2021

Long-term African dust delivery to the eastern Atlantic Ocean from the Sahara and Sahel regions: Evidence from Quaternary paleosols on the Canary Islands, Spain

Daniel R. Muhs
U.S. Geological Survey, dmuhs@usgs.gov

Joaquín Meco
Universidad de Las Palmas de Gran Canaria

James R. Budahn
U.S. Geological Survey

Gary L. Skipp
U.S. Geological Survey

Kathleen R. Simmons
U.S. Geological Survey

See next page for additional authors

Quaternary Science Reviews 265 (2021) 107024

Contents lists available at ScienceDirect

Quaternary Science Reviews

journal homepage: www.elsevier.com/locate/quascirev

Long-term African dust delivery to the eastern Atlantic Ocean from the Sahara and Sahel regions: Evidence from Quaternary paleosols on the Canary Islands, Spain

Daniel R. Muhs [a, *], Joaquín Meco [b], James R. Budahn [a], Gary L. Skipp [a], Kathleen R. Simmons [a], Matthew C. Baddock [c], Juan F. Betancort [b], Alejandro Lomoschitz [d]

[a] U.S. Geological Survey, MS 980, Box 25046, Federal Center, Denver, CO, 80225, USA
[b] Departamento de Biología, Universidad de Las Palmas de Gran Canaria, 35017, Las Palmas de Gran Canaria, Canary Islands, Spain
[c] Geography and Environment, Loughborough University, Epinal Way, Loughborough, Leicestershire, LE11 3TU, United Kingdom
[d] Instituto de Oceanografía y Cambio Global, IOCAG – Unidad Asociada de I+D+i Al CSIC, Universidad de Las Palmas de Gran Canaria, ULPGC, 35017, Las Palmas de Gran Canaria, Canary Islands, Spain

ARTICLE INFO

Article history:
Received 22 January 2021
Received in revised form
4 May 2021
Accepted 5 June 2021
Available online 25 June 2021

Handling editor: Giovanni Zanchetta

Keywords:
Pleistocene
Holocene
Paleoclimatology
Africa
Coastal geomorphology
Sediment mineralogy

ABSTRACT

Africa is the most important source of dust in the world today and dust storms from that continent frequently deposit sediment on the nearby Canary Islands. Many investigators have inferred African dust inputs to Canary Islands paleosols based only on the presence of quartz. However, some local rocks do contain this mineral, so quartz alone is insufficient proof of dust deposition. Further, it is not known whether the Sahara Desert or the Sahel region is more important as a dust source. We address these issues by study of sequences of Pleistocene aeolian sands on the islands of Lanzarote and Fuerteventura. Aeolian sands are composed mostly of marine carbonate minerals and locally derived volcanic minerals. They date from the early-middle Pleistocene to the Holocene. Trace element geochemistry shows that the soils formed from both locally derived basalt and African dust. Major element geochemistry and clay mineralogy indicate that dust additions to the Canary Islands likely come from both the Sahara and Sahel. Dust delivered from the Sahel indicates that droughts in that region have had a history extending through much of the Quaternary. Accretionary-inflationary profile development, from dust accretion, is evident in the upward growth of Canary Islands paleosols.

Published by Elsevier Ltd.

1. Introduction

Long-range-transported (LRT) dust has important effects on many of the Earth's physical systems. Dust can affect the planetary radiation balance by its influence on both incoming (solar) short-wave radiation and outgoing (terrestrial) long-wave radiation (Kohfeld and Tegen, 2007). Marine ecosystems are affected by dust inputs to the ocean, because primary productivity can be enhanced by bioavailable iron additions to primary producers (such as phytoplankton) in the oceanic food chain (Mahowald et al., 2005). Soils are affected by dust because it serves as an important parent material for what would otherwise be minimal rates of pedogenesis (McFadden, 2013). LRT dust is a valuable indicator of paleoclimate, with geologic archives found in ocean sediments, lake sediments, terrestrial sediments, soils, and glacial ice (Muhs, 2013).

The Sahara and Sahel regions of Africa are thought to be the most important sources of LRT dust in the world today (Prospero et al., 2002; Goudie and Middleton, 2006; Mahowald et al., 2006; Kohfeld and Tegen, 2007). One important dust pathway from these source regions is the northeasterly trade wind belt (Fig. 1a), which occurs at low altitudes year-round (Pye, 1987; Sarnthein et al., 1981; Stein and Sarnthein, 1984; Stuut et al., 2005). Along this trajectory, dust from the westernmost Sahara is transported to the eastern Atlantic Ocean off the coast of northwestern Africa. A second pathway occurs farther south. Dust from the Sahel and southern Sahara is transported to the Atlantic Ocean via the Saharan Air Layer, or SAL (Fig. 1a), which occurs predominantly in summer (Prospero et al., 1970; Carlson and Prospero, 1972; Prospero and Carlson, 1972; Prospero and Lamb, 2003). Near Africa, the SAL reaches altitudes as high as 5–7 km, above the trade wind zone.

* Corresponding author.
E-mail address: dmuhs@usgs.gov (D.R. Muhs).

https://doi.org/10.1016/j.quascirev.2021.107024
0277-3791/Published by Elsevier Ltd.

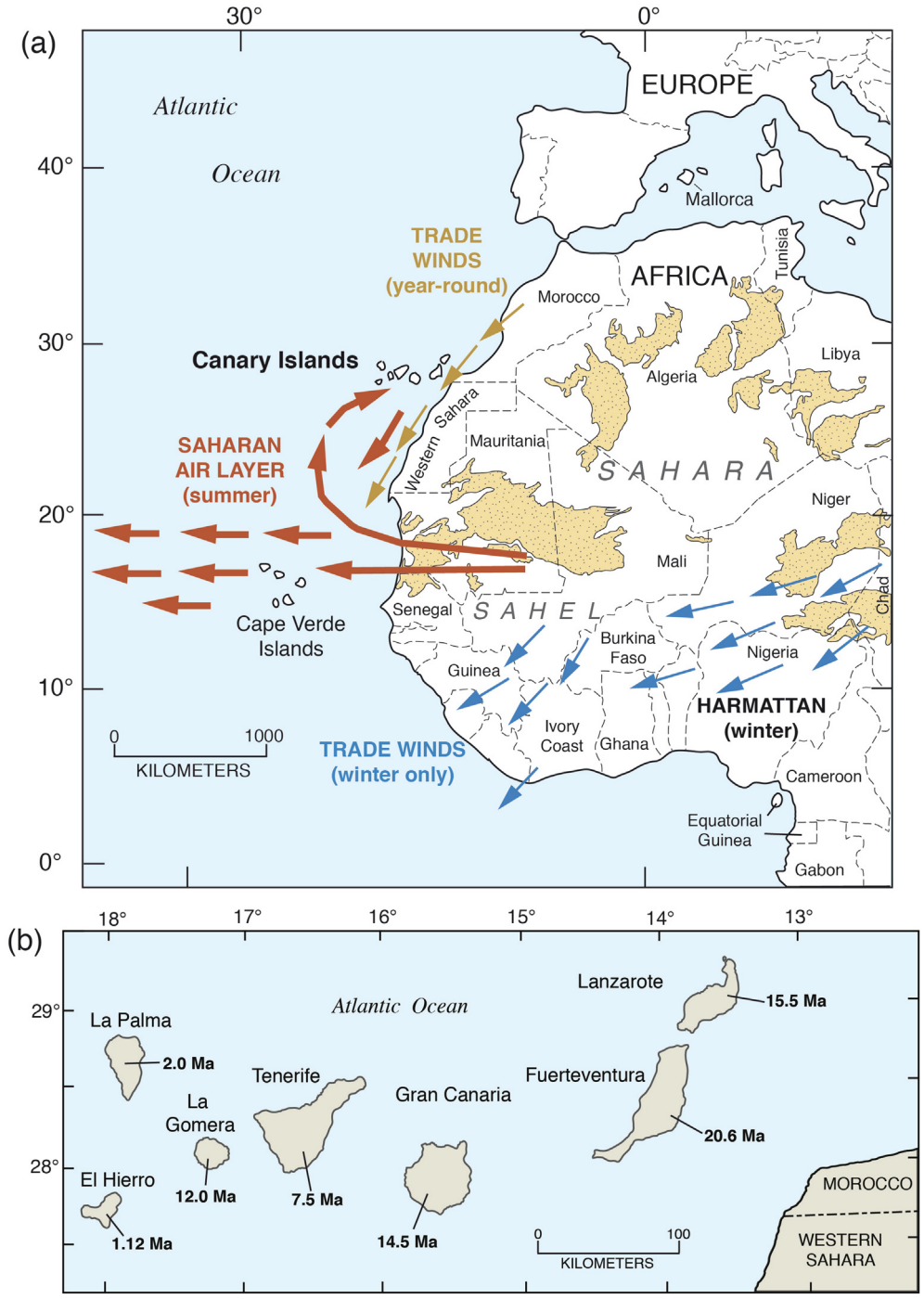

Fig. 1. (a) Map showing northwestern Africa, the Canary Islands study area, localities referred to in the text, and the main dust-transporting winds and their seasons of transport. Dust-bearing wind paths generalized from Dubief (1979), Kalu (1979), Sarnthein et al. (1981), McTainsh and Walker (1982), Stein and Sarnthein (1984), Tetzlaff and Peters (1986), Pye (1987), Stuut et al. (2005), and Schwanghart and Schütt (2008). Also shown (gold stippled areas) are major active or stable, but recently active sand seas, generalized from "Global Soil Regions" map, from U.S. Department of Agriculture, Natural Resources Conservation Service (http://www.soils.usda.gov/use/worldsoils/mapindex/order.html), in turn derived from FAO-UNESCO Soil Map of the World (Food and Agriculture Organization of the United States, UNESCO, 1974). (b) Map of the Canary Islands, with ages (in millions of years, Ma) of oldest exposed rocks given in bold type (from Guillou et al., 2004a, 2004b; Carracedo and Troll, 2016). (For interpretation of the references to color in this figure legend, the reader is referred to the Web version of this article.)

Sarnthein et al. (1981), Stein and Sarnthein (1984), Tetzlaff and Peters (1986), and Pye (1987) point out that although the main direction of dust transport in the SAL is to the west at latitudes between ~15°N and ~21°N, south of the Canary Islands (Fig. 1b), a south-to-north component of flow can occur in the lee of an easterly wave. Thus, a "hook-like" trajectory of dust movement from the Sahel to the vicinity of the Canary Islands via the SAL is observed (Figs. 1a and 2). Evidence presented by Sarnthein et al. (1981) and Grousset et al. (1998) indicates that both the trade winds and the SAL were situated approximately where they are now during the last glacial maximum, ~20,000 yr B.P., but dust fluxes may have been greater. In more recent studies, McGee et al. (2013) and

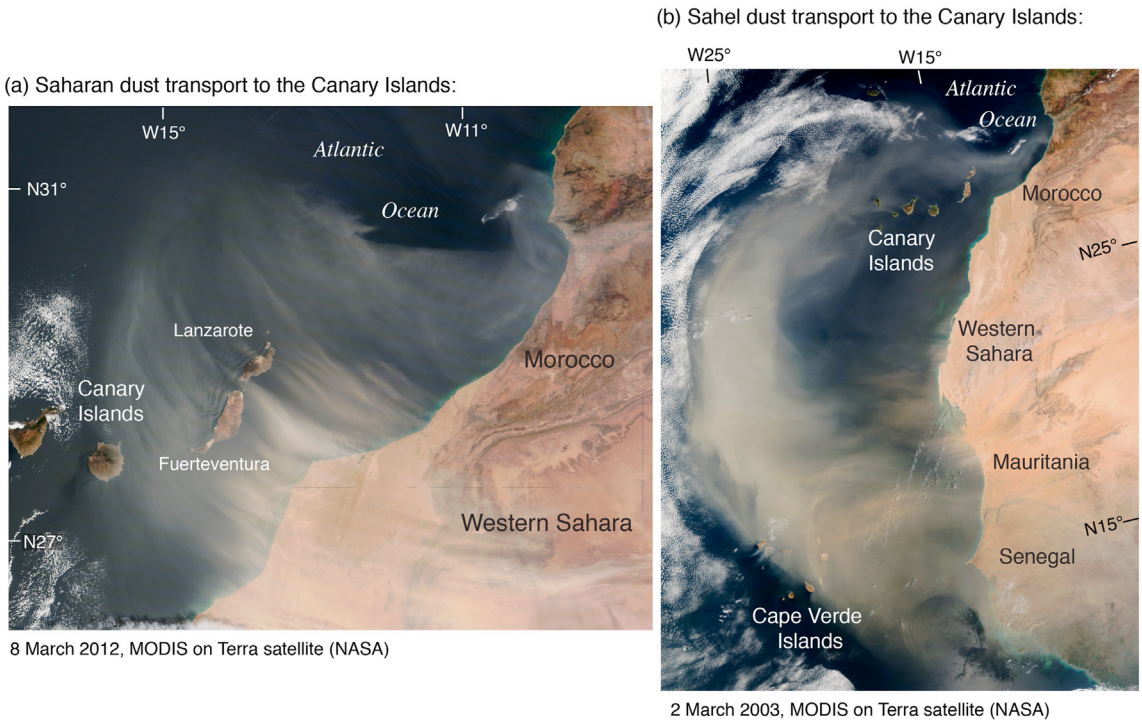

Fig. 2. Examples of dust storms over the Canary Islands that have sources from broad areas in western Africa and are derived from the SAL (Saharan Air Layer) from either (a) easterly winds, with sediment derived primarily from Sahara Desert sources, or (b) easterly winds, but with a "hook-like" form of transport northward, with a trajectory toward the Canary Islands and dust sources from both the Sahara and the Sahel. Both images acquired from the Moderate Resolution Imaging Spectroradiometer (MODIS) instrument aboard the NASA Terra satellite; image in (a) was taken on March 8, 2012; image in (b) was taken on March 2, 2003. Images are courtesy of Jeff Schmaltz (image in (a)) and Jacques Descloitres (image in (b)), both with the MODIS Rapid Response Team at NASA GSFC.

Williams et al. (2016) report that dust fluxes during "Heinrich Stadial 1" (~19 to ~15 ka) and the Younger Dryas (~13 to ~12 ka) were much higher than during the end of the African Humid Period (~8 to ~6 ka). In a third dust pathway, Sahel and southern Sahara dust are transported seasonally from Africa to the Atlantic during winter via the famous "Harmattan" dust storms (McTainsh and Walker, 1982). This trajectory is a route of dust transport to southern parts of the western African Atlantic margin (Fig. 1a).

Dust transported westward from Africa has a diverse suite of likely sources in the northern part of the continent. Formenti et al. (2010, 2014) and Scheuvens et al. (2013) have demonstrated that there are compositionally distinctive potential source areas (PSAs) for dust in Africa (Fig. 3). The PSAs in northern Africa occur across a vast part of the continent, from Western Sahara and Mauritania in the west to southern Egypt and Sudan in the east. Most of these PSAs occur within the hyperarid portions of the Sahara, but many (PSA 2, PSA 3, PSA 5 and PSA 6) include not only parts of the Sahara, but parts of the semiarid Sahel region as well. This is shown by the higher Normalized Difference Vegetation Index (NDVI) values (greener tones in Fig. 3) of the southern parts of PSAs 2, 3, 5, and 6.

With the close proximity of the Canary Islands to Africa (Figs. 1–3), dust storms originating on that continent are common on the islands, locally referred to as "calima" events (Torres-Padrón et al., 2002; Criado and Dorta, 2003; Alastuey et al., 2005). Because some of the dust from calima events accumulates on the Canary Islands, modern soils on these islands have a composition that is intermediate between the local bedrock and African dust (Muhs et al., 2010). In addition, however, stratigraphic and geochronologic studies show that the Canary Islands host a rich record of past periods of soil formation in the Quaternary. The geologic records that have been studied most thoroughly are carbonate-rich aeolian sand deposits with intercalated paleosols. A number of studies have shown that such deposits on the Canary Islands contain numerous paleosols and the records may span much of the middle and late Quaternary (Damnati et al., 1996; Damnati, 1997; Meco et al., 1997, 2006, 2008, 2011; Ortiz et al., 2006; Criado et al., 2012; Gutiérrez-Elorza et al., 2013; Muhs, 2013; Faust et al., 2015; Roettig et al., 2017, 2019, 2020). Paleosols intercalated with fluvial ("vega") deposits and lava flows have also been reported (Von Suchodoletz et al., 2008, 2009a, 2009b, 2013, 2009a). A recent study has shown that the record of paleosols within carbonate-rich aeolian sands extends back into the Pliocene (Muhs et al., 2019). Thus, the paleosols of the Canary Islands may contain valuable archives of long-term dust deposition.

Recognition that Canary Islands soils may have a record of African dust comes largely from soil mineralogy, specifically, the presence of quartz and mica. Modern dust traveling westward from Africa contains a number of constituents, but among the most abundant particles are quartz in the fine silt (20 μm–2 μm) fraction, and mica in the clay (<2 μm) fraction (Glaccum and Prospero, 1980; Chiapello et al., 1997; Caquineau et al., 1998; Stuut et al., 2005). In contrast, the Canary Islands are composed predominantly of basalt (Carracedo and Troll, 2016), and both quartz and mica are typically not found in basalt or other mafic igneous rocks. Interestingly, however, the linkage between the presence of quartz and the inference of African dust inputs has now become almost axiomatic in the interpretation of soils and paleosols on the Canary Islands. Most investigators have assumed that local rocks simply could not have contributed such particles, even though minor amounts of quartz have been reported in rocks on Lanzarote (Fuster et al., 1968a) and both quartz and mica (biotite) have been documented in rocks from Fuerteventura, particularly in what is called the Basal Complex (Fuster et al., 1968b; Carracedo and Troll, 2016). Even the historic (1730–1736) eruption of Timanfaya on Lanzarote is

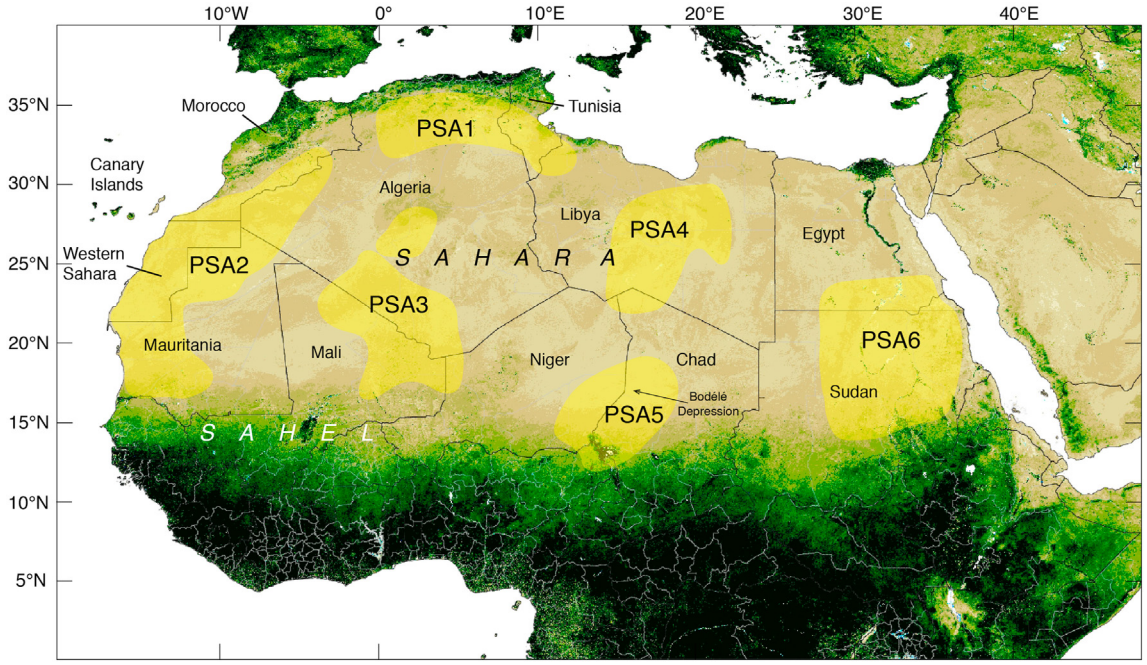

Fig. 3. Normalized Difference Vegetation Index (NDVI) image of northern Africa and adjacent regions, including the Canary Islands, compiled from NASA's MODIS sensor, showing degree of vegetation cover (denser vegetation is green; lesser density of vegetation is brown). Image was acquired from 17 November to December 2, 2019, and is presented courtesy of NASA. Also shown (light yellow shades) are Potential Source Areas (PSAs) of dust, as defined by Formenti et al. (2010, 2014) and Scheuvens et al. (2013). (For interpretation of the references to color in this figure legend, the reader is referred to the Web version of this article.)

reported to contain small amounts of quartz, based on both thin section studies and X-ray diffractometry (Carmona et al., 2009). Thus, evidence of an African dust input to the paleosols of the Canary Islands requires more than just the presence of quartz.

Another issue is the considerable debate about the most important sources of dust in Africa. Many workers have simply ascribed dust inputs in Canarian soils and paleosols to sources in the "Sahara" without much more specificity (Damnati et al., 1996; Williamson et al., 2004; Von Suchodoletz et al., 2008, 2009a, 2009b, 2013, 2009a, 2013; Menéndez et al., 2009, 2019, 2019; Criado et al., 2012; Faust et al., 2015; Varga and Roettig, 2018; Roettig et al., 2019). This is consistent with a number of studies that have emphasized the importance of the year-round trade wind dust pathway from northwestern Africa, described above (Coudé-Gaussen et al., 1987; Grousset et al., 1992, 1998, 1998; Rognon et al., 1996), implying northern, Saharan-derived sources. Nevertheless, Bergametti et al. (1989) point out that more southerly sources, such as the Sahel, also play a role in delivering dust to the Canary Islands. Based largely on particle size data, Stuut et al. (2009) inferred that Canary Islands sediments and soils could be derived largely from the Sahel region. Given modern observations that the SAL can have a hook-like trajectory to the north (Fig. 2b), such a delivery of Sahel and southern Sahara dust to the Canary Islands in the past is certainly possible. In a recent study, Heinrich et al. (2021) proposed that during Heinrich Events (collapses of ice sheets bordering the North Atlantic Ocean during glacial periods), there was a southern shift of climate zones. Under these conditions, the Sahel region of Africa becomes arid and constitutes an important dust source. Heinrich et al. (2021) consider paleosols on Lanzarote to have formed during such times.

A number of studies have proposed that one specific area within the Sahara, the Bodélé Depression of Chad (situated within PSA 5; Fig. 3), is by far the most important source of westward-traveling dust from Africa, at least at present (Goudie and Middleton, 2001; Prospero et al., 2002; Washington et al., 2003). The identification of this area as a single important dust source is based on contemporary measurements from Total Ozone Mapping Spectrometer (TOMS) imagery. From these earlier findings, it is now common for dust investigators to refer routinely to the Bodélé Depression not only as the most important source of dust in Africa, but the most important source on the entire planet (Giles, 2005; Goudie and Middleton, 2006; Washington et al., 2006; Todd et al., 2007; Warren et al., 2007; Bristow et al., 2009, 2010, 2010; Moskowitz et al., 2016; Bristow and Moller, 2018).

There are, however, challenges to the concept of the Bodélé Depression as the most important source of LRT dust from Africa, based on isotopic studies, back-trajectory reconstructions, and other modeling (Bozlaker et al., 2018; Kumar et al., 2018; Yu et al., 2020). In fact, identification of the Bodélé Depression as the most important dust source in Africa poses some simple mineralogical problems. Where African dust has been transported to the west and collected in traps on both sides of the Atlantic (Canary Islands, Cape Verde, mid-Atlantic, Barbados, and Miami), it consists of mica, quartz, kaolinite, chlorite, K-feldspar, plagioclase, and calcite (Glaccum and Prospero, 1980; Caquineau et al., 1998; Stuut et al., 2005; Menéndez et al., 2007, 2014; Patey et al., 2015; Van der Does et al., 2018). In contrast, the Bodélé Depression is dominated by diatomite (Abouchami et al., 2013; Bristow and Moller, 2018), although quartz, mica, kaolinite, and other clays also have been reported (Hudson-Edwards et al., 2014). It is, therefore, an open question as to whether the present importance of the Bodélé Depression as a dust source is mirrored in the longer-term geologic record.

LRT dust trapped on the islands of Bermuda in the 1980s and 1990s and Barbados in the 1960s by J.M. Prospero and colleagues illustrate the multiple sources of African dust transported to and across the Atlantic Ocean. Atmospheric "back-trajectory" techniques can help to identify dust sources. These sorts of models are used to reconstruct the route that an air mass takes to, or from, a given point in time and space. Dust trajectories can be examined

both "backward" and "forward," and assessments in both directions have provided considerable insight into dust source location and behavior. To accomplish this, back-trajectory models typically use three-dimensional inputs of remodeled gridded wind fields, available in varying spatial and temporal resolutions. Using LRT dust samples from both of these islands that were characterized geochemically by Muhs et al. (2007, 2010, 2012), we conducted back-trajectory analyses using the HYSPLIT method (Draxler and Hess, 1998), following the procedures recently utilized by Baddock et al. (2017). Results of these analyses show that summer (July and August) dust collected on Bermuda likely has sources in the western part of the Sahara and the northern part of the Sahel regions (Fig. 4a). On Barbados, dust collected from May through October also has its origins in the western part of the Sahara and Sahel regions (Fig. 4b and c). These results parallel those of similar back-trajectory modeling for dust collected at Barbados by Engelstaedter et al. (2009). Another recent study, also using HYSPLIT back-trajectory analyses, shows that dust collected on Barbados in 2013 and 2014 had potential sources in the Sahel, the western Sahara, and possibly the Bodélé Depression (Bozlaker et al., 2018).

Here, we test the hypotheses of Sahara and Sahel dust origins for soils and paleosols on the Canary Islands. Thick sequences of carbonate-rich aeolian sand, with intercalated paleosols, are found on the islands of Lanzarote and Fuerteventura (Figs. 5 and 6), the easternmost two islands of the Canaries (Fig. 1b). Geochronology is derived from a suite of radiocarbon, $^{40}Ar/^{39}Ar$, and calibrated Sr-isotope age estimates. We use a combination of bulk mineralogy, clay mineralogy, major element geochemistry, and trace element geochemistry to evaluate whether paleosols are derived from local bedrock sources, Saharan dust, Sahel dust or some combination of these materials, and assess the significance of the results with regard to the long-term history of dust transport out of Africa to the Atlantic Ocean.

2. Study areas

2.1. Geology of Lanzarote

Lanzarote is the easternmost of the Canary Islands and is composed dominantly of basalt, with ages ranging from Miocene to historic (Fuster et al., 1968a). Carracedo and Troll (2016) also point out that Lanzarote is one of the oldest islands and hence the Miocene rocks are highly eroded. Two volcanic massifs, Ajaches and Famara (Fig. 5) developed as shield volcanoes during the Miocene, with Ajaches forming first. There was apparently a long period of no eruptions, perhaps on the order of several million years, followed by the eruption of the Corona volcano in the late Pleistocene (Carracedo and Troll, 2016), in the area between Órzola and Arrieta (Fig. 5). The only Holocene eruptions that are known are the extensive historic flows of 1730–1736, followed by a shorter and less extensive eruption in 1824.

On Lanzarote, Fuster et al. (1968a) recognized four ages of basalts: "Series I" (Miocene), "Series II," "Series III," and "Series IV" (post-Miocene and historic). Fuster et al. (1968a) conducted detailed petrographic analyses of these rocks. In the basalts that dominate all four series, the main minerals reported are plagioclase, pyroxenes, and olivine, as well as nepheline, magnetite, apatite, and zeolite. However, in some gabbros of Series I, Fuster et al. (1968a, p. 147–148) report the occurrence of K-feldspar. Although rare, in Series II, III, and IV basalts of Lanzarote, Fuster et al. (1968a, p. 164) report the occurrence of quartz in xenoliths and scoriae. Thus, although quartz and K-feldspar are certainly not typical of minerals found in the dominantly basaltic terrain of Lanzarote, their presence in rocks on the island has been documented.

Carbonate-rich aeolian sands, with a range of ages from Pliocene to Holocene, are found over the north-central part of the island and a small area on the coast south of Arietta (Fig. 5). Because our study locality on Lanzarote (a quarry near Mala) hosts aeolian sands derived from beach or shelf sediments, it is important to document the mineralogy of contemporary beach sands, the best modern analog to what was deposited at Mala in the past. The two closest modern beaches are those at Famara and Arrieta (Fig. 5). At Famara, 13 beach sand samples contain calcite, aragonite, plagioclase, pyroxenes, and possibly hematite, in order of approximate abundances. At Arrieta, a dozen samples of beach sands collected all contain calcite, aragonite, plagioclase, pyroxenes, olivine, possibly hematite, and quartz. On both beaches, aragonite and calcite are derived from marine invertebrate skeletal fragments and plagioclase, pyroxenes, olivine, and hematite likely originate from local basalt. The origin of quartz is uncertain but could be derived from some of the rare occurrences on Lanzarote noted by Fuster et al. (1968a).

The quarry at Mala (Figs. 7 and 8), studied here, has previously been examined by Damnati et al. (1996), Williamson et al. (2004), Meco et al. (2006, 2011), Ortiz et al. (2006), Yanes et al. (2007, 2008), and Von Suchodoletz et al. (2012). Meco et al. (2006) reported optically stimulated luminescence (OSL) ages of ~130 ka near the top of the section and ~191 ka at ~7 m depth. These workers also reported U-series ages on land snails, which are now known to be unreliable, because U uptake in mollusks is secondary. Ortiz et al. (2006) used amino acid ratios in land snails to infer that the upper part of the section at Mala is ~28 ka and the lower part is ~40 ka. Von Suchodoletz et al. (2012) conducted thermoluminescence (TL) analyses of the soil or sediment immediately underlying a lava flow on the south side of the quarry. These investigators reasoned that the heat from the lava flow would have zeroed the accumulated luminescence in the underlying sediments. Von Suchodoletz et al. (2012) reported red TL (coarse grain regenerative), blue TL (fine grain additive), and blue TL (fine grain regenerative) ages of 172 ± 17 ka, 136 ± 11 ka, and 144 ± 22 ka (numbers rounded for significant figures), respectively, for this lava. They considered both of the blue TL ages to be underestimates, due to anomalous fading, and considered the red TL age to be the best estimate of the age of the lava. Thus, it is clear from these investigations that most of the section at Mala is likely Quaternary, but age estimates differ from study to study.

2.2. Geology of Fuerteventura

Basalts that were generated during the building of three Tertiary shield volcanoes (Carracedo and Troll, 2016) dominate the island of Fuerteventura (Fig. 6). Thus, much of the island is composed of volcanic rocks of Miocene ("Series I″ of Fuster et al., [1968b]), Pliocene ("Series II"), Pleistocene ("Series III"), and Holocene ("Series IV") age. An exception to this is an area in the west-central part of the island referred to as the "Basal Complex" (Fig. 6), which consists of a wide variety of rocks, ranging in age from Mesozoic to Miocene.

As is the case on Lanzarote, basalts and other mafic rocks on Fuerteventura are dominated by plagioclase, pyroxenes, and olivine (Fuster et al., 1968b). None of the basalts or other mafic rocks on the island contain quartz, based on detailed petrographic studies reported by Fuster et al. (1968b). However, an important local source of quartz on Fuerteventura is found in the sequence of Mesozoic sediments found in the Basal Complex (see Fuster et al., [1968b] and Carracedo and Troll [2016], p. 536–537). Rocks of the Basal Complex occupy a substantial part of the west-central portion of Fuerteventura (Fig. 6). Fuster et al. (1968b) also report biotite in

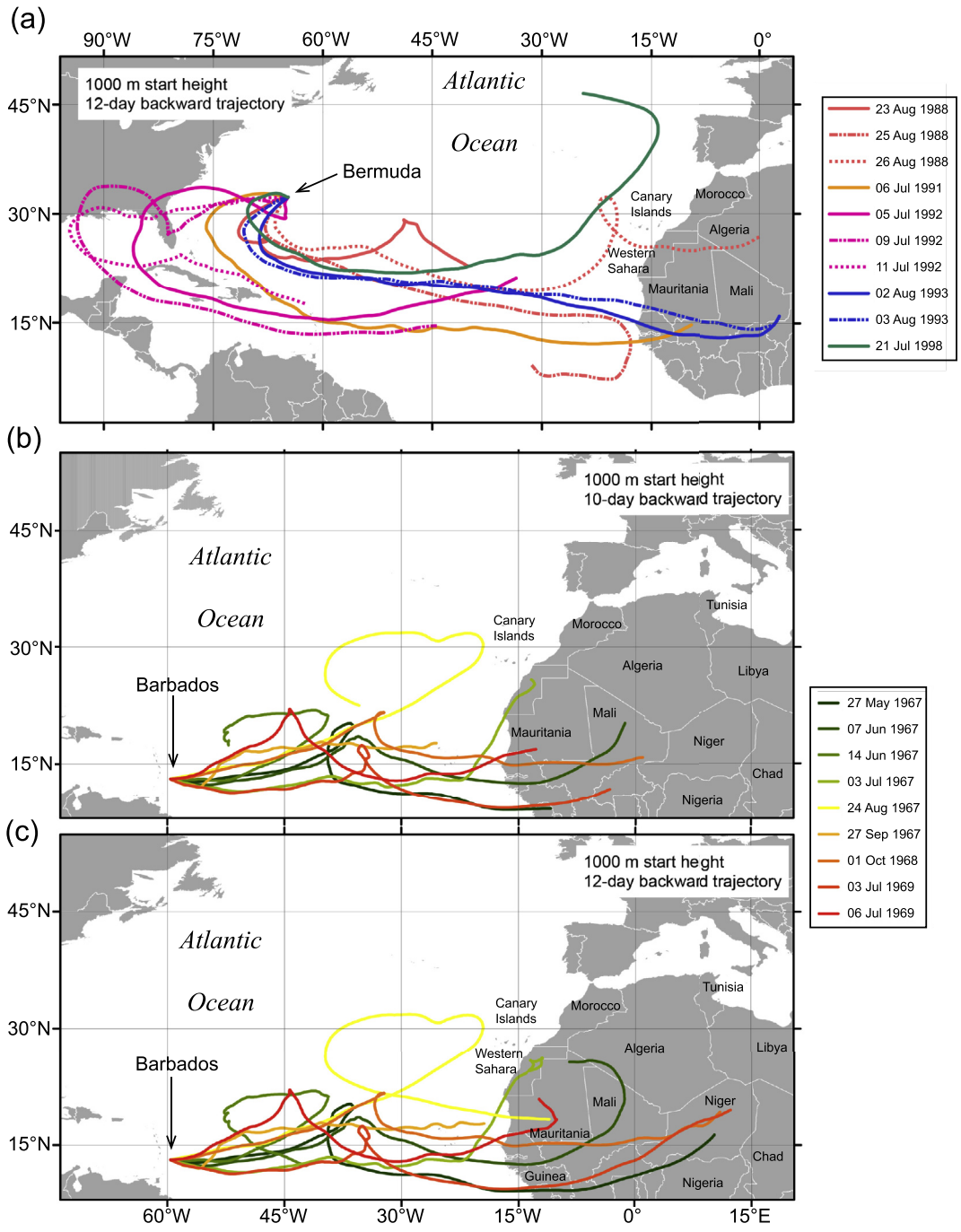

Fig. 4. Calculated back-trajectory pathways of dust transport from Africa to (a) Bermuda and (b, c) Barbados, for times of dust collection on those islands reported by Muhs et al. (2007, 2012). Back trajectories calculated by the authors using the HYSPLIT software (Draxler and Hess, 1998). Note that calculated pathways of long-range dust transport imply sediment sources in both the Sahara (Algeria, Western Sahara, and northern Mali, Mauritania, and Niger) and Sahel (southern Mali, Mauritania, and Niger, Nigeria, Burkina Faso, and Guinea) regions.

Fuerteventura pyroxenites, syenites, and "Series I″ basalts. Thus, Fuerteventura has local sources of quartz and mica within the suites of older rocks.

In addition to basalts and Basal Complex rocks, carbonate-rich surficial deposits cover much of Fuerteventura. Some of these are large areas covered by pedogenic calcretes (caliche) derived from pre-Quaternary aeolian sand (Carracedo et al., 2005; Meco et al., 2006). As is the case on Lanzarote, there are also substantial areas of active, Holocene, and Pleistocene aeolian sand (Fig. 6). In the northern part of the island (Figs. 9 and 10), a quarry is present at a locality called La Rosa Negra (called "Montaña de la Costilla" by Ortiz et al., 2006; and the "Costilla" section by Faust et al., 2015). The stratigraphy at this site has been previously studied by Damnati et al. (1996, 2005), Bouab and Lamothe (1997), Meco et al. (2006, 2008), Ortiz et al. (2006), Gutiérrez-Elorza et al. (2013), and Faust et al. (2015). In addition, a number of other localities, with similar

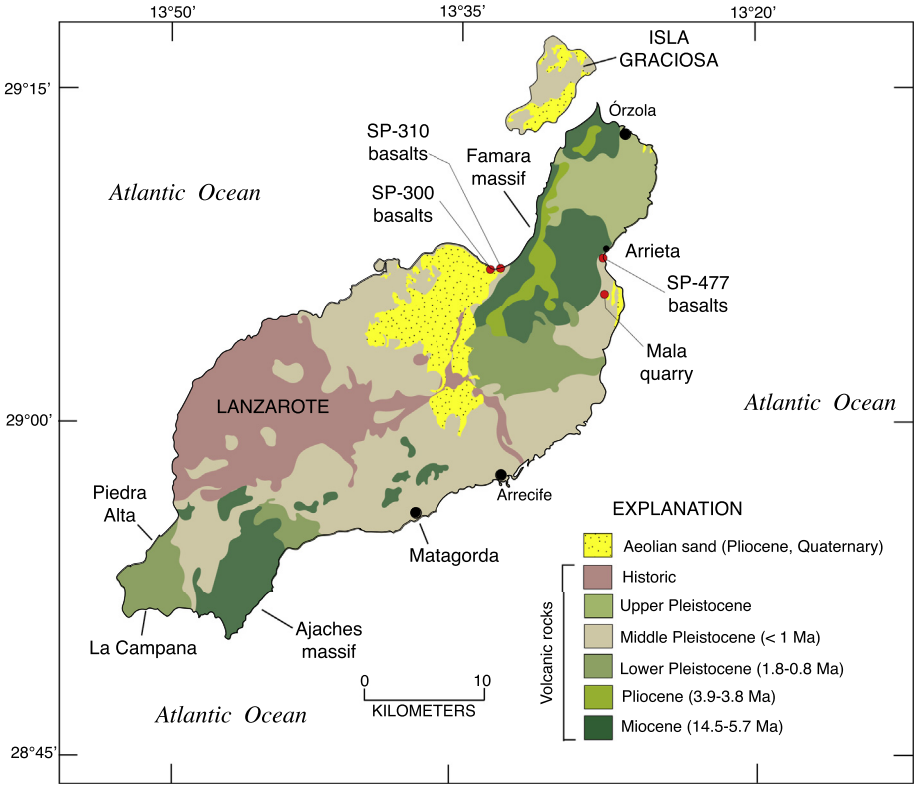

Fig. 5. Geology of Lanzarote, simplified from Carracedo and Troll (2016) for volcanic rocks and Balcells et al. (1994) for aeolian sand. Also shown is the location of the quarry at Mala and beaches at Famara and Arrietta, where both beach sands and volcanic clasts were sampled.

aeolian deposits and paleosols, have also been studied in northern Fuerteventura (Ortiz et al., 2006; Faust et al., 2015; Roettig et al., 2017, 2019, 2020).

Specifically for the locality at La Rosa Negra, Bouab and Lamothe (1997) and Meco et al. (2006) report OSL ages ranging from ~147 ka at a depth of ~1–2 m to ~253 ka at a depth of ~8–9 m. Ortiz et al. (2006) used radiocarbon dating and amino acid ratios in land snails to infer that the upper part of the section is Holocene and the oldest aeolian sands near the base of the section are ~47 ka. Gutiérrez-Elorza et al. (2013) reported radiocarbon ages of >49 ka to ~46 ka from ~3.5 m depth to ~11–12 m depth, and OSL ages of ~26 ka to ~46 ka over the same depth interval. Faust et al. (2015) reported an infrared stimulated luminescence (IRSL) age of ~228 ka at a depth of ~3–4 m. Thus, as is the case with the quarry at Mala, there are disagreements about the ages of these deposits, but all investigators agree that they are of Quaternary, and mostly Pleistocene age.

3. Methods

3.1. Geochronology

3.1.1. Radiocarbon dating

Ideal materials for radiocarbon dating, such as charcoal or wood, are lacking in Canary Islands aeolian sediments and their associated paleosols. However, unaltered fossil land snails, some of them still retaining color and/or shell patterning, are common, particularly within the paleosols themselves. Fossil land snails, most commonly of the genus *Theba* (including *T. geminata*, *T. pisana*, and *T. impugnata*), are found in most aeolian sand sequences we have examined on both Lanzarote and Fuerteventura. We sampled these fossils for radiocarbon dating. Studies by Yanes et al. (2007, 2008, 2011) from the same stratigraphic sections, as well as other sections on the Canary Islands, show that species of the genus *Theba* are very well preserved. With rare exceptions, fossil *Theba* specimens are typically 91–100% aragonite, indicating little or no diagenetic recrystallization from the original mineralogy. From the Mala, Lanzarote section, studied here, Yanes et al. (2007, 2008) reported that aragonite contents of fossil *T. geminata* and *T. impugnata* range from 94% to 100%, with the majority of specimens being 100% aragonite. From a section very close to that we studied on Fuerteventura, Yanes et al. (2007) reported aragonite contents of *T. geminata* ranging from 96% to 100%.

Radiocarbon dating of nonmarine gastropods has had a long and uncertain history (see review in Goodfriend and Hood, 1983). Particularly questionable results have come from pond or marsh snails where old, "dead" carbon can be incorporated into shell carbonate. However, in the past decade or so, studies using a careful selection of land snail samples, typically with smaller species, combined with accelerator mass spectrometric counting, has resulted in a newer view that such materials are often favorable for radiocarbon geochronology (Pigati et al., 2010). Age bias for old, "dead" carbon is often minimal with such taxa, and even where it occurs, it can be corrected because the bias seems to be genus or species controlled. A comparison of land snail radiocarbon ages with independent geochronology (luminescence ages or radiocarbon ages on wood) in calcareous loess deposits of the North American Great Plains and Alaska concluded that small terrestrial gastropods are reliable materials for dating these types of deposits (Pigati et al., 2013).

Snails were prepared for radiocarbon dating in the laboratories of the U.S. Geological Survey (samples from Lanzarote) and Lawrence Livermore National Laboratory (samples from Fuerteventura). Methods follow those given in Pigati et al. (2013). Briefly,

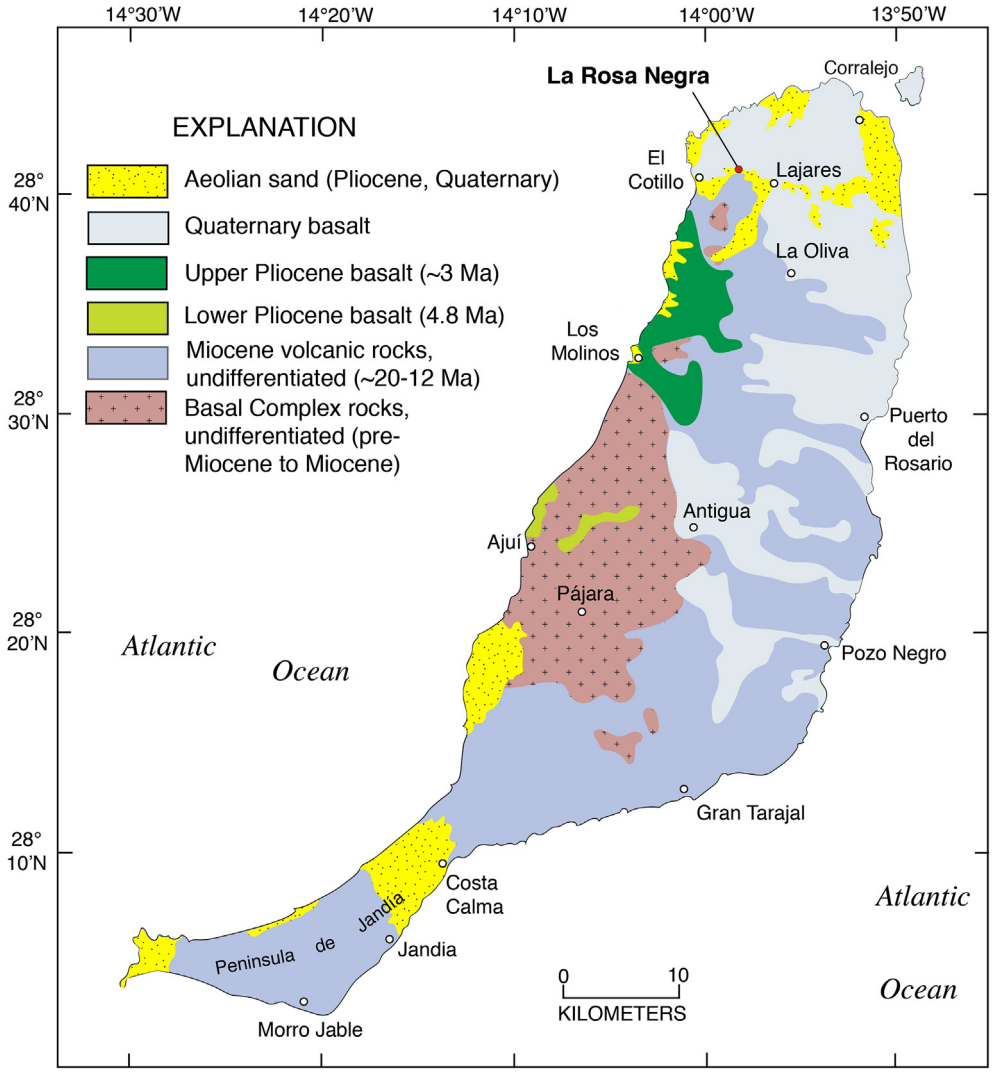

Fig. 6. Geology of Fuerteventura, redrawn from Balcells et al. (1991) and Meco et al. (2015) and location of La Rosa Negra quarry. Also shown is the distribution of aeolian sand, redrawn from Carracedo et al. (2005).

after identification to species, land snail shells were separated from the host sediment, placed in a beaker of ASTM Type 1, 18.2 MU (ultrapure) water, and subjected to an ultrasonic bath for a few seconds. The shells were then repeatedly immersed in a second beaker of ultrapure water to remove material adhering to the shell surface or lodged within the shell itself, and the process was repeated until the shells were visibly clean. In most cases, shells were selectively dissolved or etched briefly using dilute HCl to remove secondary carbonate (dust) from primary shell material. The etched shells were then washed repeatedly in ultrapure water and dried in an oven overnight at ~70 °C. The clean, dry shells were broken and examined under a dissecting microscope to ensure that the interior whorls were free of secondary carbonate and detritus. Fossil shells that were free of detritus were converted to CO_2 using A.C.S. reagent grade 85% H_3PO_4 under vacuum at 50 °C until the reaction was visibly complete (~1 h). The resulting CO_2 was converted to graphite using an iron catalyst and the standard hydrogen reduction process and submitted to the Center for Accelerator Mass Spectrometry at Lawrence Livermore National Laboratory. Radiocarbon ages for the gastropod shells were calibrated using the IntCal13 dataset and the CALIB 7.1. html calibration program (Stuiver and Reimer, 1993; Reimer et al., 2013). Ages are presented in calibrated radiocarbon years BP (ka = thousands of years; BP = Before Present; 0 yr BP = 1950 A.D.), rounded to the closest 10 years and uncertainties are given at the 95% (2 sigma) confidence level.

3.1.2. $^{40}Ar/^{39}Ar$ geochronology

A basalt sample from the quarry at Mala, Lanzarote was analyzed for $^{40}Ar/^{39}Ar$ geochronology at the New Mexico Geochronology Research Laboratory (NMGRL), New Mexico Institute of Mining and Technology in Socorro, New Mexico. The groundmass concentrate was prepared by treating crushed material with dilute HCl and then removing the phenocrysts. The mineral separate and monitors (Fish Canyon Tuff sanidine, with an age of 28.201 Ma; see Kuiper et al., [2008]) were loaded into aluminum discs and irradiated for 0.33 h at the USGS TRIGA reactor in Denver, Colorado. After irradiation, the groundmass was step-heated with a Photon Machines Diode laser and was analyzed with a Thermo Helix MCPlus mass spectrometer. Sensitivity for the Helix MCPlus with the Diode laser (step-heated samples) is 3.0 e^{-16} mol/fA. Total fusion analyses were performed on an Argus VI mass spectrometer online with an automated all-metal extraction system. Sensitivity for the Argus VI with the CO_2 laser (fused monitors) is 4.62 e^{-17} mol/fA. Typical system blanks and background were 281.7,

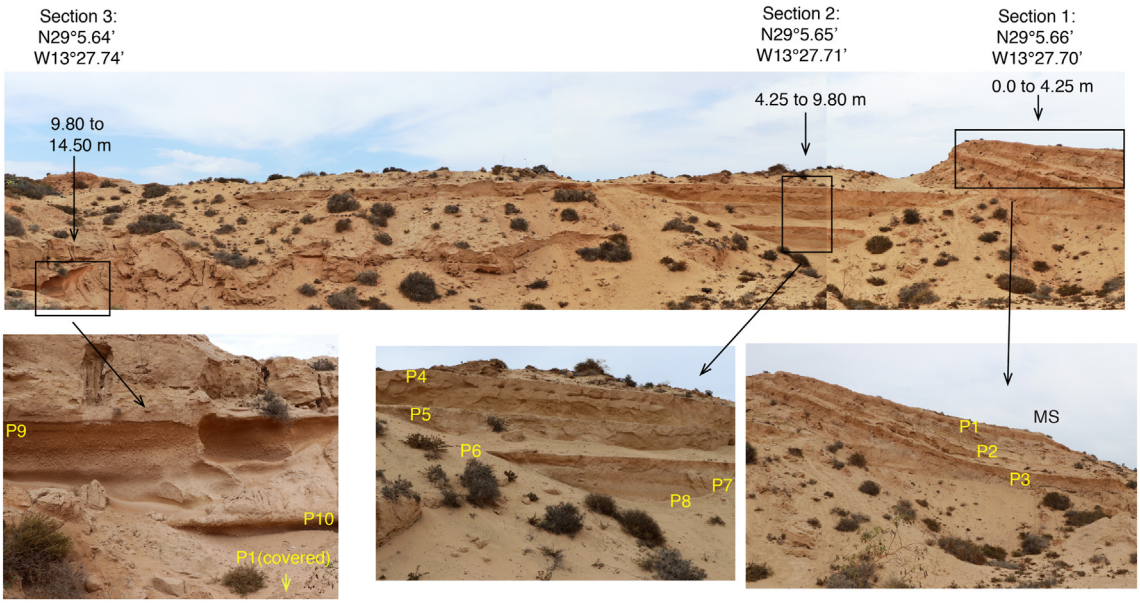

Fig. 7. Photographs of aeolian sands and paleosols (paleosols indicated by "P" prefix; "MS" is modern soil) in the quarry exposure at Mala, Lanzarote. Overall stratigraphy, shown later, is a composite of three sections (3, 2, and 1, from left to right in upper photograph) with laterally traceable units. Lower three photographs show close-ups of aeolian sands and paleosols in the three sections. All photographs by D.R. Muhs.

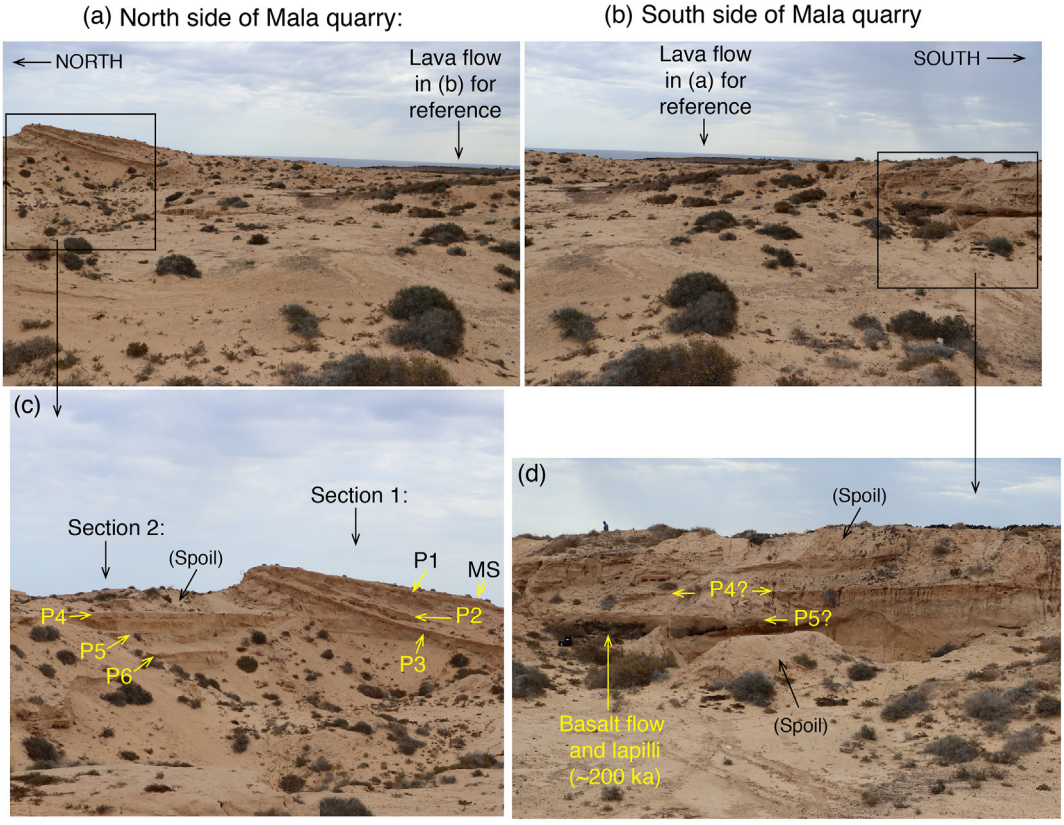

Fig. 8. (a) Photograph of aeolian sands and paleosols in the quarry exposure at Mala, Lanzarote, as in Fig. 7, for the north side of the quarry; photograph in (b) shows the south side of the quarry, where dated basalt flow and lapilli are exposed. Photographs in (c) and (d) show possible correlations of paleosols (with "P" prefixes) from north and south side exposures. All photographs by D.R. Muhs.

1.53, 8.07, 7.53, 1.05 $\times$ 10^{-18} mol at masses 40, 39, 38, 37 and 36, respectively, for the laser analyses. J-factors were determined by CO_2 laser fusion of six single crystals from each of 6 radial positions around the irradiation tray. Decay constants used are from Min et al. (2000).

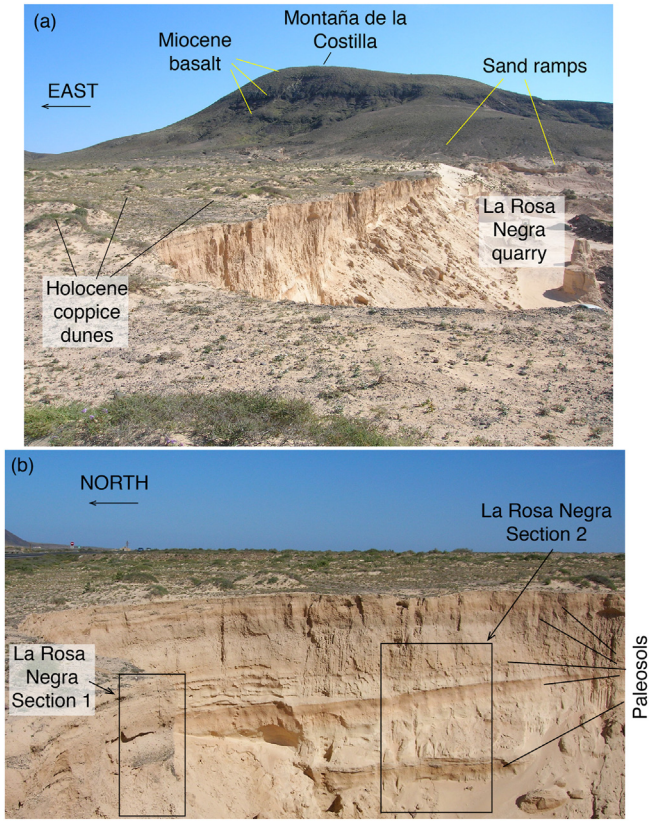

Fig. 9. Photographs of aeolian sands and paleosols in the quarry exposure at La Rosa Negra, Fuerteventura. Overall stratigraphy, shown later, is a composite of two sections with laterally traceable units. (a) Upper photograph shows overall landscape setting of the quarry exposure of the climbing dune (sand ramp) deposited on older volcanic rocks. (b) Lower photograph shows close-ups of aeolian sands and paleosols in the two sections. All photographs by D.R. Muhs.

3.1.3. Strontium isotope stratigraphy

Strontium isotopes can be utilized for assessing ages of fossil carbonate marine organisms in sediments because the Sr isotopic composition of seawater varies over geologic time (Howarth and McArthur, 1997; McArthur et al., 2001, 2020). Marine organisms that precipitate Sr (which substitutes for Ca in $CaCO_3$, whether aragonite or high-Mg calcite) in their skeletons do so without measurable fractionation of Sr isotopes. Thus, $^{87}Sr/^{86}Sr$ values in unaltered fossil carbonate skeletons reflect the $^{87}Sr/^{86}Sr$ isotopic composition of seawater at the time of precipitation. Since ~37 Ma, the $^{87}Sr/^{86}Sr$ isotopic composition of seawater has been increasingly radiogenic, i.e., there has been a steady increase in the $^{87}Sr/^{86}Sr$ value, albeit at different rates in different time intervals (Howarth and McArthur, 1997; McArthur et al., 2001).

The host aeolian sands of the paleosols we studied are dominantly aragonite- and high-Mg-calcite-rich marine organisms, as well as some secondary calcite (total $CaCO_3$ values range from 76 to 95% at Mala quarry and 69–93% at La Rosa Negra quarry; see below). Although Sr-isotope compositions of such sediments do not give the age of aeolian sand entrainment or deposition, they do provide maximum-limiting ages of these events, as $^{87}Sr/^{86}Sr$ values will give approximate average ages of the mix of marine organisms that constitute the dominant sources of the aeolian sediment packages. We specifically chose for analysis those aeolian sand samples that were highest in aragonite and high-Mg calcite content (i.e., those dominated by marine bioclasts) to minimize any contributions from detrital secondary carbonates.

Carbonate-dominated aeolian sand samples were subjected to repeated ultrasonication in deionized water, removal of detrital clays, drying of the cleaned carbonate skeletal sands, and inspection under magnification. This procedure resulted in clean, clay-free carbonate sands dominated by primary marine bioclasts. Cleaned samples processed at the USGS isotope laboratory in Denver were dissolved in 5 M acetic acid to minimize Sr contamination from any remaining non-carbonate material. The soluble fraction was then centrifuged and separated by standard ion-exchange techniques. Strontium was loaded on a single oxidized Ta filament. Isotopic ratios were measured on a VG54 sector multi-collector mass spectrometer in dynamic mode. Uncertainties are given at the 95% confidence level. SRM-987 from the U.S. National Institute of Standards and Technology (https://www-s.nist.gov/m-srmors/certificates/987.pdf) was used as a reference $^{87}Sr/^{86}Sr$ standard. Age estimates were made for each sediment package analyzed using the calibrated $^{87}Sr/^{86}Sr$ values in McArthur et al. (2020), LOWESS Version 6.

3.2. Mineralogy and geochemistry

Volcanic rocks, sediments, and paleosols from all localities were analyzed as bulk samples after pulverization and homogenization. Total inorganic carbon (TIC) concentrations in aeolian sediments and paleosols were measured using a rapid and precise method that utilizes automated coulometric titration (Engleman et al., 1985). Samples were pulverized to a fine powder and analyzed for weight percentages of TIC using a UIC Inc. carbon-dioxide coulometer (Engleman et al., 1985). Calcium carbonate content was calculated as TIC/0.12, where 0.12 is the molar fraction of carbon in $CaCO_3$. Based on internal standards and sample replicates, the accuracy and precision for TIC is 0.10%.

Mineralogy of bulk samples was determined by X-ray diffractometry (XRD) of randomly oriented mounts. Calcite is identified by a peak at 29.4° and high-Mg calcite can sometimes be distinguished from low-Mg calcite by a peak at a slightly higher angle (29.7–29.8°). Unfortunately, unambiguous identification of high-Mg calcite is precluded by the presence of a pyroxene peak at or near the same position. Aragonite is identified by a peak at 26.2°. A second aragonite peak near 27.2° makes it difficult to confirm or reject the presence of K-feldspar, which has a peak at about 27.4°–27.5°. Plagioclase is identified by a peak at 27.8°. Quartz is identified by a prominent peak at 26.6° and a much smaller peak at 20.9°. Because the mica (003) peak coincides with the 26.6° quartz peak, we measured the 20.9° quartz peak for estimates of relative abundances of this mineral. Thus, some samples that show no apparent quartz in our plots might contain it but did not display 20.9° peaks above background.

The clay (<2 μm) fractions of paleosols were isolated from separate unpulverized splits by sedimentation, after removal of organic matter by 30% H_2O_2 and removal of most or all carbonates by either acetic acid buffered to pH = 5 or weak HCl, followed by dispersion with sodium hexametaphosphate. Mineralogy of the clay fraction was determined by XRD from three treatments: air-dried, glycolated, and heat-treated (550 °C, 1 h) samples, all from oriented mounts. Clay mineral identifications follow guidelines in Moore and Reynolds (1997). Smectite has a prominent peak at ~5.2° (001) when glycolated and this peak collapses after heating to 550 °C for 1 h. Mica has peaks at 8.9° (001), 17.7° (002), and 26.6° (003) when air-dry or glycolated and these peaks persist after heat treatment. Kaolinite has peaks at 12.5° (001) and 24.9° (002) when air-dried or glycolated and these peaks collapse after heat treatment. Chlorite is identified by peaks at 6.2° (001) and 18.8° (003) on heat-treated samples.

Major element geochemistry of sediments and paleosols from

Fig. 10. Map of the islands of Lanzarote and Fuerteventura, showing localities referred to in the text. Also shown are the 100-m and 200-m isobaths, indicating insular shelf areas that could have been sources of the carbonate skeletal sands in the sections at Mala and La Rosa Negra during glacial-age, low sea-level stands of the Pleistocene. Bathymetric data are from the U.S. National Oceanic and Atmospheric Administration (NOAA) Bathymetric Data Viewer (https://maps.ngdc.noaa.gov/viewers/bathymetry/).

both the Mala quarry and La Rosa Negra was determined by wavelength-dispersive X-ray fluorescence (WD-XRF). Trace element geochemistry, including the rare earth elements (REE), was determined by instrumental neutron activation analysis (INAA), following methods in Budahn and Wandless (2002). All geochemical data presented here are available as supplementary files at the journal website and at this url: https://doi.org/10.5066/P9ZI4Y63.

4. Results

4.1. Stratigraphy, paleosols, and geochronology

4.1.1. Mala quarry, Lanzarote

At Mala (Figs. 7, 8 and 10), we examined a south-facing wall with a composite thickness of ~16 m. The composite stratigraphy, shown in later figures, is the result of descriptions of three individual sections (Figs. 7 and 8) that provide what were perceived to be the best exposures of individual units. A similar approach was taken on the island of Fuerteventura (Figs. 9 and 10). On both islands, section-to-section correlation was achieved by lateral tracing of individual paleosols within the host aeolian sands.

Aeolian sand units at Mala consist of well-sorted fine to medium sands, with thicknesses ranging from less than a meter to as much as ~2 m (Fig. 7). Bedding, if present, was not apparent. Most aeolian sands are very pale brown (10 YR 7/3, 7/4, 8/3, 8/4) or white (10 YR 8/2, 7/2) when dry (all colors given here are from Munsell soil color charts). Sands are composed of skeletal fragments of marine invertebrate organisms (bivalves, gastropods, and echinoids, particularly sea urchin spines; less commonly, foraminifera and sponge spicules), and volcanic (basaltic) rock fragments.

Paleosols are distinguished from their host aeolian sands by changes in color and texture and the presence of fossils and trace fossils. In contrast to the very pale brown or white aeolian sands, dry colors of paleosols are usually light brown (7.5 YR 6/4), pink (7.5 YR 7/3, 7/4), pinkish white (7.5 YR 8/2), or reddish yellow (7.5 YR 6/6). A noticeable feature of almost all paleosols is that the degree of redness and the amount of silt and clay increase upward through the soil profiles. By greater "redness," it is meant that there is a shift from 10 YR hues in the aeolian sands to 7.5 YR hues in the

paleosols, with an accompanying increase in chromas. Unlike the aeolian units, paleosols, while sandy, contain substantial amounts of silt and clay and some exhibit weak to moderate development of subangular blocky structure. Based on field estimates, the content of fine silt and clay is on the order of ~10% in the lower parts of paleosols increasing to 30% or more in the upper parts of the paleosols. The paleosols have very gradual lower boundaries and sharp contacts with overlying aeolian sand units. When paleosol samples are examined under the microscope, silt- and clay-sized particles can be seen coating sand-sized carbonate skeletal and volcanic rock grains. Land snails (most commonly of the genus *Theba*) are abundant in the paleosols and are less common in the underlying aeolian sands. Also present in the paleosols are "ootecas," trace fossils of the Moroccan locust, *Dociostaurus maroccanus*, described in detail by Meco et al. (2011), and also discussed by Genise et al. (2013) and Roettig et al. (2017). Ootecas in these sections are typically ~2 cm long, ~1 cm in diameter, and composed of a sandy tubular structure bound together by silts and clays, with remarkable durability.

Part of our chronology for the Mala section utilizes Sr-isotope stratigraphy. A prerequisite to such an approach is good preservation of the skeletal fragments that make up the carbonate fraction. Results of XRD analyses indicate that although low-Mg calcite is present, there is also abundant high-Mg calcite and aragonite. This mineralogy indicates that little, if any, diagenetic or pedogenic alteration of the host carbonate skeletal fragments has taken place.

Results of Sr isotopic analyses at Mala indicate that most or all aeolian sediment packages could be of Pleistocene age (Table 1). Averages of 5–7 analyses of each sediment package yield Sr isotope age estimates ranging from ~850 ka to ~550 ka, but results did not yield (and were not expected to yield) an entirely consistent suite of ages with stratigraphic position. The oldest two units sampled, at ~1450 cm and ~1338 cm (from section 3) gave apparent average ages of ~790 ka to ~730 ka and ~850 ka to ~800 ka, respectively. The next two youngest units analyzed, at ~1160 cm and ~920 cm, have apparent ages of ~690 ka to ~620 ka, and ~810 ka to ~750 ka respectively. The aeolian unit at ~695 cm gave much older average ages of ~850 ka to ~750 ka, but the youngest unit sampled, at ~150 cm, gave average ages of ~630 ka to ~550 ka.

It is recognized that the ages of oldest grains in each of these units could be considerably older than these estimates and the ages of the youngest grains in each unit could be considerably younger. Nevertheless, in all cases the time of actual aeolian sediment emplacement must be no older than the youngest grains and also must be younger than the average Sr isotope age for that respective unit. The results, while uncertain for ages of specific units, do indicate that the entire sequence is likely of Pleistocene age, and some units could certainly date back to the early or middle Pleistocene. Given the ranges of measurements from each depth interval, the instrumental analytical uncertainties for each analysis, and the uncertainties in the Sr isotope calibration curve (Howarth and McArthur, 1997; McArthur et al., 2001, 2020), all that can be said with certainty is that the aeolian sediment packages likely have an average age range that could span an interval from ~950 ka to ~400 ka.

On the south side of the quarry at Mala, a basaltic lava flow crops out in part of the exposure (easternmost part at N29°05.614'; W13°27.723′). This flow is found at a depth of 3.5 m below the quarry access road and extends laterally for ~11–12 m to the west, grading from basalt to lapilli, before pinching out (Fig. 8). It is the same lava flow studied by Von Suchodoletz et al. (2012) discussed earlier. It is difficult to determine with certainty where this lava fits stratigraphically with the main sections we studied on the north side of the quarry, as the lava is not exposed there. Using soil morphology, careful leveling, GPS methods, and lateral tracing to the extent possible, our best estimate is that the paleosol that immediately overlies the lava on the south side of the quarry corresponds to paleosol P5 on the north side of the quarry (Figs. 7 and 8).

We collected a sample of this lava for $^{40}Ar/^{39}Ar$ dating to compare with the age estimate given by Von Suchodoletz et al. (2012). The basalt from Mala yielded a flat age spectrum over the initial 63.7% of the gas released (Table 2). The remaining steps gave an increase in apparent age from 240 ka to 870 ka. A weighted mean age of 220 ± 20 ka is calculated from the flat initial 63.7% of the age spectra. The radiogenic yields range from 0.6% to 16.3%. Inverse isochron analysis of steps A-K (see Table 2) reveals points that cluster near the y axis and an isochron age that agrees within error to the age calculated from the age spectra, 170 ± 90 ka, and a $^{40}Ar/^{36}Ar$ intercept that agrees within error to the atmospheric intercept 305 ± 11. The isochron age agrees with the red TL age, although the plateau age is somewhat older. Nevertheless, all the age estimates are in broad agreement that the lava is on the order of ~200 ka.

Land snails were collected from the uppermost paleosols at Mala for radiocarbon dating. Here it is important to note that as is the case with paleosols in many locations (Birkeland, 1999; Schaetzl and Thompson, 2015), our inference is that soil A horizons, if they were once present, could have been eroded prior to emplacement of the overlying aeolian sands. Thus, for radiocarbon dating, snails sampled are mostly from the remnant clay-rich (possibly argillic) soil B horizons. These included snails from the B horizon of the modern soil (MS on Fig. 7), as well as snails from the B horizons of paleosols P1, P2, P3, P4, and P5. We also collected and analyzed three dead, but modern specimens of *Theba geminata* for radiocarbon dating from the island of Fuerteventura, at the quarry at La Rosa Negra, described in more detail below. As pointed out by Pigati et al. (2010), each genus of land snail will incorporate a certain amount of "dead" carbon (i.e., carbon with little or no ^{14}C), giving an apparent nonzero age, even for a living specimen. The three specimens of modern (dead) *T. geminata* gave apparent radiocarbon ages of 1665 ± 30 ^{14}C yr, 1925 ± 25 ^{14}C yr, and 2385 ± 30 ^{14}C yr (Table 3). Thus, all fossil land snails can be considered to have "real" ages that are ~1700–2400 ^{14}C yr younger than their apparent reported ages.

At Mala, snails from the B horizons of the modern soil and the uppermost part of paleosol P1 gave middle Holocene, calibrated radiocarbon ages of ~6.7 ka and ~7.4 ka, respectively. All other *Theba* snails analyzed, from the lower B horizon of paleosol P1 and the B horizons of paleosols P2, P3, P4, and P5 gave significantly older ages, ranging from ~43.4 ka (calibrated, from P1) to ~45.5 ka (calibrated, from P5). With one exception (the upper B horizon of paleosol P3), all these snails yielded apparently finite ages, but we regard all of them as minimum-limiting ages. Apparent ages that are at the practical limit of the radiocarbon dating technique may be older, because very small amounts of modern carbon contamination can yield apparently finite ages in a material that is beyond the limit of radiocarbon dating (Pigati et al., 2007). Thus, paleosols P1 and P2 are very likely older than ~43 ka to ~50 ka, and paleosols P3, P4, and P5 are all likely older than ~50 ka (Table 3).

Although there are substantial uncertainties in all three methods of geochronology employed here, it is possible to put some broad limits on the timing of aeolian sand deposition and paleosol formation at Mala. Collectively, the entire sequence is of Quaternary age. The Sr isotope values of carbonate particles in the section indicate that the aeolian sands are likely ~950 ka to ~400 ka. The carbonate particles in these units could be composed of grains with a range of ages (for example, older Pliocene grains mixed with middle or late Quaternary grains). Aeolian units high in the section have grains with average ages that differ only slightly than the

Table 1
Strontium isotope values and age estimates (from McArthur et al., 2020, LOWESS version 6) for aeolian sands at the Mala section, Lanzarote.

Sample #	Depth (cm)	$^{87}Sr/^{86}Sr$	+/−	% error	$^{87}Sr/^{86}Sr$ age	lower limit	upper limit	
SP - 406	150	**0.709154**	0.000004	0.0006				
		0.709157	0.000010	0.0014				
		0.709162	0.000004	0.0006				
		0.709157	0.000011	0.0016				
		0.709158	0.000009	0.0012				
		0.709158	0.000008	0.0011				
		0.709156	0.000004	0.0006				
SP - 406 avg		**0.709157**	**0.000002**	**0.0003**	**0.60 Ma**	0.55 Ma	0.63 Ma	n = 7
SP - 434	695	**0.709142**	0.000019	0.0027				
		0.709150	0.000009	0.0012				
		0.709151	0.000009	0.0012				
		0.709145	0.000008	0.0011				
		0.709143	0.000007	0.0009				
		0.709151	0.000006	0.0008				
SP - 434 avg		**0.709147**	**0.000004**	**0.0006**	**0.80 Ma**	0.75 Ma	0.85 Ma	n = 6
SP - 445	860	**0.709149**	0.000004	0.0006				
		0.709161	0.000006	0.0008				
		0.709163	0.000009	0.0013				
		0.709148	0.000010	0.0013				
		0.709142	0.000010	0.0014				
SP - 445 avg		**0.709153**	**0.000010**	**0.0014**	**0.66 Ma**	0.62 Ma	0.69 Ma	n = 5
SP - 448	920	**0.709146**	0.000007	0.0009				
		0.709151	0.000006	0.0008				
		0.709144	0.000006	0.0008				
		0.709145	0.000008	0.0011				
		0.709152	0.000007	0.0009				
		0.709149	0.000008	0.0011				
SP - 448 avg		**0.709148**	**0.000004**	**0.0005**	**0.78 Ma**	0.75 Ma	0.81 Ma	n = 6
SP - 460	1160	**0.709151**	0.000009	0.0013				
		0.709149	0.000013	0.0018				
		0.709152	0.000007	0.0010				
		0.709147	0.000003	0.0005				
		0.709157	0.000005	0.0008				
		0.709154	0.000005	0.0008				
		0.709153	0.000008	0.0012				
SP **- 460 avg**		**0.709153**	**0.000006**	**0.0008**	**0.66 Ma**	0.62 Ma	0.69 Ma	n = 7
SP - 470	1338	**0.709152**	0.000008	0.0011				
		0.709151	0.000010	0.0014				
		0.709140	0.000010	0.0014				
		0.709142	0.000006	0.0008				
		0.709145	0.000007	0.0010				
SP - 470 avg		**0.709146**	**0.000006**	**0.0009**	**0.83 Ma**	0.80 Ma	0.85 Ma	n = 5
SP - 476	1450	**0.709160**	0.000008	0.0011				
		0.709143	0.000025	0.0035				
		0.709149	0.000008	0.0011				
		0.709142	0.000011	0.0015				
		0.709150	0.000005	0.0008				
		0.709147	0.000006	0.0009				
SP - 476 avg		**0.709149**	**0.000006**	**0.0008**	**0.76 Ma**	0.73 Ma	0.79 Ma	n = 6

lower units, indicating a substantial amount of reworked aeolian sediment with successive periods of deposition. If we are correct in our correlation of the basaltic lava on the south side of the quarry with sediment underlying P5, then the lower ~1000 cm of sediment is older than ~200 ka and younger than ~400 ka to ~950 ka. Because snails at ~70 cm depth (in paleosol P1) and all older snails are likely beyond the range of radiocarbon dating, this implies that the sequence of aeolian sediments and paleosols between the upper part of P1 (70 cm) and P5 (~580 cm) all date from between ~43 ka and ~200 ka. The thin modern soil, its parent aeolian sand parent material, and the upper part of paleosol P1 date to the Holocene.

4.1.2. *La Rosa Negra quarry, Fuerteventura*

The aeolian sediments exposed at La Rosa Negra (Figs. 6 and 10) appear to be part of a stabilized sand ramp, or climbing dune, that covers the lower flanks of a volcanic edifice called Montána de la Costilla, which is composed of Miocene basalt (Fig. 9). In the quarry, more than 800 cm of section are exposed, consisting of more than 6 aeolian-colluvial units, each capped by a paleosol or (for the youngest unit) the modern soil. Although the dominant sediments are aeolian sands, a distinctive feature of the deposits here, which distinguishes them from Mala, is the presence of gravel layers, of local alluvial or colluvial origin, within what are otherwise very

Table 2
$^{40}Ar/^{39}Ar$ analytical data for lava flow from Mala quarry.

ID	Power	$^{40}Ar/^{39}AR$	$^{37}Ar/^{39}Ar$	$^{36}Ar/^{39}Ar$	$^{39}Ar_k$	K/Ca	$^{40}Ar^*$	^{39}Ar	Age	± 1 σ
	(Watts)			(x 10^{-3})	(x 10^{-15} mol)		(%)	(%)	(Ma)	(Ma)
A	0.8	392.1	0.6263	1318.6	0.4	0.81	0.6	1.7	0.37	0.31
B	1.3	46.51	0.6817	152.3	2	0.75	3.4	10.6	0.23	0.04
C	1.6	17.46	0.8098	54.75	2.6	0.63	7.7	22.2	0.2	0.02
D	2	14.68	0.8347	45.47	3.5	0.61	8.9	37.8	0.2	0.01
E	2.5	14.7	0.885	44.85	3.4	0.58	10.3	53.1	0.23	0.01
F	3	16	1.009	49.09	2.4	0.51	9.8	63.7	0.24	0.01
X G	4	26.07	1.433	82.26	2.5	0.36	7.2	75	0.28	0.02
X H	5	29.37	3.298	91.79	2.3	0.15	8.6	85.1	0.38	0.02
X I	7	29.16	8.131	90.85	2.2	0.063	10.2	95.1	0.45	0.02
X J	10	35.84	13.66	116.7	0.8	0.037	6.8	98.4	0.37	0.04
X K	15	35.29	16.19	104.4	0.4	0.032	16.3	100	0.87	0.06
Integrated age ± 2σ			n = 11		22.5	0.2	K_2O = 1.05%		0.28	0.02
Plateau ± 2σ	**steps A-F**		**n = 6**	**MSWD = 1.35**	**14.3**	**0.61 ± 0.23**		**63.7**	**0.22**	**0.02**
Isochron ± 2σ	steps A-K		n = 11	MSWD = 22.26		$^{40}Ar/^{36}Ar$ = 305 ± 11			0.17	0.09

Analyses by Lisa Peters, New Mexico Geochronology Research Laboratory, Socorro, New Mexico, U.S.A.

well sorted sands.

Similar to Mala, however, the aeolian sediments at La Rosa Negra exhibit a dominance of sand-sized particles composed of marine invertebrate skeletal debris, including fragments of bivalves, gastropods, echinoids, and other taxa. Dry colors of aeolian sands range from light brown (7.5 YR 6/4) to very pale brown (10 YR 8/3, 8/4). Also similar to Mala, paleosols can be distinguished by soil color, texture, and structure. Paleosols at La Rosa Negra are pink (7.5 YR 7/3, 7/4, 8/3, dry) or less commonly reddish yellow (7.5 YR 6/6, dry). Field estimates of the content of fine silt and clay are on the order of ~5–10% (lower parts of some paleosols) increasing to 25–30% (upper parts of other paleosols). At La Rosa Negra, the presence of fossils and trace fossils is less diagnostic of paleosols, as ootecas and land snails are found in both aeolian sands and paleosols.

Our only geochronology for the section at La Rosa Negra is based on radiocarbon ages of *Theba* land snails (Table 3). The results are similar to those at Mala. The upper meter, including the modern soil, its aeolian sand parent material, and the youngest paleosol and its parent material are all Holocene, with calibrated ages ranging from ~5.9 ka (parent material of the uppermost paleosol) to ~3.7–3.8 ka (parent material of the modern soil). One much older age of ~33.5 ka, at a depth of 20–32 cm, is considered to be a reworked, older fossil snail. All other analyses, down to ~650 cm, gave calibrated ages of ~44 ka to ~45 ka, all of which are considered to be minimum ages.

4.2. Mineralogy and geochemistry

4.2.1. Mala quarry, Lanzarote

The bulk mineralogy of aeolian sediments at Mala, obtained by XRD, confirms field observations that marine-derived skeletal grains are one of the major constituents. Aeolian sediments at all depths are dominated by carbonate minerals, aragonite, high-Mg calcite, and low-Mg calcite. Geochemistry is consistent with these observations. Total $CaCO_3$ contents range from 76 to 95%, and most samples are 85–95% (Fig. 11). CaO content (measured by XRF) parallels the plot for $CaCO_3$ content and has values that are slightly less than half those of total $CaCO_3$ content, indicating that almost all of the CaO is found in carbonate minerals. A correlation/regression analysis of $CaCO_3$ content vs. CaO content yields a regression equation of Y = 0.465X + 5.711, where "Y" = CaO content and "X" = $CaCO_3$ content, with a coefficient of determination of r^2 = 0.99. Marine invertebrate organisms composed of either aragonite or high-Mg calcite typically have relatively high concentrations of Sr, a trace element that is found in solution in seawater and which substitutes for Ca in aragonite or calcite structures. Concentrations of Sr in many marine bivalves, gastropods, echinoids, and foraminifera, the major constituents of the aeolian sands at Mala, range from ~1300 to ~3700 ppm (Milliman, 1974). At Mala, aeolian sands have Sr concentrations (measured by INAA) that range from ~2000 to ~2500 ppm, with a depth function that closely parallels those of $CaCO_3$ and CaO concentrations (Fig. 11). These concentrations, within the range of modern marine taxa, indicate that, consistent with the mineralogy dominated by aragonite and high-Mg calcite, the aeolian sands at Mala have undergone little or no dissolution after deposition.

The second source of aeolian sediments at Mala is minerals derived from the local volcanic rocks of Lanzarote. Plagioclase was detected in almost all of the aeolian sediments and is reflected in bulk Na_2O contents of 0.45–0.8%. Most aeolian sediments analyzed also have pyroxenes and possibly hematite, both reflected in concentrations of Fe_2O_3 of 0.35–2.8%. Interestingly, quartz was detected in almost half of the aeolian sediments analyzed, similar to what was observed in the composition of beach sands collected at Arrieta, described earlier.

Paleosols at Mala host a bulk mineralogy with both similarities to and differences from the aeolian sediments. Aragonite and calcite are found in all horizons of all paleosols, indicating that no soil horizon has been totally leached of carbonate minerals. Total $CaCO_3$, CaO, and Sr concentrations are, however, lower in all of the paleosol horizons, compared to their host aeolian sediments (Fig. 11). Further, concentrations of carbonates are lowest in the upper horizons of each paleosol and highest in lower horizons of each paleosol. Plagioclase, pyroxenes, and hematite were detected in almost all soil horizons as well. Quartz, present in only small amounts and found in only some aeolian sediments, is prominent in all horizons of all paleosols. Peak-height ratios of quartz to aragonite and quartz to low-Mg calcite parallel SiO_2 abundances and are highest in upper paleosol horizons (Fig. 12).

Two major elements, Al_2O_3 and Fe_2O_3, show measurable amounts at all depths, but have substantial enrichments within the paleosols (Fig. 13). The concentrations of these elements likely reflect, at least in part, the presence of locally derived volcanic minerals, such as plagioclase, pyroxenes, magnetite, and hematite, as noted above. However, the enrichment of Al_2O_3 and Fe_2O_3 in the paleosols compared to aeolian sediments could also be due to the presence of phyllosilicate clay minerals that commonly host, and

Table 3
Radiocarbon ages of land snails from Lanzarote and Fuerteventura, Canary Islands, Spain.

USGS Laboratory #	CAMS Laboratory #	Field #	Location	Latitude	Longitude	Elevation at top (m)	Depth in section (cm)	Species	$\delta^{13}C$ (per mil)	^{14}C age (yr)	Uncertainty 1s	Calibrated age (yr)	Uncertainty 2s	P
WW-8516	Na	SP-213-m-1	La Rosa Negra, Fuerteventura	N28°41.343′	W13°58.239′	54	Modern	*Theba geminata*	−5.02	1925	25			
WW-8517	Na	SP-213-m-2	La Rosa Negra, Fuerteventura	N28°41.343′	W13°58.239′	54	Modern	*Theba geminata*	−2.55	2385	30			
WW-8518	Na	SP-213-m-3	La Rosa Negra, Fuerteventura	N28°41.343′	W13°58.239′	54	Modern	*Theba geminata*	−7.32	1665	30			
Na	CAMS-177646	SP-213-a	La Rosa Negra, Fuerteventura	N28°41.343′	W13°58.239′	54	0–20	*Theba geminata*	−1.5	2280	60	**2310**	**160**	0.99
Na	CAMS-177647	SP-214-a	La Rosa Negra, Fuerteventura	N28°41.343′	W13°58.239′	54	20–32	*Theba geminata*	−6.2	29,080	120	**33,530**	**310**	1.00
Na	CAMS-177648	SP-215-a	La Rosa Negra, Fuerteventura	N28°41.343′	W13°58.239′	54	32–46	*Theba geminata*	1.2	3445	30	**3670**	**60**	0.75
										3445	30	**3760**	**20**	0.10
										3445	30	**3810**	**20**	0.15
Na	CAMS-177649	SP-217-a	La Rosa Negra, Fuerteventura	N28°41.343′	W13°58.239′	54	46–76	*Theba geminata*	2.3	2880	25	**2970**	**90**	1.00
Na	CAMS-177650	SP-218-a	La Rosa Negra, Fuerteventura	N28°41.343′	W13°58.239′	54	76–90	*Theba geminata*	−6.6	5130	30	**5950**	**50**	1.00
Na	CAMS-177651	SP-227-a	La Rosa Negra, Fuerteventura	N28°41.343′	W13°58.239′	54	275–290	*Theba geminata*	−5.0	39,760	370	**43,520**	**680**	1.00
na	CAMS-177652	SP-231-a	La Rosa Negra, Fuerteventura	N28°41.343′	W13°58.239′	54	400–420	*Theba pisana*	−0.6	40,360	420	**43,950**	**790**	1.00
na	CAMS-177653	SP-233-a	La Rosa Negra, Fuerteventura	N28°41.343′	W13°58.239′	54	440–460	*Theba geminata*	−0.5	41,270	440	**44,720**	**830**	1.00
na	CAMS-177654	SP-241-a	La Rosa Negra, Fuerteventura	N28°41.343′	W13°58.239′	54	605–613	*Theba impugnata*	−2.2	39,070	830	**45,240**	**3420**	1.00
na	CAMS-177655	SP-244-a	La Rosa Negra, Fuerteventura	N28°41.343′	W13°58.239′	54	642–660	*Theba geminata*	−6.3	40,290	390	**43,920**	**740**	1.00
WW-10729	CAMS-172939	SP-398	Mala, Lanzarote	N29°05.66′	W13°27.70′	53	0–20	*Theba geminata*	−4.2	5865	25	**6690**	**50**	1.00
WW-10730	CAMS-172940	SP-401	Mala, Lanzarote	N29°05.66′	W13°27.70′	53	40–60	*Theba impugnata*	−6.2	6480	25	**7360**	**40**	0.63
										6480	25	**7420**	**10**	0.37
WW-10731	CAMS-172941	SP-402	Mala, Lanzarote	N29°05.66′	W13°27.70′	53	60–80	*Theba impugnata*	−3.4	39,310	670	**43,230**	**1050**	1.00
WW-10732	CAMS-172942	SP-403	Mala, Lanzarote	N29°05.66′	W13°27.70′	53	80–100	*Theba geminata*	−3.6	39,690	710	**43,510**	**1120**	1.00
WW-10733	CAMS-172943	SP-404	Mala, Lanzarote	N29°05.66′	W13°27.70′	53	100–120	*Theba impugnata*	−0.4	39,010	640	**42,990**	**990**	1.00
WW-10734	CAMS-172944	SP-408	Mala, Lanzarote	N29°05.66′	W13°27.70′	53	180–200	*Theba geminata*	−1.1	39,920	720	**43,680**	**1150**	1.00
WW-10735	CAMS-172945	SP-409	Mala, Lanzarote	N29°05.66′	W13°27.70′	53	200–220	*Theba geminata*	−3.9	42,170	950	**45,560**	**1840**	1.00
WW-10736	CAMS-172947	SP-410	Mala, Lanzarote	N29°05.66′	W13°27.70′	53	220–240	*Theba geminata*	−4.5	45,900	1500	**exceeds calibration range**	na	
WW-10737	CAMS-172948	SP-413	Mala, Lanzarote	N29°05.66′	W13°27.70′	53	270–300	*Theba impugnata*	−4.8	51,100	2900	**exceeds calibration range**	na	
WW-10738	CAMS-172949	SP-416	Mala, Lanzarote	N29°05.66′	W13°27.70′	53	340–360	*Theba impugnata*	−4.4	45,600	1500	**exceeds calibration range**	na	
WW-10739	CAMS-172950	SP-422	Mala, Lanzarote	N29°05.65′	W13°27.71′	53	450–470	*Theba geminata*	−4.4	45,000	1400	**exceeds calibration range**	na	
WW-10740	CAMS-172951	SP-428	Mala, Lanzarote	N29°05.65′	W13°27.71′	53	570–590	*Theba geminata*	−5.3	42,130	950	**45,510**	**1830**	1.00

• Samples with a "WW" prefix were processed at the ^{14}C laboratory of the U.S. Geological Survey in Reston, Virginia; all others were processed at the Center for Accelerator Mass Spectrometry (CAMS), Lawrence Livermore National Laboratory, Livermore, California.
• ^{14}C ages for all samples were determined at the Center for Accelerator Mass Spectrometry (CAMS), Lawrence Livermore National Laboratory, Livermore, California.
• The quoted age is in radiocarbon years (BP) using the Libby half life of 5568 years.
• The WW number is the identification assigned to a sample by the USGS ^{14}C laboratory.

are enriched in, Al and Fe, including smectite, mica, and kaolinite (Weaver and Pollard, 1973). Taylor and McLennan (1985) and McLennan (1989) point out that the REE are concentrated within clay minerals. A plot of total REE content parallels those of Al_2O_3 and Fe_2O_3, indicating common host minerals for all these elements that are likely dominated by clay minerals.

We undertook XRD studies of clay (<2 μm) separates in order to determine if enrichments in Al_2O_3, Fe_2O_3, and REE in the paleosols are due to the presence of clay minerals that host these elements. Results indicate that paleosols exposed in the Mala quarry host three main phyllosilicate clay minerals. All paleosols studied contain smectite, mica, and kaolinite (Fig. 14). Glycolated samples show a smectite peak at ~5.2°, mica peaks at 8.9°, 17.7°, and 26.6°, and kaolinite peaks at 12.5°and 24.9°. Retention of peaks at 6.2° and 18.8° on heat-treated samples indicates the possible presence of some chlorite. It is likely that the paleosols also contain some clay-sized quartz, but the main quartz peak at 26.6° is coincident with the mica (003) peak. In mica-bearing sediments with an absence of quartz, the 8.9° (001) mica peak is typically higher than the 26.6° (003) mica peak (Moore and Reynolds, 1997). The heights of the peaks at 26.6° in many of the paleosols studied here are higher than the 8.9° mica peaks. Thus, this higher 26.6° peak in the paleosols indicates the presence of some clay-sized quartz as well as mica. Overall, the results indicate that much of the enrichment of Al_2O_3, Fe_2O_3, and REE in the paleosols is likely due to the presence of smectite, mica, kaolinite, and possibly some chlorite.

Identification of mica in the paleosols is also supported by other major element (K) and trace element (Ba, Rb, Cs) concentrations. Although many of the volcanic rocks on Lanzarote are alkali basalts, concentrations of K_2O are typically low (Fuster et al., 1968a). In contrast, concentrations of K_2O are high in the paleosols and low in the aeolian sands in the section at Mala (Fig. 15). Thus, the depth function for this element closely parallels those of Al_2O_3, Fe_2O_3, and SiO_2 (Figs. 12 and 13), supporting an inference of mica as the main carrier of K_2O in the paleosols. Three trace elements, Ba, Rb, and Cs, commonly substitute for K in K-bearing minerals, such as micas and K-feldspar. Depth functions of these three trace elements closely parallel that of K_2O, providing additional geochemical support for the presence of mica in the clay fraction of the paleosols.

4.2.2. La Rosa Negra quarry, Fuerteventura

Much of what is observed in the way of mineralogy and complementary geochemistry in the aeolian sediments and paleosols at Mala on Lanzarote is also seen in the composition of sediments and paleosols at La Rosa Negra on Fuerteventura. Bulk mineralogy in aeolian sediments at La Rosa Negra shows a somewhat simpler composition, however. Sediments at all depths host aragonite, calcite, and plagioclase. A minority of aeolian sediments have detectable quartz but only a few depth intervals contain pyroxenes that are detectable by XRD. The high aragonite and calcite content of the aeolian sediments is apparent in the high $CaCO_3$, CaO, and Sr concentrations (Fig. 16). Similar to the section at Mala, a correlation/regression analysis of $CaCO_3$ content vs. CaO content yields a regression equation of $Y = 0.439X + 8.460$, where "Y" = CaO content and "X" = $CaCO_3$ content, with a coefficient of determination of $r^2 = 0.97$.

Paleosols at La Rosa Negra host calcite, aragonite, plagioclase, and quartz, also similar to what is observed at Mala. Paleosols at La Rosa Negra show higher SiO_2 contents and higher quartz-to-aragonite and quartz-to-calcite values (Fig. 17). Higher concentrations of Al_2O_3, Fe_2O_3, and REE are also found in the paleosols at La Rosa Negra (Fig. 18). We hypothesize that here too, higher concentrations of Al_2O_3, Fe_2O_3, and REE in the paleosols are due to enrichment of phyllosilicate clay minerals.

Unfortunately, clay separates from paleosols at La Rosa Negra did not yield particularly satisfactory mounts, despite multiple attempts using a variety of methods. Nevertheless, resultant XRD patterns do confirm that smectite, mica, kaolinite, and possibly clay-sized quartz are the dominant minerals in the <2 μm fraction, similar to Mala (Fig. 19). Thus, the presence of smectite, mica, and kaolinite likely explain much of the enrichment in Al_2O_3, Fe_2O_3, and REE that is apparent in the paleosols. One difference we note here is that smectite appears to be in lower abundance compared to mica and kaolinite, in contrast to paleosols at Mala, but this could in part be a function of the poor mounting and subsequent higher background.

As with the section at Mala on Lanzarote, the presence of mica in the paleosols at La Rosa Negra is supported by concentrations of K_2O, Ba, Rb, and Cs. All four elements show relatively high values in the paleosols with lower values in the aeolian sands (Fig. 20). The depth functions for K_2O, Ba, Rb, and Cs at La Rosa Negra parallel those for Al_2O_3, Fe_2O_3, and SiO_2 (Figs. 17 and 18), supporting an inference of mica as the main carrier of K_2O in the clay fraction of the paleosols.

4.3. Major element geochemistry as a source-area indicator

Major element geochemistry can provide insights for dust source areas provided that such regions have a variable enough mineralogy that major elements can distinguish them. Chiapello et al. (1997) pioneered this approach for identifying specific dust source regions in Africa. These investigators showed that dust derived from the northwestern Sahara (PSA 2 in Fig. 3), the south-central Sahara (northern part of PSA 3 in Fig. 3), and the Sahel (southern parts of PSA 2 and PSA 3) have distinctive Si/Al, Ca/Al, Fe/Ca, and K/Ca values. Higher Fe/Ca values in Sahel dusts are related to higher abundances of pedogenic Fe-oxyhydroxides, particularly hematite, in lower-latitude soils, whereas higher K/Ca values in Saharan dusts are linked to higher mica and lower kaolinite contents in desert soils farther north. Mineralogical data for dust from these three regions reported by Caquineau et al. (1998) are consistent with this geochemistry. Unfortunately, because of the high carbonate mineral content of the host aeolian sediments on the Canary Islands, use of Fe/Ca and K/Ca values is precluded, as the high Ca contents from the marine carbonate particles dominate these elemental ratios, even in the paleosols. Dr. Isabelle Chiapello (LOA, CNRS/Université Lille) and Dr. Gilles Bergametti kindly supplied Si, Al, and K data from a study of theirs (Chiapello et al., 1997), conducted at the Laboratoire Interuniversitaire des Systèmes Atmosphériques. Using these data, Si/Al and K/Al ranges can be plotted for the three dust source regions in Africa identified by Chiapello et al. (1997), along with the ranges of these values for local basalts on Lanzarote and Fuerteventura.

Results indicate that although the south-central Sahara region has considerable overlap with the geochemical fields defined by the northwestern Sahara and the Sahel, there is a general trend of a north-to-south decrease in K/Al values, consistent with the decreasing mica (rich in K) abundances and increasing kaolinite (rich in Al) abundances going north to south (Fig. 21). As shown previously by Chiapello et al. (1997), there is also an overall north-to-south decrease in Si/Al values, which is consistent with the change in mineralogy, because micas have higher Si/Al values than kaolinite (Weaver and Pollard, 1973). Further, all three dust source areas have geochemical fields distinctive from those defined by the local Canary Islands basalts (Fig. 21).

Later studies by Formenti et al. (2008, 2011, 2014), Klaver et al. (2011), McConnell et al. (2008), and Scheuvens et al. (2013) also have demonstrated that dust collected from many potential source areas in Africa have distinctive major element ratios, again using Si/Al and K/Al. Using data reported in or compiled by Formenti et al.

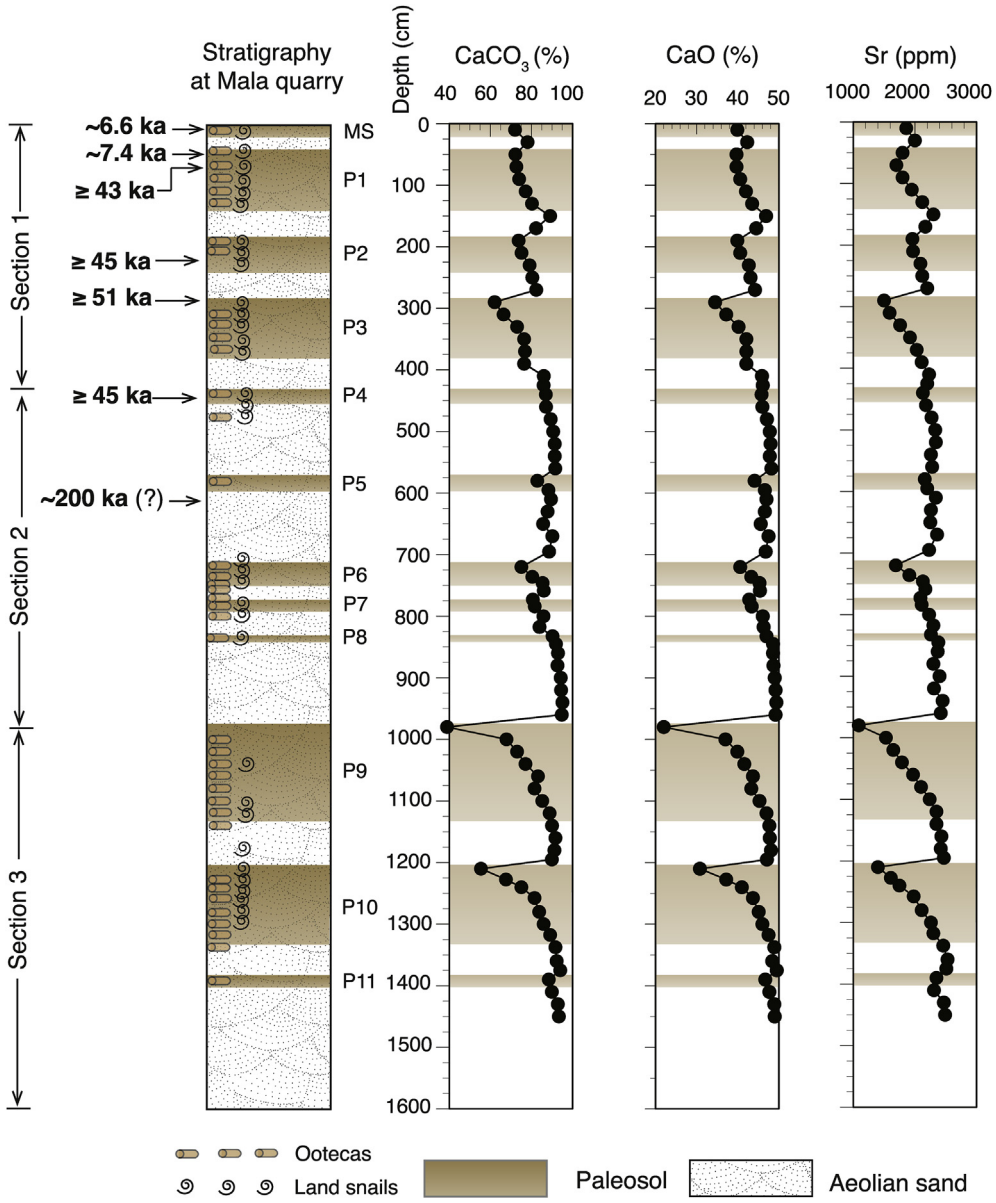

Fig. 11. Composite stratigraphy of aeolian sands (stipple pattern) and paleosols (brown shades) at Mala (see Figs. 7 and 8 for location of sections 1, 2, and 3) and concentrations of $CaCO_3$, CaO, and Sr as a function of depth. Numbers to the left of the section are age estimates in thousands of years (ka), based on radiocarbon, $^{40}Ar/^{39}Ar$, and Sr isotope methods (Tables 1–3). (For interpretation of the references to color in this figure legend, the reader is referred to the Web version of this article.)

(2008, 2011, 2014), Klaver et al. (2011), and McConnell et al. (2008), we plotted Si/Al vs. K/Al values for airborne dust samples collected above various PSAs across Africa, as well as the composition of local Canary Islands basalt (Fig. 22). We also plotted Si/Al vs. K/Al values for Bodélé Depression sediments (within PSA 5), collected on the ground (Fig. 3), reported by Abouchami et al. (2013). Results again show distinctive geochemical signatures for a number of the PSAs (Fig. 22). Western Saharan sources (PSA 2 and PSA 3) have the highest K/Al values, consistent with the data of Chiapello et al. (1997). Dust samples from PSA 5, where the Bodélé Depression is situated, have a geochemical signature that is distinctive from that of PSA 2 and PSA 3, as do dust samples derived from a combination of PSA 5 and PSA 6. Ground-collected Bodélé Depression samples have lower K/Al values and a wider range of Si/Al values than airborne dust samples from PSA 5. The higher range of Si/Al values in ground-collected Bodélé Depression samples could be due to the presence of high-silica diatomite as well as quartz (Abouchami et al., 2013; Formenti et al., 2014). Nevertheless, it would appear that much of the dust from PSA 5 does not include material from the Bodélé Depression, at least at the time of sampling represented by the materials plotted in Fig. 22.

Sahel dust collected over Niger overlaps much of the compositional field of dust from PSA 5 and PSA 6, areas which include parts of the Sahel. The field defined by these Sahel dust samples have considerable overlap with the geochemical field for Sahel dust from the Chiapello et al. (1997) data (compare Fig. 21 with Fig. 22b,d, but note horizontal scale change). As noted above, the generally lower K/Al values in both Sahel dust and Bodélé Depression sediments likely reflect relatively lower amounts of mica (rich in K) and higher amounts of kaolinite (rich in Al). The geochemical fields from most of the PSAs do not overlap substantially with the field defined by local basalt on Lanzarote (Fig. 22a and b) and have only partial

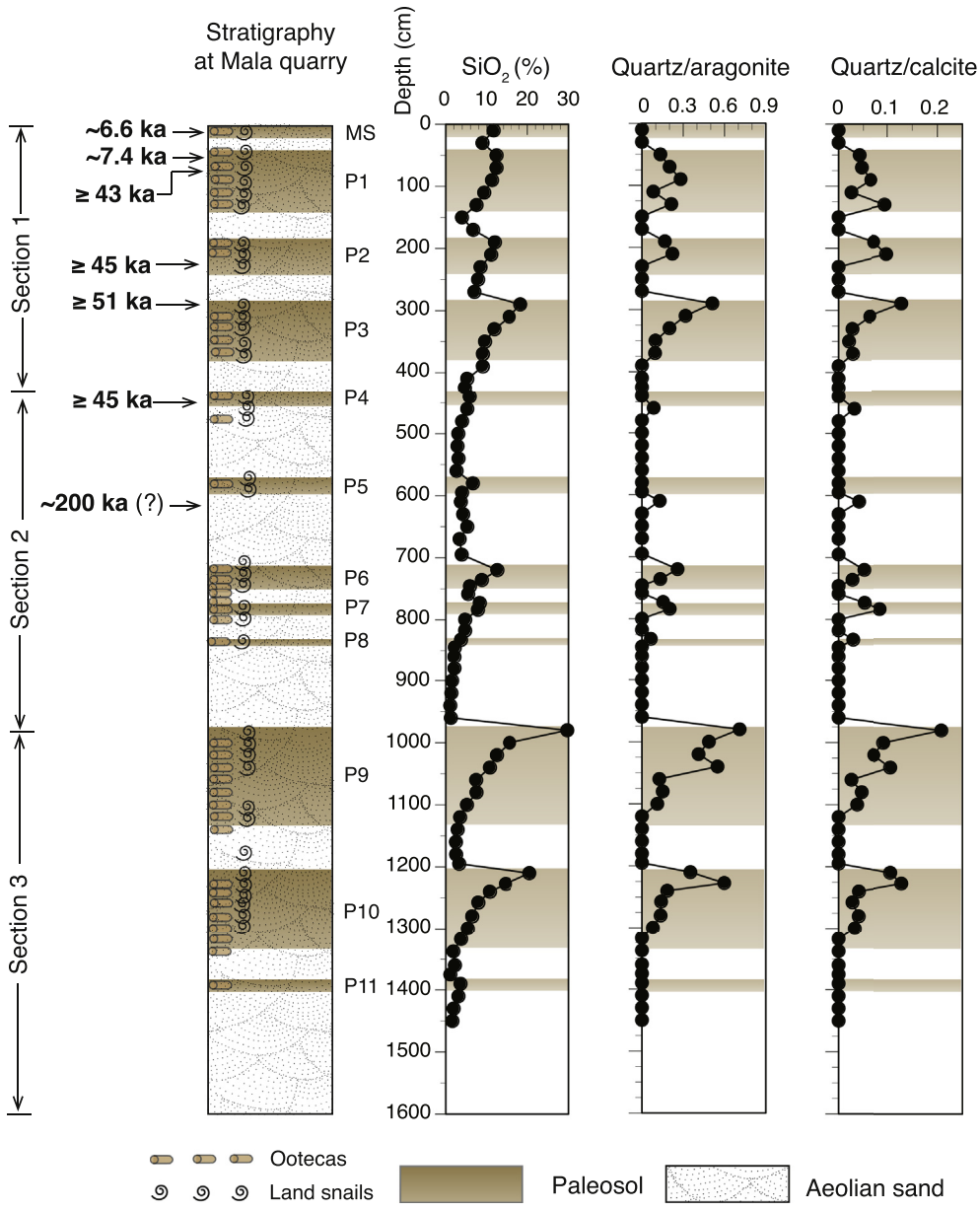

Fig. 12. Composite stratigraphy of aeolian sands (stipple pattern) and paleosols (brown shades) at Mala (see Figs. 7 and 8 for location of sections 1, 2, and 3), concentrations of SiO_2, quartz-aragonite bulk XRD peak-height values, and quartz-calcite bulk XRD peak-height values as a function of depth. (For interpretation of the references to color in this figure legend, the reader is referred to the Web version of this article.)

overlap with the field defined by local basalt on Fuerteventura (Fig. 22c and d). Interestingly, the Bodélé Depression has the only substantial overlap in composition with basalts on both islands.

With compilations of Si/Al vs. K/Al compositional fields for various PSAs defined, it is possible to make comparisons with aeolian sands and paleosols from the Canary Islands. Aeolian sands from the Mala and Rosa Negra sections plot within or just above the fields for the local volcanic rocks and have substantially lower K/Al values than all of the paleosols (Fig. 21). Using either set of PSA compositional fields, paleosols from both the Mala and Rosa Negra sections plot between the dust PSAs and volcanic fields (Figs. 21 and 22). K/Al values in paleosols from both sections are similar to those for dust samples from PSA 2, PSA 3, and PSA 4, and have partial overlap with K/Al values for Sahel dust collected over Niger (Figs. 21 and 22). The compositions of the paleosols differ from those of most of the PSAs with higher Si/Al values, which overlap those of the island basalts. K/Al values in the paleosols all plot above the field for the Bodélé Depression but have overlap with Si/Al values from this dust source.

4.4. Trace element geochemistry as a source-area indicator

Trace element abundances can be powerful tools for determining soil or sediment provenance. Muhs et al. (2010) used Sc-Th-Ta, Cr-Hf-Th, La_N/Yb_N-Eu/Eu*, and Gd_N/Yb_N-Eu/Eu* successfully to distinguish late Quaternary basalt on Lanzarote from African dust in a study of the origin of modern soils on that island. Such an approach was also used by Huerta et al. (2015) in determining the influence of African dust in the origin of calcretes on Lanzarote and Fuerteventura. Here, we use similar geochemical indicators to evaluate the relative contributions of local volcanic rocks and African dust to the paleosols at Mala and La Rosa Negra.

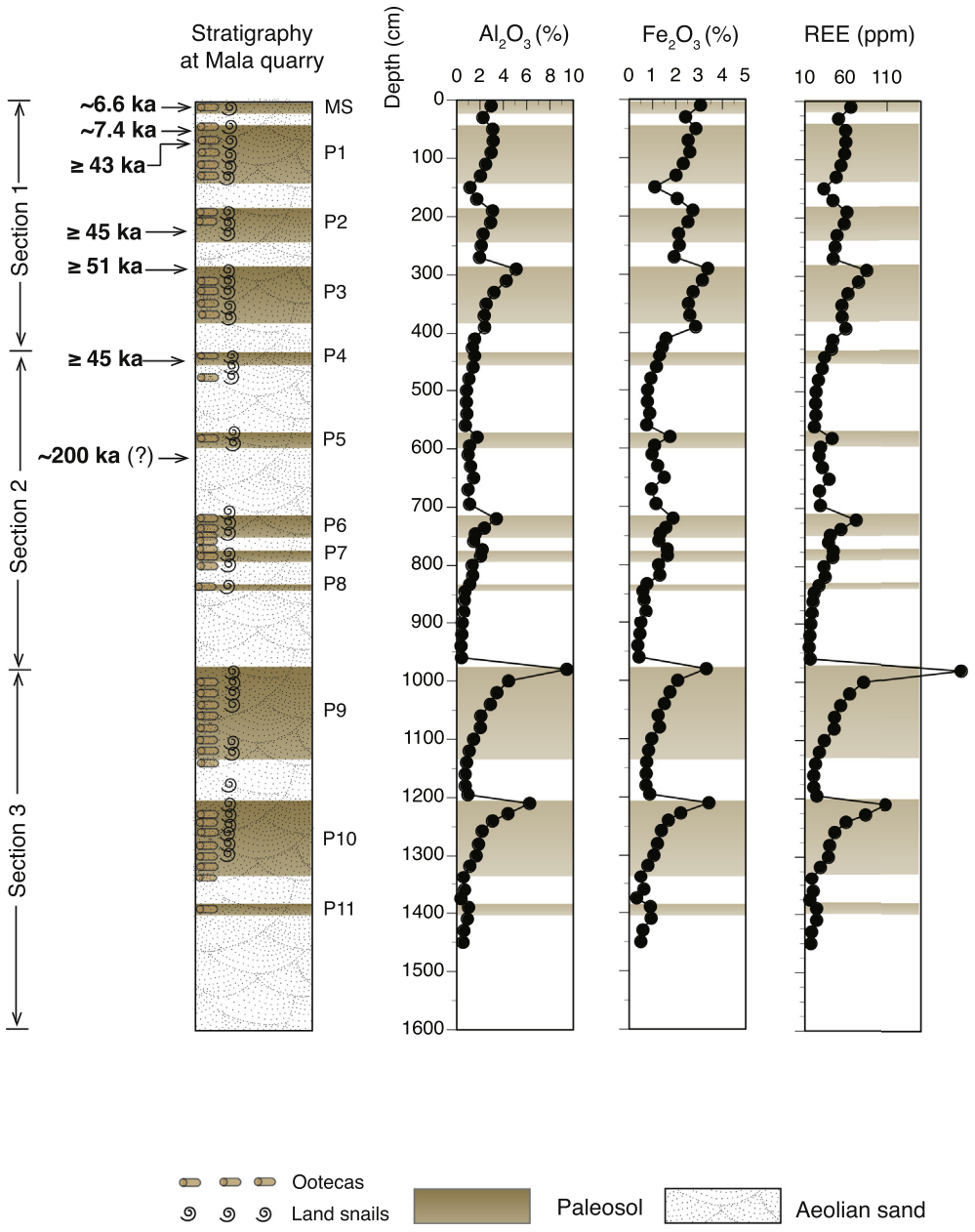

Fig. 13. Composite stratigraphy of aeolian sands (stipple pattern) and paleosols (brown shades) at Mala (see Figs. 7 and 8 for location of sections 1, 2, and 3), and concentrations of Al_2O_3, Fe_2O_3, and total REE (La, Ce, Nd, Sm, Eu, Gd, Tb, Ho, Yb, Lu) as a function of depth. (For interpretation of the references to color in this figure legend, the reader is referred to the Web version of this article.)

Unfortunately, there are few REE or other trace element data available for most of the PSAs shown in Fig. 3. An exception is the Bodélé Depression, for which Abouchami et al. (2013) reported some REE data for a few samples.

For the Mala quarry, we compared the trace element composition of the paleosols with (1) the volcanic rocks collected at Famara and Arrieta and (2) African dust collected on Barbados (Muhs et al., 2007, 2010) and Bermuda (Muhs et al., 2012). Dust collected on Barbados and Bermuda is derived from a mix of source regions in Africa, as shown by the HYSPLIT-derived back trajectories (Fig. 4). On a Sc-Th-Ta x 10 ternary plot, African dust and local volcanic rocks have distinctive compositions (Fig. 23a). With one exception (for which we have no explanation), paleosols from Mala have Sc-Th-Ta x 10 compositions that fall between the geochemical fields defined by the two sources. On a Cr/10-Hf-Th ternary plot, local volcanic rocks from Lanzarote and dust collected on Barbados and Bermuda show an even greater compositional difference (Fig. 23b). As expected, based on known compositions of average ocean crust and average upper continental crust (Taylor and McLennan, 1985), volcanic rocks from Lanzarote are enriched in Cr and depleted in Hf and Th, similar to oceanic crust. African dust collected on Barbados and Bermuda, in contrast, falls near the center of the plot, showing relative enrichments in Hf and Th and depletions in Cr, similar to average upper continental crust. Some paleosols from Mala fall within the range for local volcanic rocks whereas most plot between the fields defined by the two sources (Fig. 23b), consistent with the Sc-Th-Ta x 10 plot (Fig. 23a).

In an extensive review, McLennan (1989) noted that the REE can be sensitive indicators of sediment provenance. Here, a comparison is made between the REE composition of the paleosols with the

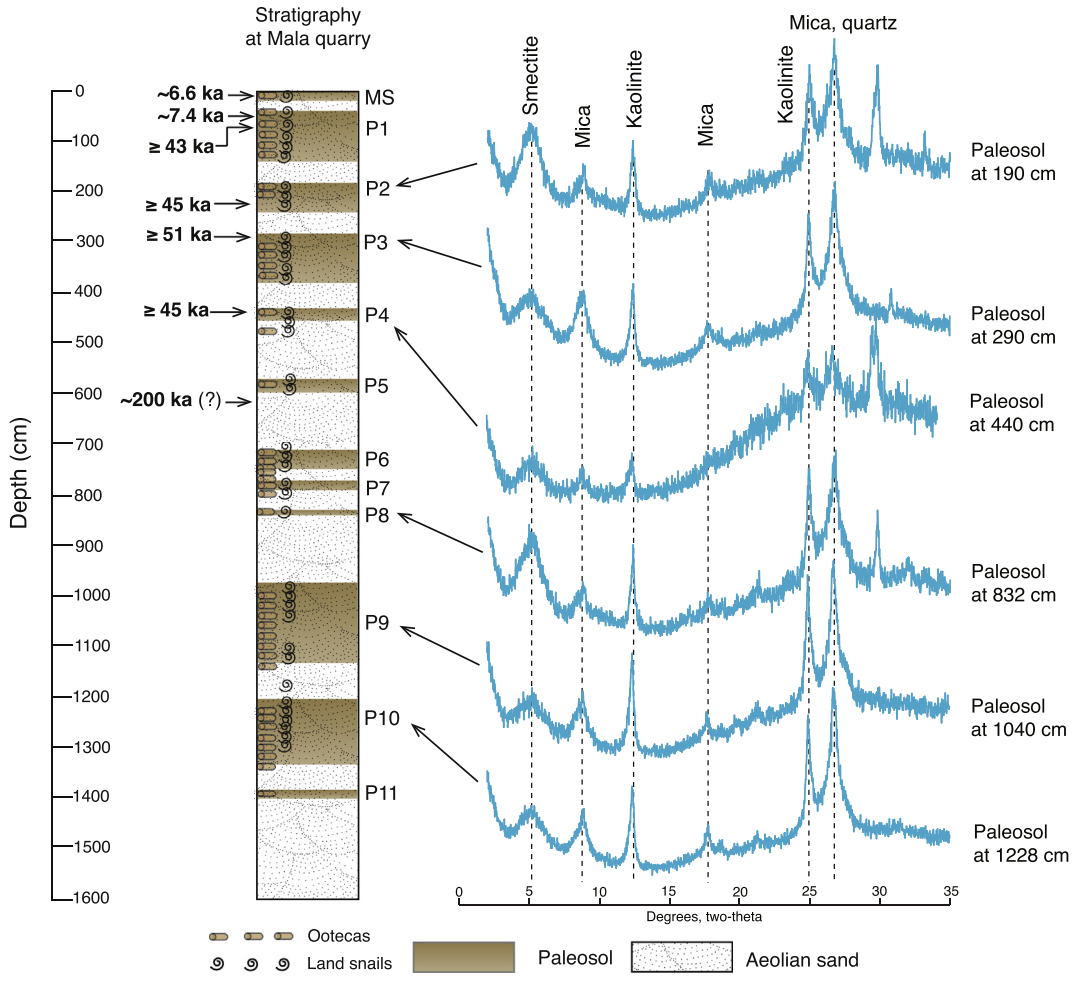

Fig. 14. Composite stratigraphy of aeolian sands (stipple pattern) and paleosols (brown shades) at Mala and X-ray diffraction patterns of glycolated clay samples from paleosol separates, showing mineralogy of the <2 μm fraction. (For interpretation of the references to color in this figure legend, the reader is referred to the Web version of this article.)

volcanic rocks collected at Famara and Arrieta and African dust collected on Barbados (Muhs et al., 2007, 2010) and Bermuda (Muhs et al., 2012), plus dust trap REE data from Barbados reported by Pourmand et al. (2014) and REE data derived from shipboard dust collections made in the Atlantic Ocean (Van der Does et al., 2018). We also make comparisons with REE data from the small collection from the Bodélé Depression reported by Abouchami et al. (2013).

As with the other trace elements, local volcanic rocks on Lanzarote and African dust display geochemical fields that are distinct from one another for overall REE composition (Fig. 23c and d). The REE element data from Pourmand et al. (2014) overlap the field defined by mixed-source African dust reported by Muhs et al. (2007, 2010). Bodélé Depression sediments overlap much of this field as well. Thus, REE do not allow for a clear distinction between Sahara and Sahel sources of dust. For both La_N/Yb_N vs. Eu/Eu* and Gd_N/Yb_N vs. Eu/Eu*, some paleosols from Mala have compositions that are intermediate between those of African dust and local volcanic rocks, but most either fall directly within the fields for African dust or very close to them.

For comparison of paleosol compositions in the quarry section at La Rosa Negra on Fuerteventura, we use the same data sources for African dust as described above, along with published data for local bedrock on this island. Although rocks on the island of Fuerteventura are dominated by basalt, a substantial area of what has been called the Basal Complex, as noted earlier, has a considerably more diverse composition (Fuster et al., 1968b; Carracedo and Troll, 2016). The composition of the Basal Complex is important because this formation is rich in quartz (Carracedo and Troll, 2016, p. 535–537). Thus, in comparing the trace element composition of paleosols at La Rosa Negra with potential source sediments, it is necessary to consider the compositions of both the extensive Tertiary and Quaternary basalts and the diverse lithologies of the Basal Complex. For the Tertiary and Quaternary basalts, we use trace element data reported by Schneider et al. (2014) and Tornare et al. (2016). For rocks of the Basal Complex, we use trace element data reported by Holloway and Bussy (2008) and Allibon et al. (2011).

Tertiary and Quaternary basalts from Fuerteventura have a broadly similar composition to basalts from Lanzarote but with a greater range of variability (Fig. 24). Nevertheless, these rocks have a range of compositions that are distinct from African dust for all trace elements considered. Similar to the paleosols at Mala on Lanzarote, on a Sc-Th-Ta x 10 plot, paleosols from La Rosa Negra plot between the compositional fields for volcanic rocks and African dust (Fig. 24a). On a Cr/10-Hf-Th plot, some paleosols plot within the field for local volcanic rocks, but most plot between this field and the fields for African dust (Fig. 24b). On the two REE plots, La_N/Yb_N vs. Eu/Eu* and Gd_N/Yb_N vs. Eu/Eu*, results for La Rosa Negra are also similar to those for the paleosols at Mala: some samples plot between the volcanic rock and African dust fields (but closer to African dust), whereas others fall directly in the fields defined by

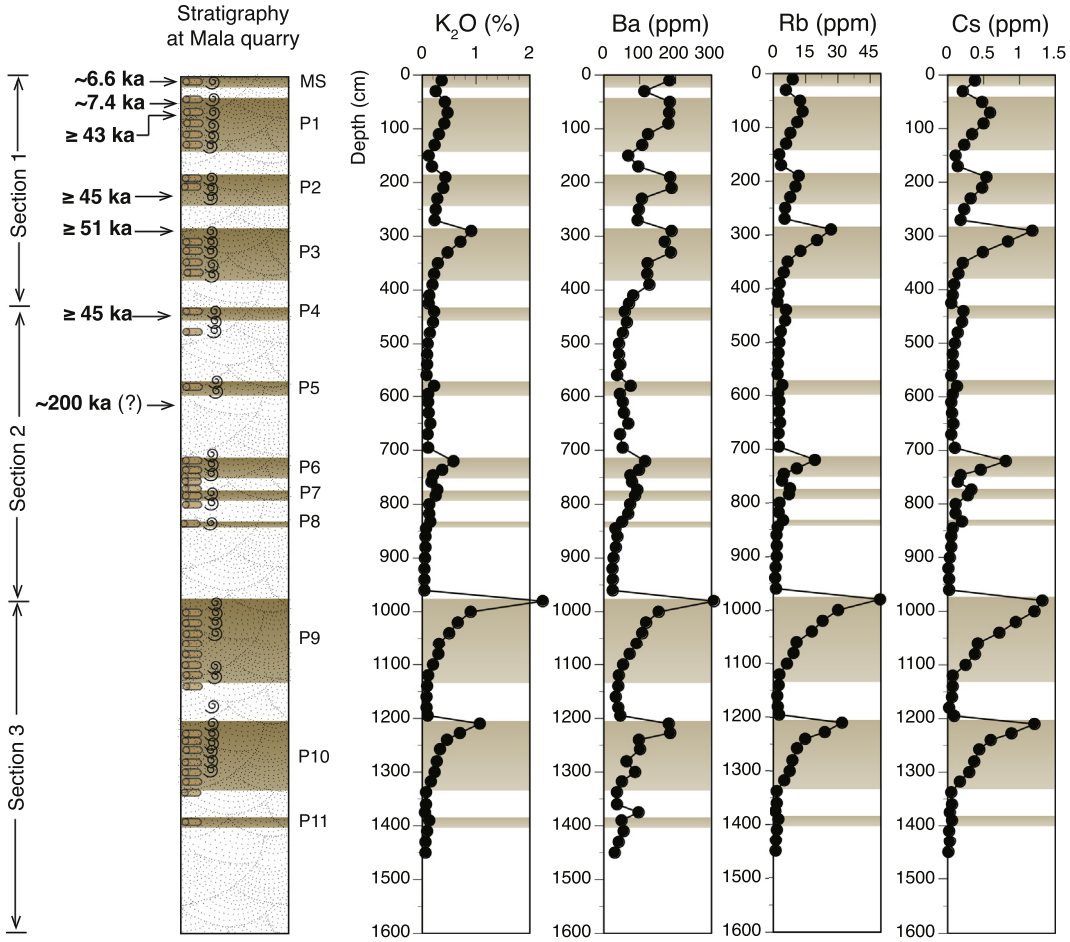

Fig. 15. Composite stratigraphy of aeolian sands (stipple pattern) and paleosols (brown shades) at Mala (see Figs. 7 and 8 for location of sections 1, 2, and 3), and concentrations of K_2O, Ba, Rb, and Cs as a function of depth. (For interpretation of the references to color in this figure legend, the reader is referred to the Web version of this article.)

African dust (Fig. 24c and d).

For all trace elements considered, Basal Complex rocks and intrusions also show a wide range of variability (Fig. 25). Nevertheless, the trace element compositions of these rocks do not overlap with those of African dust, which allows us to assess the importance of these rocks to the composition of paleosols at La Rosa Negra. Results are similar to those in the comparison with the Tertiary and Quaternary volcanic rocks: paleosols from La Rosa Negra plot between the fields for Basal Complex rocks and African dust for Sc-Th-Ta x 10 (Fig. 25a). For Cr/10-Hf-Th, some paleosols overlap the Basal Complex field, but most plot between this field and that of African dust (Fig. 25b). On the REE plots, some paleosols fall between the two fields, but others plot squarely within the African dust fields (Fig. 25c and d). None of the paleosols plot within the fields defined for Basal Complex rocks.

5. Discussion

5.1. Alternation of carbonate aeolian sand deposition and paleosol formation

The age estimates of carbonate aeolian sands and paleosols reported here are evaluated in the context of how we envision the timing of these deposits with respect to sea level history. Rognon and Coudé-Gaussen (1987) were among the first investigators to note that Fuerteventura hosts aeolian sands, locally derived from marine bioclasts, and alternating with paleosols. These workers presented a model showing that when aeolian sand sedimentation ceased, African dust was trapped on the island by what had become a denser vegetation cover. Rognon et al. (1989) expanded this concept to point out that aeolian sands, recognized to be detrital bioclastic sediments, were derived from the insular shelves (Fig. 10). These investigators proposed that at the close of the last glacial period, vegetation cover increased, aeolian sand was stabilized, and the enhanced vegetation cover allowed trapping of African dust. This sequence of events was developed further by Coudé-Gaussen and Rognon (1993) and Rognon and Coudé-Gaussen (1996a, 1996b).

Specifically for the sections at Mala and La Rosa Negra, Bouab and Lamothe (1997), Damnati (1997), Meco et al. (1997), and Damnati et al. (2005) provided descriptions of the stratigraphy and also proposed that these sequences represented alternations of insular-shelf-derived bioclastic sands and paleosols derived from African dust. Importantly, Meco et al. (1997) also pointed out that at least some of the bioclastic sands within the Quaternary aeolian sequences had their origins from bioclastic materials of Tertiary age, found on the insular shelves. Indeed, later Meco et al. (2006, 2008) described a model of aeolian sand formation for Fuerteventura during the Pliocene, where marine skeletal sands accumulated on the insular shelf (Fig. 10) during a relatively high stand or stands of sea. Remnants of carbonate-rich aeolian sands dating to the Pliocene have been reported by Lomoschitz et al. (2016) on the northern part of Lanzarote. During a subsequent sea-level regression (or regressions), these newly exposed sands were entrained by

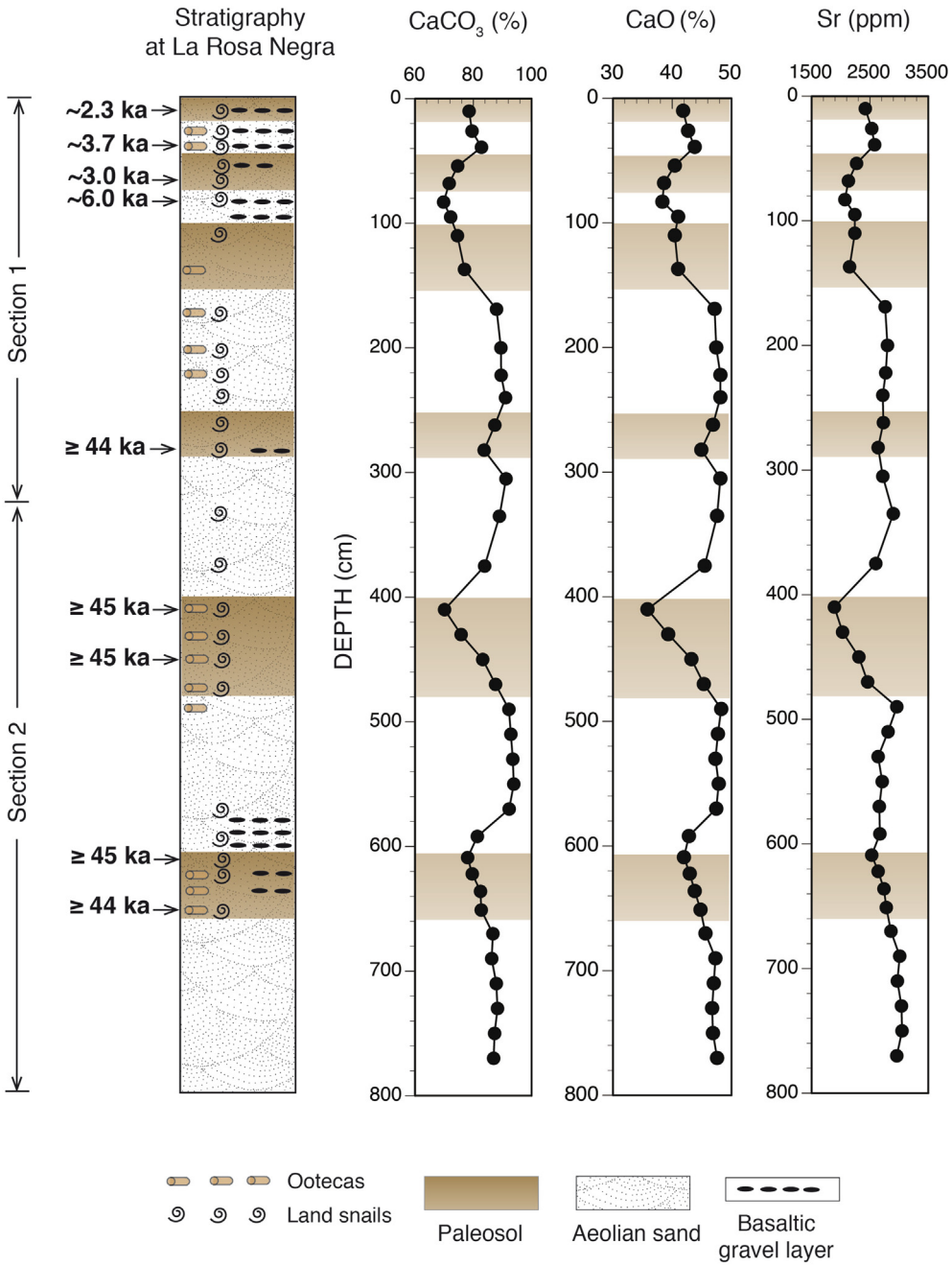

Fig. 16. Composite stratigraphy of aeolian sands (stipple pattern) and paleosols (brown shades) at La Rosa Negra (see Fig. 9 for location of sections 1 and 2) and concentrations of $CaCO_3$, CaO, and Sr as a function of depth. Numbers at left are age estimates in thousands of years (ka), based on radiocarbon ages (Table 1). (For interpretation of the references to color in this figure legend, the reader is referred to the Web version of this article.)

wind and deposited on Fuerteventura.

Following from Meco et al. (2006, 2008), Meco et al. (2011) inferred that a similar sequence of events took place in the Quaternary on Lanzarote, using the Mala section as a case study. The cycle they envisioned was one of deposition of carbonate aeolian sands derived from bioclastic insular shelf sands during a glacial period of lowered sea level, formation of a paleosol during an succeeding interglacial period, derived at least in part from African dust, and burial of this paleosol during a succeeding glacial period, when sea level falls again. Meco et al. (2011) used the Mala section, with the same stratigraphy as presented here, to show that this cycle could have occurred numerous times during the Quaternary. Criado et al. (2012) also noted the alternations of bioclast-derived aeolian sands alternating with African-dust-derived paleosols. For the sequence at Mala described by Meco et al. (2011), Muhs (2013) proposed that the African-dust-derived paleosols appear to have grown upwards by dust accretion, rather than having developed downward, by weathering of the carbonate aeolian sands. In a similar line of reasoning, Roettig et al. (2019) also thought that little or no chemical weathering was responsible for the paleosols and that African dust deposition was the dominant process of soil formation. Further, these investigators added detail to the models described above by pointing out that the optimal time for aeolian sand accumulation would be at the start of glacial-period sea-level

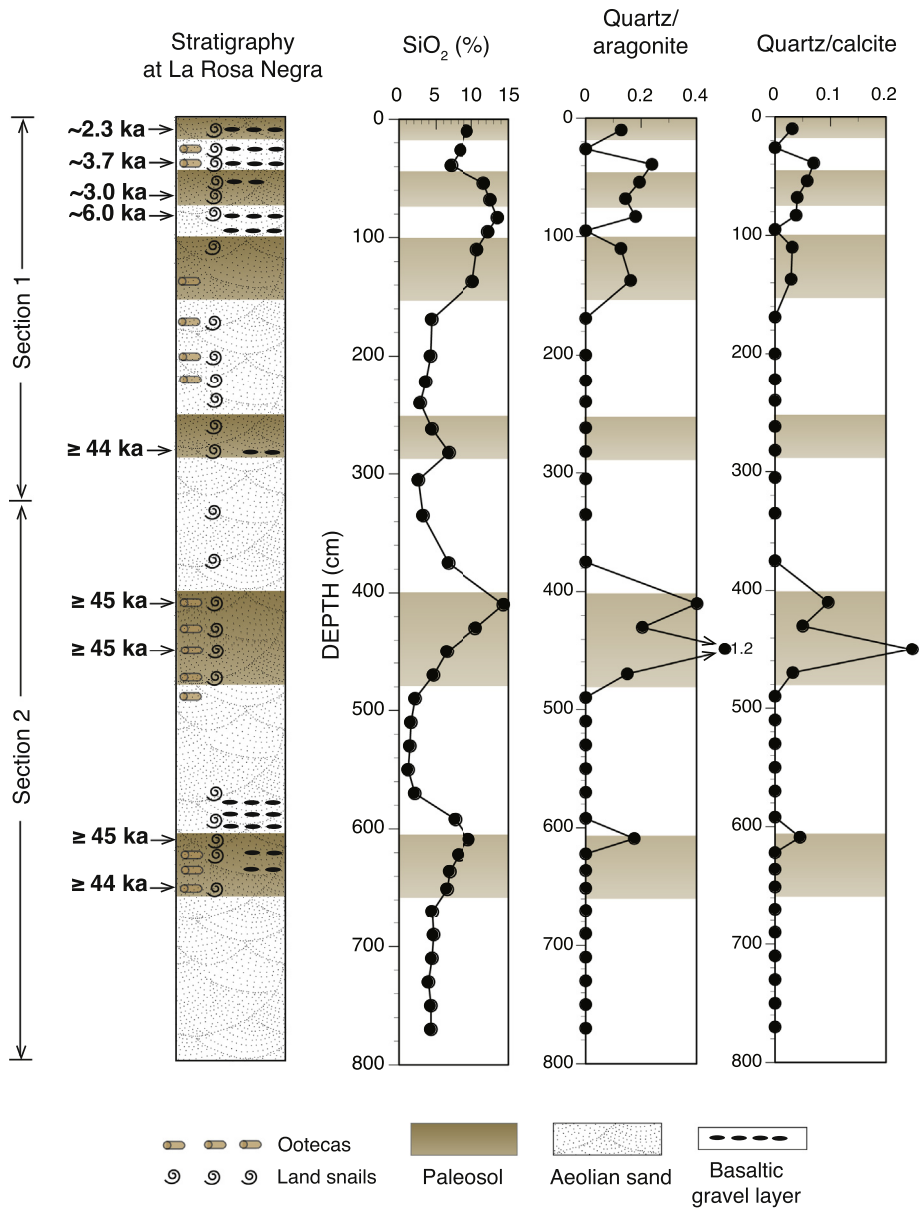

Fig. 17. Composite stratigraphy of aeolian sands (stipple pattern) and paleosols (brown shades) at La Rosa Negra (see Fig. 9 for location of sections 1 and 2) concentrations of SiO_2, quartz-aragonite bulk XRD peak-height values, and quartz-calcite bulk XRD peak-height values as a function of depth. (For interpretation of the references to color in this figure legend, the reader is referred to the Web version of this article.)

regressions, whereas times of surface stability would occur when sea-level transgressions occur, at the start of interglacial periods.

Here we evaluate the chronology reported in the present study in the context of the models of alternating periods of aeolian sand deposition and stability with paleosol formation. Noting the observations of Meco et al. (1997, 2006, 2008), it is expected that the Sr isotope compositions of aeolian sands will represent a mix of skeletal fragments of different ages, including carbonate grains inherited from sediments that may have formed as far back as the Tertiary. In the Quaternary, depending on carbonate production rates during each successive interglacial period when sediments are accumulating on the insular shelf, a wide variety of grain ages could also be expected. In addition, it is not expected that insular shelf sediments will be completely removed by aeolian transport during each glacial-regressive period of exposure. Hence, subsequent periods of aeolian transport will almost certainly include older skeletal grains as well as younger ones. If this reasoning is correct, then Sr-isotope age estimates of aggregates of skeletal grains should be regarded as maximum-limiting ages of aeolian packages only.

Given the high content of marine invertebrate carbonate skeletal grains in the aeolian sands, we infer that deposition of the host sediments likely took place primarily when sea level was low and insular shelves were exposed, in agreement with most previous workers cited above. On the island of Bermuda, in the western Atlantic, Rowe and Bristow (2015a, 2015b) pointed out that the optimal time of carbonate aeolian sand entrainment would have been during the transition between an interglacial high-sea stand and a glacial period, when sea level is beginning to regress and expose insular shelf sands. In agreement with this, on the California Channel Islands, Muhs et al. (2018) found that the most recent period of carbonate aeolian sand deposition began shortly before

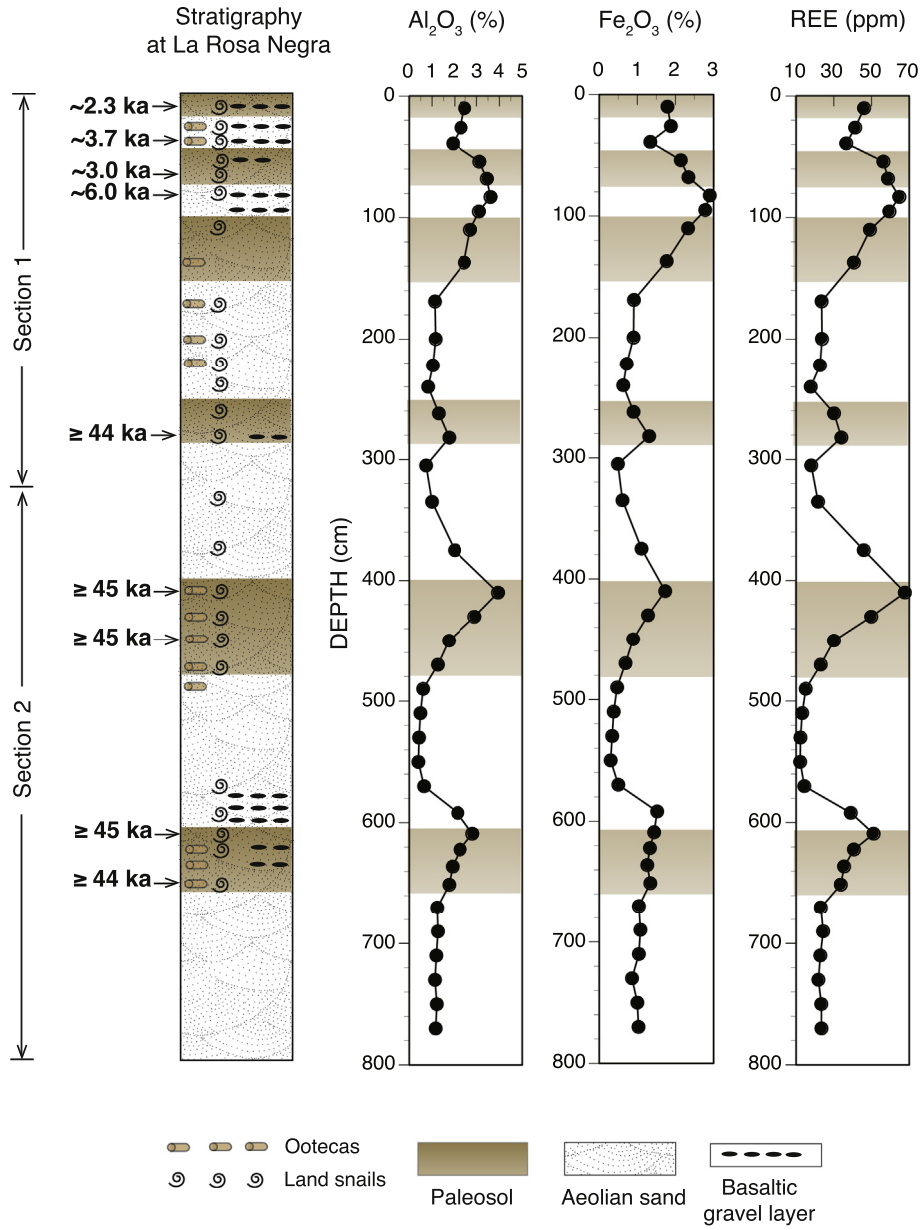

Fig. 18. Composite stratigraphy of aeolian sands (stipple pattern) and paleosols (brown shades) at La Rosa Negra (see Fig. 9 for location of sections 1 and 2) and concentrations of Al_2O_3, Fe_2O_3, and total REE (La, Ce, Nd, Sm, Eu, Gd, Tb, Ho, Yb, Lu) as a function of depth. (For interpretation of the references to color in this figure legend, the reader is referred to the Web version of this article.)

the end of the last high-sea stand of interglacial marine isotope stage [MIS] 5, at about 80 ka, and continued, episodically, through the last glacial-interstadial-glacial periods, MIS 4, 3, and 2. Working on Fuerteventura in the Canary Islands, Roettig et al. (2019, 2020) inferred a similar timing for carbonate aeolian sand entrainment, with aeolian sand entrainment beginning as sea level starts to fall (start of a glacial period) and stability beginning as sea level begins to rise (start of the next interglacial period).

Based on the Sr-isotope geochronology presented here, the Quaternary paleosol record on Lanzarote could conceivably span much of the past ~400 ka and possibly as much as the past ~950 ka, given the age uncertainties in the Sr isotope data presented here (Table 1). If our $^{40}Ar/^{39}Ar$ age (Table 2) is correct, then somewhat less than half of the section at Mala could represent the past ~200 ka, conceivably spanning the penultimate glacial period, MIS 6, as well as MIS 5, 4, and 3, and the Holocene (MIS 1). There does not appear to be a record of the last glacial period, MIS 2 at Mala, at least in the sections studied here.

Unfortunately, we have no Sr isotope or $^{40}Ar/^{39}Ar$ data for the aeolian sequence at La Rosa Negra. The upper meter or so of the section is Holocene (Table 3), but we regard all of the land snail radiocarbon ages below this depth as minima. Luminescence ages reported by Faust et al. (2015) and Roettig et al. (2019, 2020) show that elsewhere on Fuerteventura, there were several cycles of aeolian sand deposition alternating with times of paleosol formation during the past ~500 ka. Set in this context, the minimum-limiting radiocarbon ages presented here for La Rosa Negra could represent a wide range of age possibilities.

If the inferences made above about the optimal times of aeolian sand entrainment and deposition are correct, then the paleosols intercalated within the aeolian sands represent periods of relative landscape stability, most likely forming during the beginning and

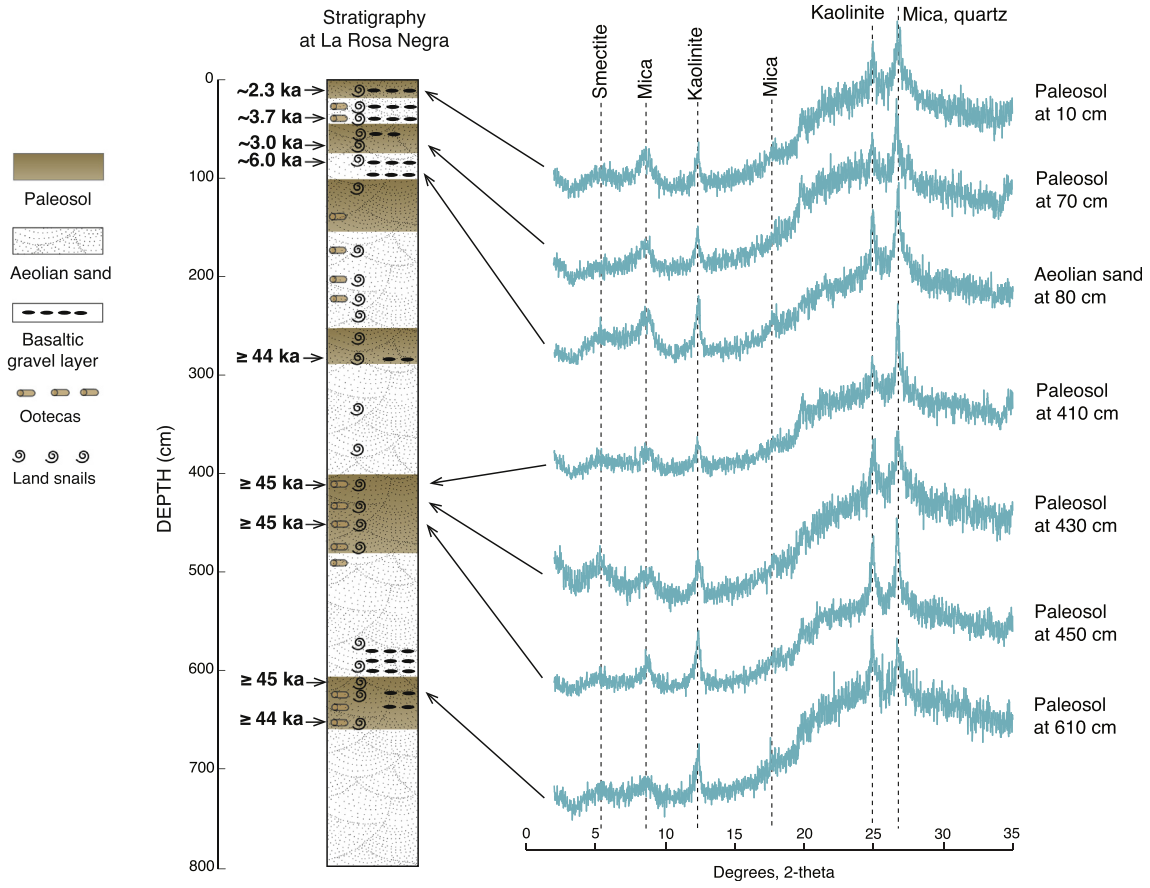

Fig. 19. Composite stratigraphy of aeolian sands (stipple pattern) and paleosols (brown shades) at La Rosa Negra (see Fig. 9 for location of sections 1 and 2) and X-ray diffraction patterns of glycolated clay samples from paleosol separates, showing mineralogy of the <2 μm fraction. (For interpretation of the references to color in this figure legend, the reader is referred to the Web version of this article.)

main parts of interglacial or interstadial periods, when offshore sand supplies were diminished and vegetation could colonize dunes or sand sheets. Under these conditions, pedogenesis, dominated by LRT dust accretion, could take place. On both Lanzarote and Fuerteventura, this inference is supported by the presence of modern soils dating to the Holocene (based on radiocarbon ages) and stratigraphically deeper soils having ages greater ~45 ka, preceding the last glacial period.

5.2. Mineralogy of aeolian sands and paleosols on the Canary Islands

Because the Canary Islands are composed dominantly of basalt, the presence of quartz in soils and sediments of these islands logically could be used to infer exotic, LRT mineral additions from Africa. As noted earlier, it has become a common practice, therefore, to assume that if quartz is present, there must have been externally derived, probably African dust additions to the soils or sediments under study. Furthermore, many studies have assumed that not only does quartz indicate an African origin, but the presence of this mineral indicates derivation specifically from the Sahara. We consider that the assumptions of quartz on the Canary Islands having an exclusively exotic origin, and strictly from the Sahara, are oversimplified views. Fuster et al. (1968a, 1968b), Carmona et al. (2009), and Carracedo and Troll (2016) have all pointed out that quartz, while rare on the eastern Canary Islands, can be found in rocks of these islands, particularly in the Basal Complex of Fuerteventura (see Fig. 8.4 of Carracedo and Troll [2016]), but also in the igneous rock suites. In our own studies, reported here, we found quartz in modern beach sands on the northeastern coast of Lanzarote, near Arrieta (Fig. 5). The same concern applies to an interpretation of mica as an exotic mineral. Although mica is rare in Canary Islands rocks, biotite has been reported in several rock types on Fuerteventura (Fuster et al., 1968b). Quartz and mica are the two most important minerals in LRT African dust (see Glaccum and Prospero, 1980). Thus, while there is no question that the presence of these minerals in Canary Islands paleosols *permits* an interpretation of an African dust origin, in principle, both minerals could be locally derived.

The results presented here show that aeolian sands in the sections of both islands have likely experienced little or no chemical weathering, either diagenetically, such as during slow aeolian sand accretion (syndepositional weathering), or pedogenically, during periods of stability. All aeolian sand units and even all the paleosols contain aragonite and high-Mg calcite, two minerals that are very susceptible to loss by dissolution in a subaerial environment. Geochemical data are consistent with the mineralogy. Total $CaCO_3$ and CaO contents are high throughout the sections (Figs. 11 and 16). Furthermore, Sr, which substitutes for Ca in aragonite and high-Mg calcite skeletons of marine organisms, has concentrations that differ little or not at all from what is found in the skeletons of modern marine organisms. Because the Sr concentrations, measured in bulk carbonate sands, are similar to those of modern marine organisms, this implies little or no loss of Sr from what was originally in the bioclastic sands. From this and the survival of the metastable minerals aragonite and high-Mg calcite, even during

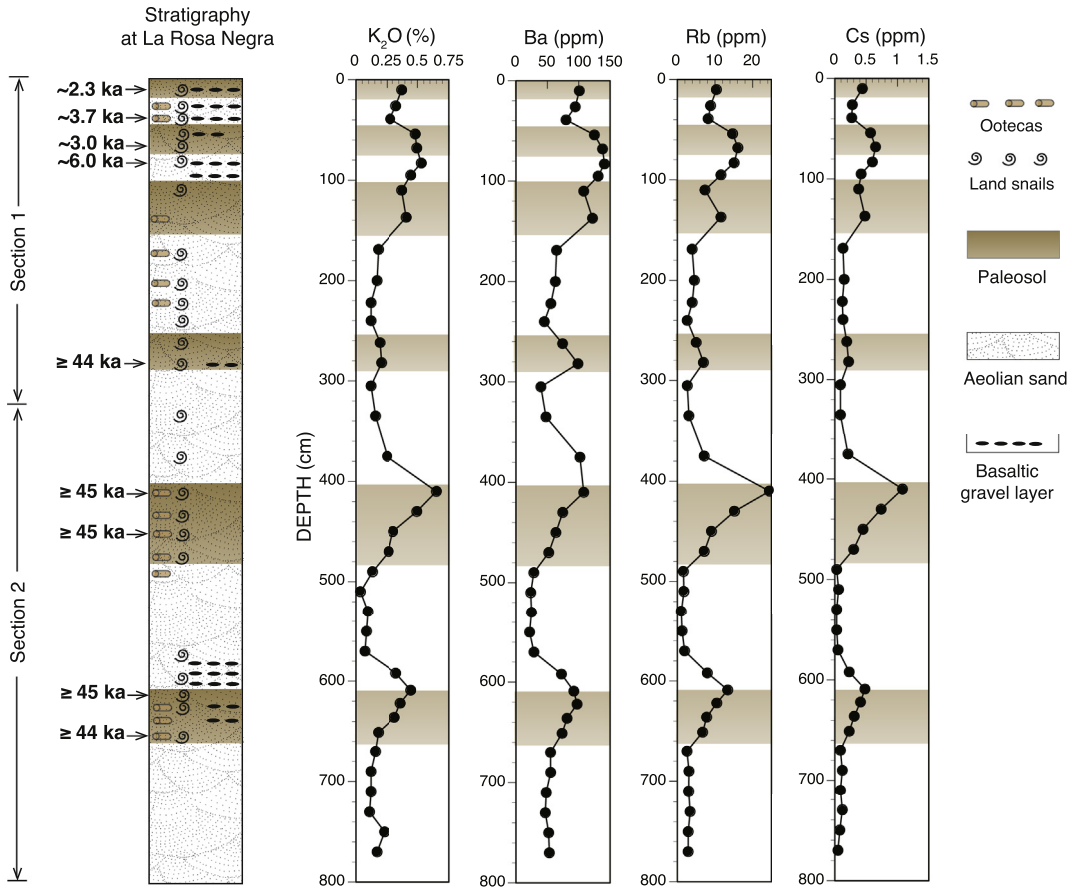

Fig. 20. Composite stratigraphy of aeolian sands (stipple pattern) and paleosols (brown shades) at La Rosa Negra (see Fig. 9 for location of sections 1 and 2) and concentrations of K_2O, Ba, Rb, and Cs as a function of depth. (For interpretation of the references to color in this figure legend, the reader is referred to the Web version of this article.)

soil formation, we infer that little chemical weathering has taken place during the long history of sedimentation and pedogenesis.

We confirm that quartz (in bulk analyses) is present in all the paleosols at both Mala and La Rosa Negra. We stress that the presence of quartz as a dust accretion indicator needs qualification due to the presence of this mineral in rocks of both islands, and our own findings that it is present in modern beach sands of Lanzarote. Nevertheless, the relative abundances of quartz are highest within the paleosols on both islands, and these concentrations increase upward through the soil profiles, in parallel with depth functions of SiO_2 (Figs. 12 and 17). Concentrations of SiO_2 are, in part, a geochemical proxy for quartz.

Two other major elements, Al_2O_3 and Fe_2O_3, also show distinct enrichments in the paleosols of both sections (Figs. 13 and 18). It has long been recognized that in many sediments concentrations of Al_2O_3 and Fe_2O_3, are positively correlated with phyllosilicate clay mineral content, because Al and Fe are found in the octahedral layers of clay minerals (Weaver and Pollard, 1973; Birkeland, 1999). Taylor and McLennan (1985) also noted that REE are concentrated in clay minerals. The inference of Al and Fe in Canary Islands paleosols as proxies for clay minerals is supported by parallel plots of total REE concentrations at both Mala and La Rosa Negra, where the REE are enriched in the buried soils (Figs. 13 and 18).

Clay mineralogical analyses confirm the presence of clay-sized (<2 μm) smectite, mica, and kaolinite in all paleosols of both sections (Figs. 14 and 19). Although smectite and kaolinite could conceivably form from chemical weathering of primary minerals in detrital basalt particles of local origin, a similar inference cannot be made for micas. True cases of pedogenic mica are extremely rare and occur only under particularly favorable circumstances (Fanning and Keramidas, 1977). Mica is present in very small amounts, as biotite, in some of the rocks of the Canary Islands, as noted earlier. However, if mica in these sections had a local, detrital origin, we would not expect to see geochemical proxies for this mineral to have any systematic depth function. We observe just the opposite, with K_2O, one of the major constituents of all micas, showing enrichments in the paleosols and depletions in the subjacent aeolian sands (Figs. 15 and 20). On both islands, Ba, Rb, and Cs, three trace elements that substitute for K, also show enrichments in the paleosols, with depth functions closely paralleling those of K_2O, SiO_2, Al_2O_3, and Fe_2O_3. Thus, the clay mineralogy and concentrations of K_2O, Ba, Rb, and Cs in the paleosols all support the conclusion of an exotic origin for mica.

With the evidence for a minimal amount of chemical weathering, as indicated by the presence of primary carbonate minerals in all paleosols, then the presence of kaolinite (Figs. 14 and 19) must also be explained. Plagioclase is abundant in the basaltic volcanic rocks of the Canary Islands and its presence is documented in all aeolian sands and paleosols studied here. Kaolinite can be an alteration product of plagioclase by hydrolysis, a process which is observed in many soils worldwide (Birkeland, 1999; Brady and Weil, 2002; Schaetzl and Thompson, 2015). Hydrolysis is not, however, a process that is expected to occur at any substantial rate in an arid climate. Both Lanzarote and Fuerteventura currently receive only 100–200 mm of precipitation annually (García Herrera et al., 2001). Furthermore, the Canary Islands were probably arid during the last glacial period as well (Hooghiemstra et al., 2006). Thus, it seems possible that both Lanzarote and Fuerteventura

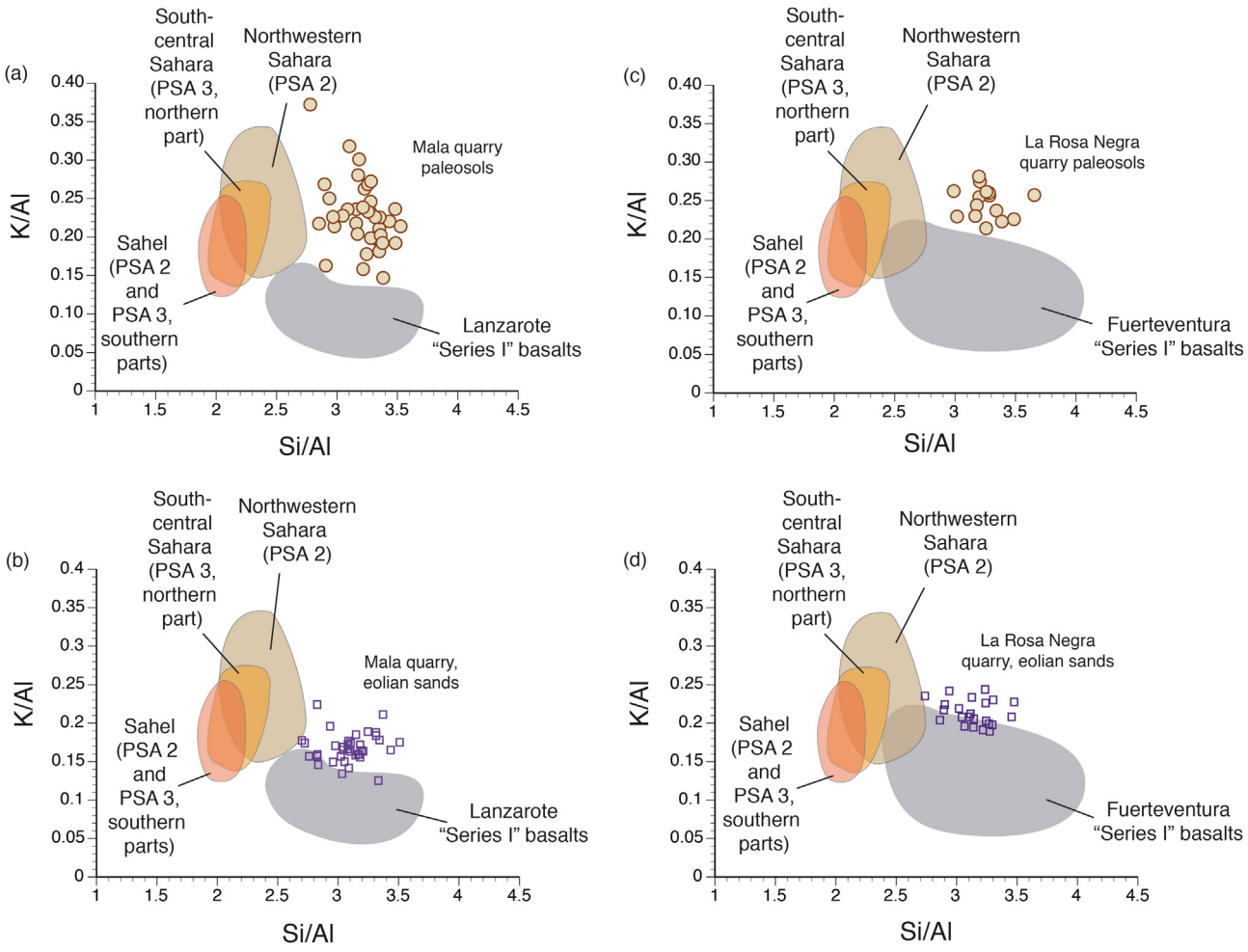

Fig. 21. Comparison of ranges Si/Al and K/Al values in dust samples whose origins are in the northwestern Sahara, south-central Sahara, and Sahel (colored shaded areas; data courtesy of Dr. Isabelle Chiapello; see also Chiapello et al., 1997), local basalt on Lanzarote and Fuerteventura (data from Fuster et al., 1968a, 1968b), and paleosols from sections exposed in the quarries at Mala and La Rosa Negra [(a) and (c)] and aeolian sands from these same sections [(b) and (d)].

could have been relatively arid islands during both interglacial and glacial periods, climatic conditions not conducive to plagioclase alteration to kaolinite. Even if one assumed past periods of higher precipitation, weathering as an origin for kaolinite is unlikely. If kaolinite owed its origin to alteration of plagioclase under past periods of higher rainfall, both aragonite and high-Mg calcite would be expected to have been depleted first, yet both minerals are present in all paleosols. Thus, kaolinite in the paleosols of Lanzarote and Fuerteventura, in addition to quartz and mica, is considered to have an external, aeolian origin.

5.3. Geochemical evidence for African dust inputs for Canary Islands paleosols

Thus far, we have emphasized the mineralogical evidence for aeolian inputs to the paleosols of the Canary Islands, but our cautionary statements about mineralogy lead us to examine the geochemical evidence. Comparison of Lanzarote paleosol compositions to those of local basalt and PSAs allows inferences about possible soil parent material, assuming there has been no loss of Si, K, or Al in the Canary Islands aeolian sections during pedogenesis. Loss of these elements due to chemical weathering is unlikely, given that all three constituents are found dominantly in aluminosilicate minerals. As just noted with regard to plagioclase, weathering of any aluminosilicate minerals would have almost certainly have been preceded by loss of less-stable minerals, aragonite and calcite. The paleosols have Si/Al and K/Al compositions that do not overlap those of the local island basalt, and those that are close to the basalt geochemical field are transitional BC or lower Bw horizons that contain higher proportions of locally derived volcanic grains (Fig. 21). These observations indicate that the non-carbonate components of the paleosols cannot be derived solely from the local island basalts.

The Si/Al and K/Al values in the paleosols not only imply an exotic origin for many of the paleosol constituents, but also can be used to make some inferences about what PSAs in Africa (Fig. 3) could have been contributors. Along with some inherited components from the local island basalt, the paleosols at Mala on Lanzarote have compositions with Si/Al and K/Al values that permit an inference of contributions from PSA 2 (northwestern Sahara and western Sahel), PSA 3 (central Sahara), PSA 4 (Libyan Sahara), PSA 5 (south-central Sahara and Sahel), and PSA 6 (southeastern Sahara) or combinations of these sources (Fig. 21). With these geochemical fields, it is possible to propose a variety of hypotheses about relative contributions of source sediments to the paleosols. For example, dust from PSA 2 (northwestern Sahara), combined with the local volcanic rocks, could account for many of the observed paleosol compositions. A mix of sources from PSA 2 (northwestern Sahara)

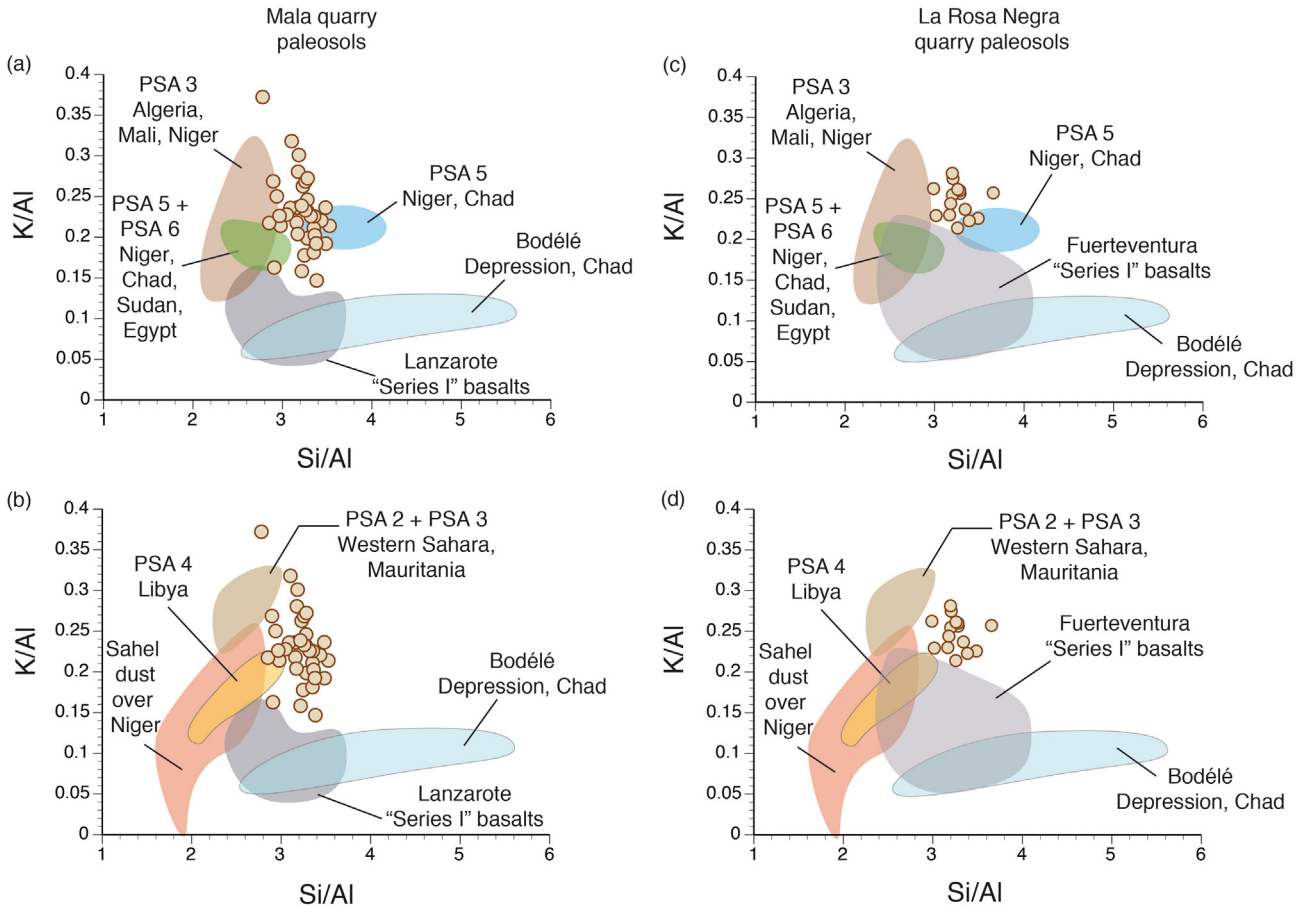

Fig. 22. (a) (b) Comparison of the Si/Al and K/Al values of paleosols at the Mala quarry on Lanzarote (brown filled circles) with those in local Lanzarote "Series I" basalt (data from Fuster et al., 1968a) and various PSAs and other source areas of African dust (data courtesy of P. Formenti; see also Formenti et al. (2008, 2011, 2014, Klaver et al., 2011, and McConnell et al., 2008). (c) (d) Same as for (a) and (b), but showing data for paleosols from the quarry at La Rosa Negra, and local Fuerteventura "Series I" basalt (data from Fuster et al., 1968b). Note horizontal scale change from Fig. 21. (For interpretation of the references to color in this figure legend, the reader is referred to the Web version of this article.)

and PSA 5 (south-central Sahara and Sahel), along with small, local volcanic contributions could also explain the composition of most of the paleosols. Many of the paleosols at Mala have a composition that could be explained simply by a mix of dust from PSA 5 and PSA 6, which would imply both Saharan and Sahel sources. Interestingly, paleosols at Mala fall farthest from the geochemical field defined by Si/Al and K/Al values of sediments collected from the Bodélé Depression, but data from this area are limited.

As with the paleosols at Mala, none of the paleosols at La Rosa Negra have Si/Al vs. K/Al compositions that fall within the field defined by the local basalt, which requires at least some derivation from exotic sources (Fig. 22). As with the paleosols on Lanzarote, contributions from a number of PSAs are possible, however, such as a mix of contributions from both the northwestern and central Sahara (PSA 2 and PSA 3) along with local volcanic rocks. Other combinations of sources are possible, with a mix of dust from PSA 3 (central Sahara) combined with more easterly sources from PSA 5 (south-central Sahara and Sahel). Overall, at both Mala and La Rosa Negra, it seems likely that more than one external (i.e., African dust) source is responsible for the composition of the paleosols, based on the Si/Al and K/Al data.

Trace element geochemistry is complementary to the major element geochemistry in understanding of the genesis of Canary Islands paleosols. Ternary plots of Sc-Th-Ta and Cr-Hf-Th for both the Mala and La Rosa Negra paleosols show that these soils have compositions that are intermediate between African dust from mixed Sahara-Sahel sources and local rocks (Figs. 23–25). On Lanzarote, the Sc-Th-Ta plot indicates about equal contributions from local island basalt and African dust, whereas the Cr-Hf-Th plots imply a broad continuum, with varying degrees of influence from African dust and local island volcanic parent materials (Fig. 23). The same conclusions would apply to paleosols at the quarry at La Rosa Negra on Fuerteventura (Figs. 24 and 25). Here, however, comparisons hold for both the local island basalt and the Basal Complex rocks with a much more diverse mineralogy. Whereas the Sc-Th-Ta and Cr-Hf-Th plots imply contributions from both local rocks and African dust to the paleosols on both islands, the REE imply a much greater influence from African dust (Figs. 23–25). Plots of Gd_N/Yb_N vs. Eu/Eu* indicate that African dust from mixed Sahara-Sahel sources is more important than local rocks as a parent material for paleosols on both Lanzarote and Fuerteventura. In fact, plots of La_N/Yb_N vs. Eu/Eu* would imply that African dust is absolutely dominant as a parent material. Unfortunately, too few trace element data are available from various PSAs across Africa to make confident inferences about which specific dust-source regions are most important for Canary Islands paleosols. Bodélé Depression sediments, for example, have considerable overlap in REE composition with African dust collected on Barbados, which has both Sahara and Sahel sources.

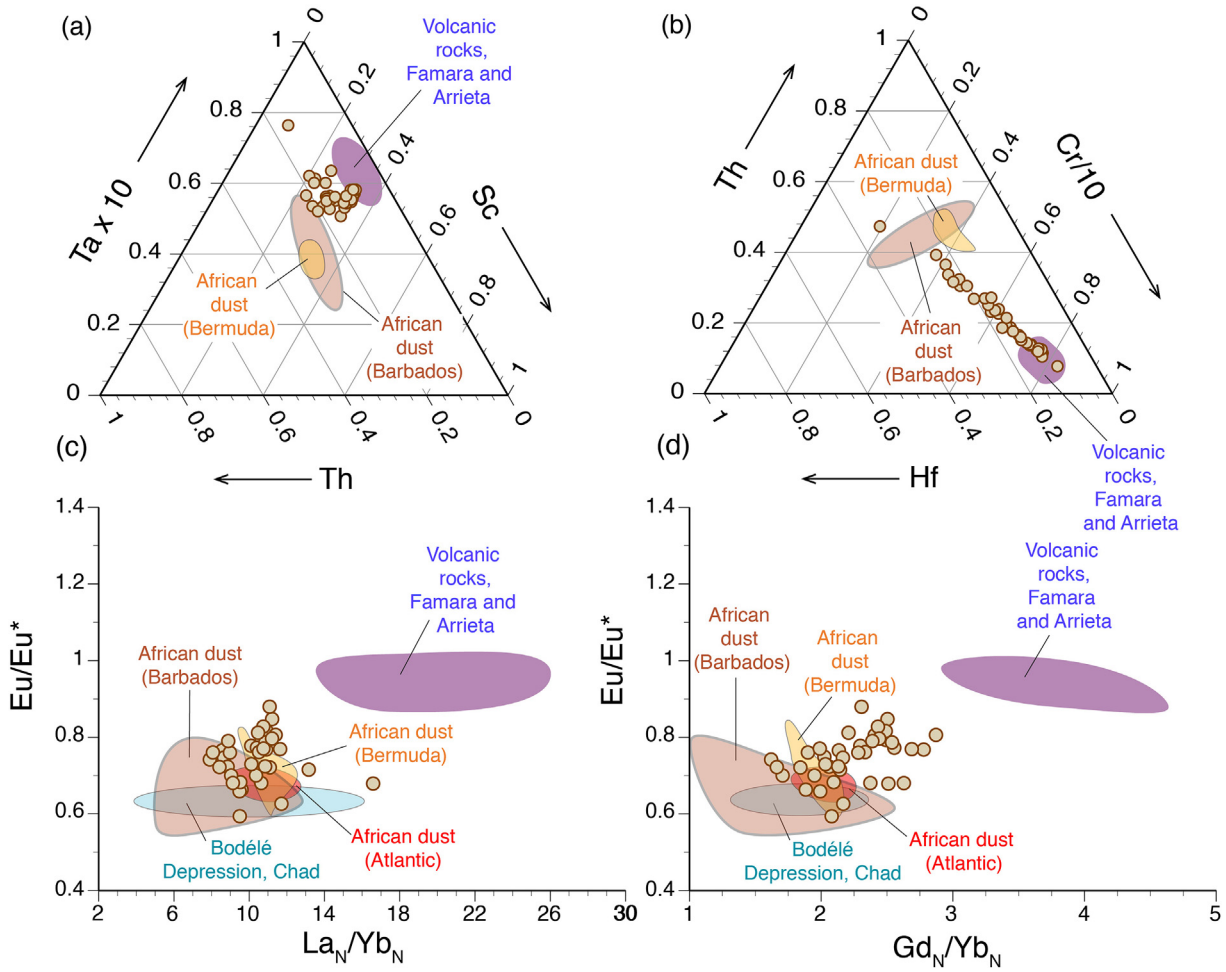

Fig. 23. Plots of (a) Sc-Th-Ta x 10, (b) Cr/10-Hf-Th, (c) La_N/Yb_N vs. Eu/Eu* and (d) Gd_N/Yb_N vs. Eu/Eu* for paleosols at the Mala quarry, Lanzarote (light brown circles) compared to African dust collected on Barbados (data from Muhs et al., [2007, 2010] and Pourmand et al., 2014), Bermuda (data from Muhs et al., 2012), the Bodélé Depression (Abouchami et al., 2013), and in the Atlantic (data from Van der Does et al., 2018) and Quaternary and Miocene volcanic rocks (SP-300, SP-310, SP-477; see Fig. 5 for localities) collected from Famara and Arrietta beaches (data from this study). (For interpretation of the references to color in this figure legend, the reader is referred to the Web version of this article.)

5.4. Evidence for multiple aeolian sources for paleosols from clay mineralogy

A distinct north-to-south change in the geography of soil clay minerals in northern Africa has long been recognized (Fig. 26). Walker (1979) conducted a study of soils (Aridisols and Entisols) and modern alluvium in an ~800-km-long north-south transect (from ~33°N to ~27°N) across the Sahara in western Libya. He reported that mica (illite) is dominant over kaolinite all along this traverse. Paquet et al. (1984) studied a north-south transect of Aridisols and Entisols across the Sahara in Algeria, from ~35°N to ~19°N. They report that mica and chlorite are dominant at higher latitudes, consistent with the Walker (1979) findings. These investigators, however, report greater amounts of kaolinite at lower latitudes. Still farther south, soils in the Sahel region (Alfisols, Ultisols, Oxisols) have relatively high kaolinite contents and high Fe-oxyhydroxide contents (e.g., Ambrost et al., 1986; Faure and Volkoff, 1998; Ducloux et al., 2002).

The changes in clay mineralogy as a function of African soil geography are mirrored in dust collections made off the west coast of Africa. Chester et al. (1972) and Stuut et al. (2005), in shipboard studies of African dust, reported a decrease in the mica/kaolinite ratio of offshore dust from the Canary Islands southward. The decrease in mica and increase in kaolinite contents of dust southward probably reflect the decreasing mica and increasing kaolinite content of adjacent African soils, moving from the Aridisols and Entisols of the Sahara to the Alfisols, Ultisols, and Oxisols of the Sahel and tropical regions (Fig. 26). This conclusion is supported by the back-trajectory analyses made by Stuut et al. (2005) in the collections they made, where dust samples with high mica-kaolinite values have origins in Algeria and Libya (Sahara) and dust samples with low mica-kaolinite values have origins farther south, in the Sahel region of Niger, Nigeria, and southern Chad (Fig. 26).

Paleosols on both Lanzarote and Fuerteventura studied here contain both mica and kaolinite (Figs. 14 and 19). Stuut et al. (2005), in studying shipboard dust collections off Africa, calculated mica/kaolinite values by measuring XRD peak heights at 8.92° 2-theta (mica/illite) and 12.38° 2-theta (kaolinite) (J-B. Stuut, written communication, February 5, 2019). Their results indicate that for dust originating in the Sahara, mica/kaolinite values range from ~1.35 to ~0.8, with one exceptionally high value of ~2.3 (Fig. 26). In contrast, mica/kaolinite values for dust originating from the Sahel range from ~0.65 to ~0.35. For the paleosols on Lanzarote and Fuerteventura, we calculated mica/kaolinite values using this same method. Results indicate that some paleosols have mica/kaolinite values that fall into the range for Sahel dust, some have values in the range of Saharan dust, and several have intermediate values

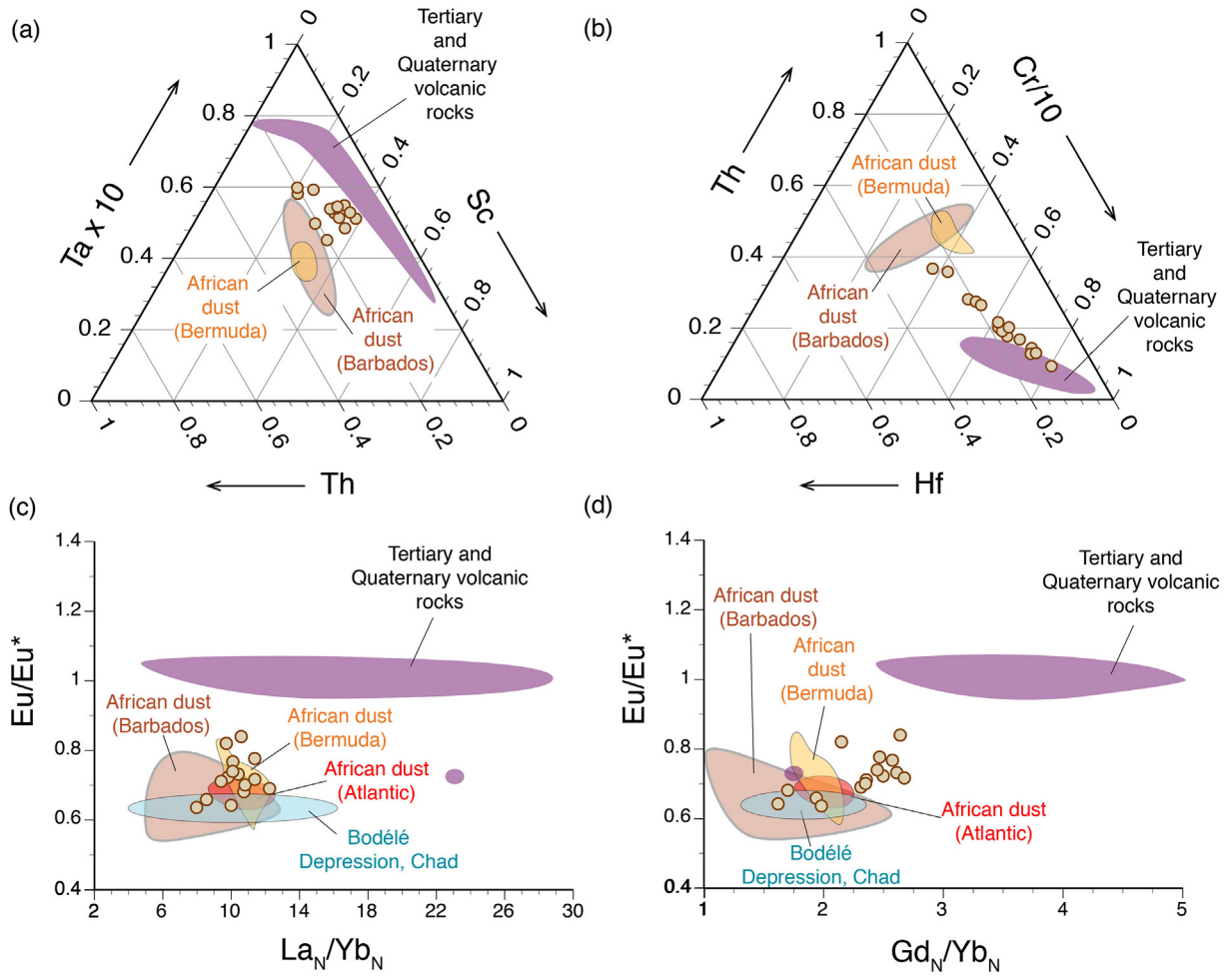

Fig. 24. Plots of (a) Sc-Th-Ta x 10, (b) Cr/10-Hf-Th, (c) La_N/Yb_N vs. Eu/Eu*, and (d) Gd_N/Yb_N vs. Eu/Eu* for paleosols at La Rosa Negra quarry, Fuerteventura (light brown circles) compared to African dust collected on Barbados (data from Muhs et al., [2007, 2010] and Pourmand et al., 2014), Bermuda (data from Muhs et al., 2012), the Bodélé Depression (Abouchami et al., 2013), and in the Atlantic (data from Van der Does et al., 2018) and Quaternary and Miocene volcanic rocks on Fuerteventura (data from Schneider et al., [2014] and Tornare et al., [2016]). (For interpretation of the references to color in this figure legend, the reader is referred to the Web version of this article.)

(Fig. 27). With mica dominant in Saharan source areas and kaolinite dominant in Sahel source areas, the presence of both mica and kaolinite indicates that clays in the paleosols are likely derived from both Sahara and Sahel sources, consistent with the geochemical data.

Despite the common practice of researchers referring to dust reaching the Canary Islands as "Saharan" (Damnati et al., 1996; Williamson et al., 2004; Von Suchodoletz et al., 2008, 2009a; 2009b, 2013; Menéndez et al., 2009, 2019; Criado et al., 2012; Faust et al., 2015; Varga and Roettig, 2018; Roettig et al., 2019), a number of investigations have shown that modern African dust reaching the Atlantic Ocean can have its origins in the Sahel. Indeed, several decades ago, Prospero and Nees (1977) demonstrated that increased African dust fluxes to Barbados in the 1970s were likely related to a major drought period in the Sahel. A more recent study has extended the time period of this relationship, showing that the magnitude of African dust transport to South America over the period 2002–2017 is negatively correlated with rainfall in the Sahel (Prospero et al., 2020). A Sahel origin for some of the LRT dust reaching Barbados and Bermuda is also demonstrated by the HYSPLIT trajectory reconstructions shown in Fig. 4. Other studies, using back-trajectory calculations, have shown that dust transported from Africa can have its origins in both the Sahara and Sahel regions (Stuut et al., 2005; Engelstaedter et al., 2009; Skonieczny et al., 2013; Patey et al., 2015; Bozlaker et al., 2018; Heinrich et al., 2021). The geochemistry and clay mineralogy of Canary Islands paleosols permit an interpretation of both Saharan and Sahel sources of dust.

5.5. Implications for the "accretionary-inflationary profile" (AIP) model of soil genesis

In a simple view, soil development in unconsolidated Quaternary sediments is often perceived to be a process that proceeds dominantly in a downward direction. In this time-honored model, pedogenesis begins after stabilization of a soil parent material by cessation of sedimentation and vegetation colonization. Subsequently, as wetting fronts migrate downward through the sediment repeatedly through time, mechanical movement of clays progresses downward and chemical weathering alters the original parent material to successively greater depths. Thus, B horizons become thicker over time, increasing downward from the original land surface (see Figs. 2.31 and 2.33 of Brady and Weil, 2002). Almond and Tonkin (1999) refer to this model as "topdown pedogenesis." A number of soil chronosequence studies have demonstrated that this concept has validity, at least in many humid climates (see reviews in Birkeland, 1999 and Schaetzl and Thompson, 2015). Importantly, however, as noted by Schaetzl and Thompson (2015),

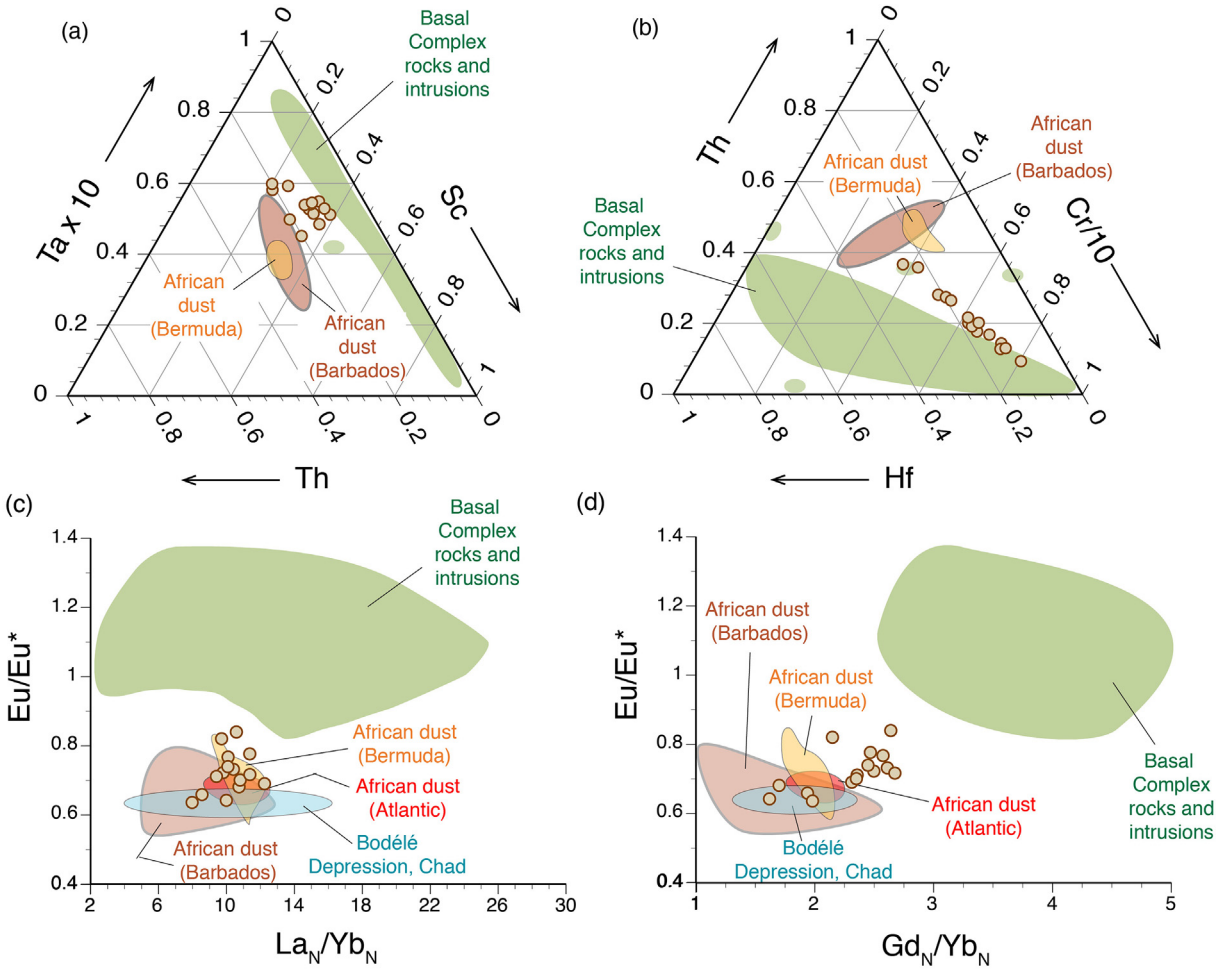

Fig. 25. Plots of (a) Sc-Th-Ta x 10, (b) Cr/10-Hf-Th, (c) La_N/Yb_N vs. Eu/Eu*, and (d) Gd_N/Yb_N vs. Eu/Eu* for paleosols at La Rosa Negra quarry, Fuerteventura (light brown circles) compared to African dust collected on Barbados (data from Muhs et al., [2007, 2010] and Pourmand et al., 2014), Bermuda (data from Muhs et al., 2012), the Bodélé Depression (Abouchami et al., 2013), and in the Atlantic (data from Van der Does et al., 2018) and Basal Complex rocks, dykes, and other intrusions (data from Ahijado et al., [2001], Holloway and Bussy [2008], and Allibon et al., [2011]). (For interpretation of the references to color in this figure legend, the reader is referred to the Web version of this article.)

this concept assumes that the original land surface is static or unchanging.

In contrast, "accretionary" soils are those that develop as new soil parent material is added while pedogenesis is ongoing (Birkeland, 1999, p. 258), or what has been termed a soil "up-building" process (Johnson, 1985). It has long been recognized that hillslope erosion removes soil and/or sediment from the steepest parts of slopes, with deposition of the eroded material at the base of the slope, thus increasing the thickness of the original parent material at that lower slope position (Brady and Weil, 2002). Accretionary soils can be the result of this kind of process and produce what are also sometimes referred to as "cumulic" soil profiles. However, accretionary soils can also develop without slopewash inputs, from accumulation of aeolian deposits. Recognition that both carbonate and clay particles are added to soils from airborne dust in the arid southwestern USA (Gile et al., 1981) led to the understanding that soils can grow upward over time (accretion) and increase mass per unit volume (inflation). This concept has been reviewed in detail by McFadden (2013; see his Fig. 1).

Muhs (2013) hypothesized that paleosols on the Canary Islands also develop by an upward-growing process as long-term dust accretion proceeds. If so, they are good examples of what McFadden (2013) refers to as "accretionary-inflationary profile" (AIP) development. Paleosols P2, P3, P6, P9, and P10 at Mala on Lanzarote are particularly striking examples of this type of soil development, where SiO_2 (quartz, mica, kaolinite), Al_2O_3 (mica, kaolinite), K_2O, Ba, Rb, Cs (mica), and REE (all clay minerals) contents all show distinct upward increases within each paleosol profile (Figs. 12, 13 and 15).

A rigorous test of hypothesized AIP development via dust accretion within an upward-growing soil can be made by plotting element concentrations that proxy for exotic minerals, calculated on a carbonate-free basis. As noted earlier, mica, as a K-bearing mineral, can be proxied by K_2O concentrations, as well as by Rb and Cs concentrations, two trace elements that substitute for K. Using the total $CaCO_3$ contents, along with the bulk K_2O, Rb, and Cs abundances, we recalculated K_2O, Rb, and Cs concentrations within the non-carbonate fraction. Results indicate that K_2O concentrations in the aeolian sands at Mala, on a carbonate-free basis, have values mostly within the range of local volcanic rocks (Fig. 28). In contrast, paleosols at Mala generally have K_2O concentrations that are substantially higher than the range found in volcanic rocks on Lanzarote. Further, most paleosols have K_2O concentrations that fall within the range of African dust (based on the composition of dust collections made on Barbados, described earlier). Concentrations of Rb and Cs, on a carbonate-free basis, parallel the depth function for K_2O values. These two trace elements show an even more distinctive trend of low concentrations in aeolian sands (but within the

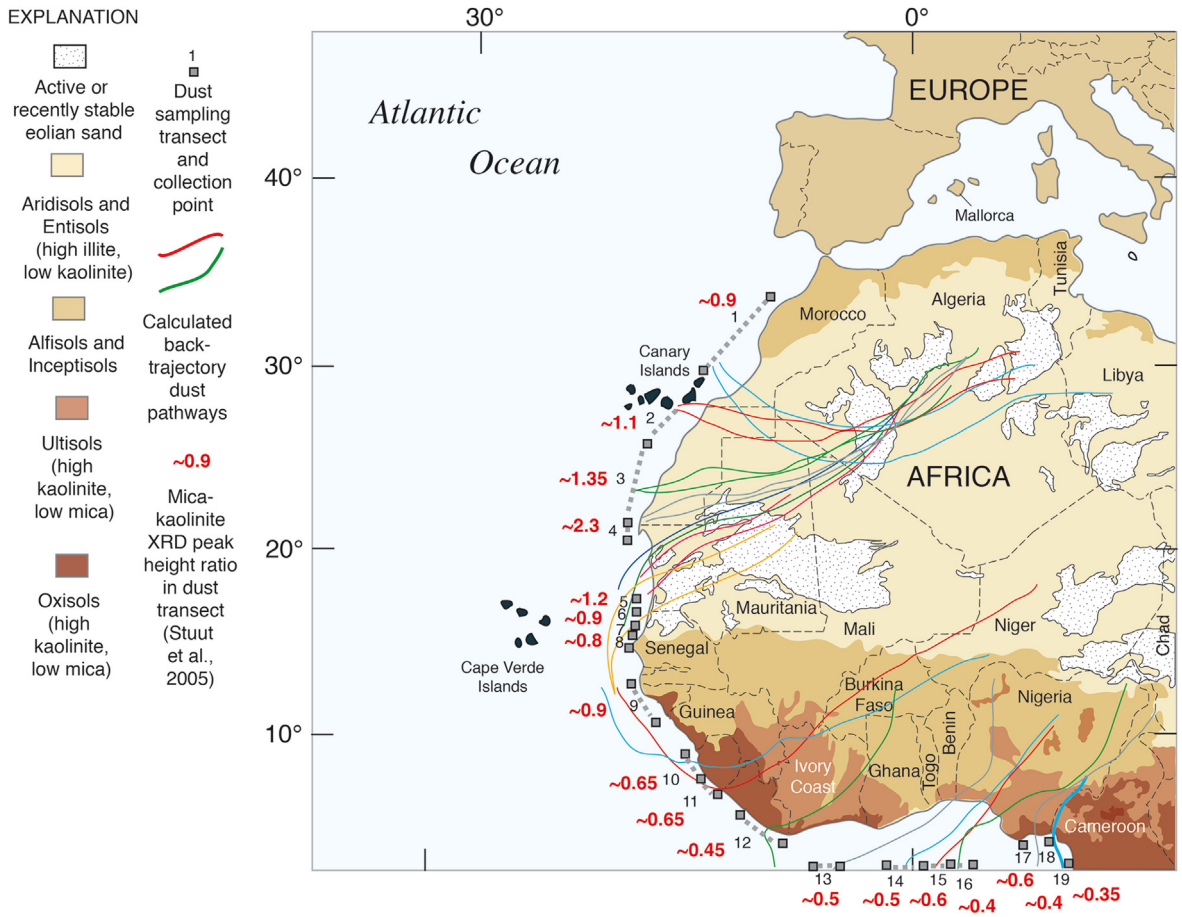

Fig. 26. Soil geography of western Africa, redrawn and generalized from U.S. Department of Agriculture, Natural Resources Conservation Service "Global Soil Regions" map (http://www.soils.usda.gov/use/worldsoils/mapindex/order.html), in turn derived from FAO-UNESCO Soil Map of the World (Food and Agriculture Organization of the United States, UNESCO, 1974). Also shown are dust sampling localities of Stuut et al. (2005), their calculated back trajectories to dust sources in the Sahara (northern pathways) and the Sahel (southern pathways), and approximate mica/kaolinite ratios in the collected dust samples (estimated from graphical presentation in Stuut et al., 2005). Note that samples with higher mica/kaolinite values originate from dune fields, Aridisols, and Entisols in the Sahara, whereas samples with lower mica/kaolinite values originate from Inceptisols, Alfisols, Ultisols and Oxisols in the Sahel and areas to the south of it.

range of Lanzarote rocks) and higher values (within the range of African dust) in paleosols. Concentrations of all three elements (K_2O, Rb, and Cs) show the lowest values in the lower horizons of each paleosol, and highest values in the upper horizons of each paleosol, consistent with an accretionary, upward-growing soil.

6. Conclusions

Thick sequences of carbonate-rich aeolian sands are found on the Canary Islands, examined here on Lanzarote and Fuerteventura. Aeolian sand deposition was not constant, but episodic, with periods of sand stability marked by the development of reddish-brown, silt and clay-rich paleosols. A combination of radiocarbon, $^{40}Ar/^{39}Ar$, and Sr-isotope dating indicates that aeolian sand deposition may have begun as long ago as ~400 ka to ~950 ka and has continued into the Holocene. Most aeolian sands were likely deposited when sea levels began to lower, during the start of glacial periods, and insular shelf sands were freshly exposed. Paleosols formed during periods when aeolian sand deposition ceased, likely during the initial phases of interglacial or interstadial periods.

The paleosols were studied as possible archives of LRT dust originating from Africa, because the presence of aragonite and calcite throughout the sections indicates that little or no chemical weathering has occurred to generate the fine-grained (silt and clay) fractions of the paleosols. Although many previous investigations have appealed to African dust as a parent material for such soils, much of the evidence cited in support of this interpretation has been based mainly on the presence of quartz, which is not typically found in basalt, the main lithology of the Canary Islands. However, previous studies have shown that quartz and even mica are present in some of the rocks of the islands, so independent evidence must be presented to confirm an African dust origin. Following from this, opinions also have been divided as to whether sources in the Sahara or Sahel regions could be the most important sources of African dust on the Canary Islands.

The paleosols contain quartz and mica, present, though not in abundance, in the local rocks of the Canary Islands, but common in LRT dust from Africa. Kaolinite is also found in the paleosols. Because of the evidence for little or no chemical weathering, kaolinite is also likely derived from western African soils of the Sahel region that are rich in this mineral. The presence of these minerals in the paleosols is supported by major and trace element geochemistry. High concentrations of SiO_2 (quartz, mica, kaolinite), Al_2O_3 (mica and kaolinite), K_2O, Ba, Rb, and Cs (mica), and REE (all clay minerals) are found in the paleosols, whereas these elements show low concentrations in the aeolian sands.

Major element geochemistry also allows assessment of PSAs in Africa because previous studies have shown that Si/Al and K/Al

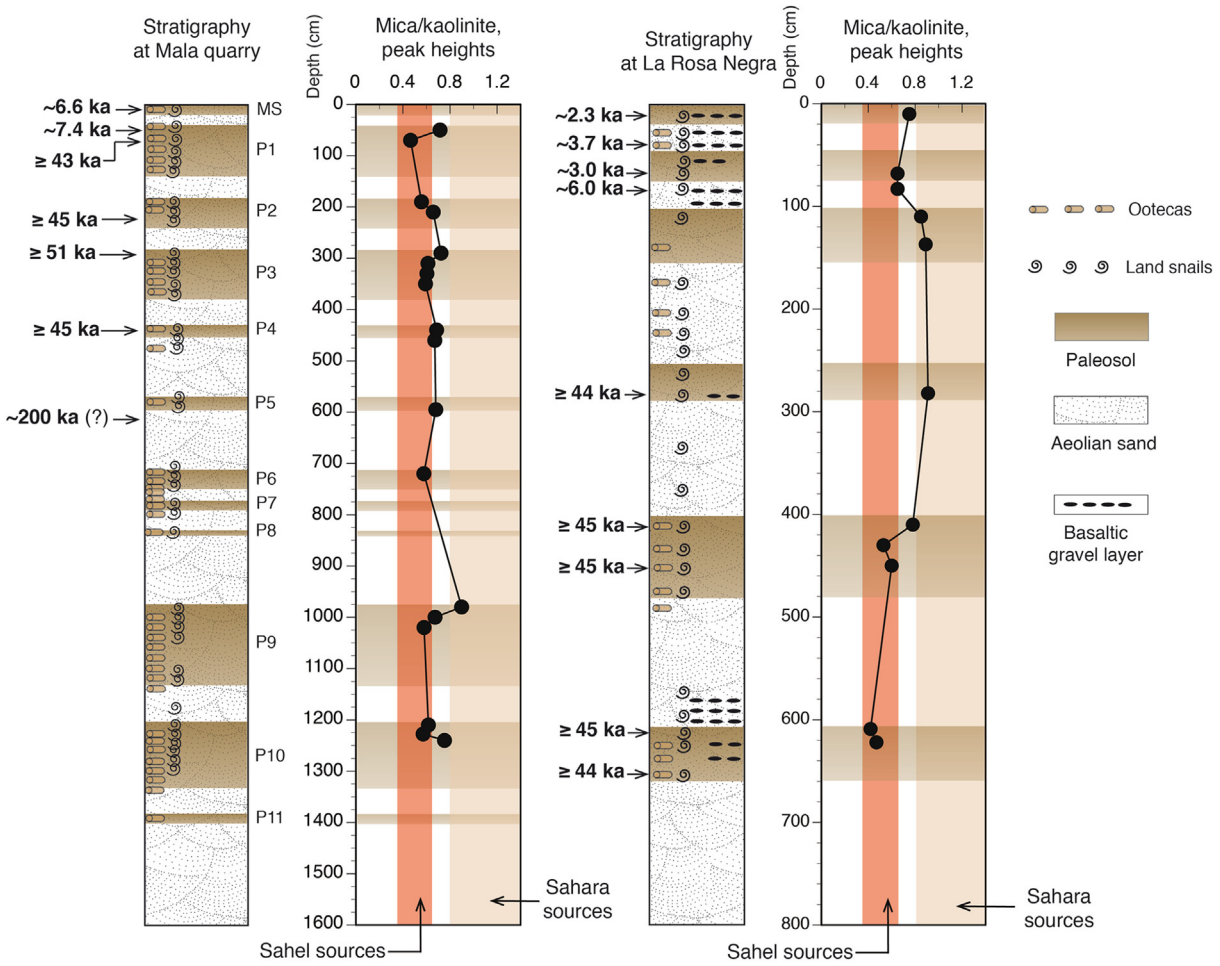

Fig. 27. Stratigraphy of the Mala and La Rosa Negra quarry localities (brown shades are paleosols), with plots of ratios of mica to kaolinite in the clay (<2 μm) fraction of paleosols, based on XRD peak heights (8.9° 2-theta for mica; 12.1° 2-theta for kaolinite) of glycolated samples, identical to the peak heights used by Stuut et al. (2005). Shaded areas show the ranges of mica/kaolinite values in dust samples collected from the Sahara and Sahel (shown in Fig. 26) reported by Stuut et al. (2005). (For interpretation of the references to color in this figure legend, the reader is referred to the Web version of this article.)

values are distinctive for many LRT dust source regions. Comparison of Si/Al and K/Al values in Canary Islands paleosols with published data shows that a variety of combinations of different PSA sediments can explain the composition of the soils, in addition to inheritance of local volcanic particles. In all cases, major element geochemistry shows that local rocks cannot be the only source of non-carbonate minerals in the paleosols. Although it is not possible with these data to identify a unique combination of source regions to explain the composition of the paleosols, it appears likely that more than one external source must be invoked.

Trace element geochemistry also supports the inferences made from mineralogy and major element geochemistry that local rocks are not the sole, or even the primary source of the non-carbonate minerals in the paleosols. Plots of Sc-Th-Ta and Cr-Hf-Th for African dust and local island rocks imply that the paleosols are derived from a combination of the two sources. REE plots (La_N/Yb_N vs. Eu/Eu* and Gd_N/Yb_N vs. Eu/Eu*) of African dust and local island rocks show that African dust may actually be the most important component of REE-bearing minerals, such as clay minerals.

Mica/kaolinite values have been shown to vary latitudinally in shipboard dust collections along the western African coast, reflective of the changing soil geography from the hyperarid Sahara to the semiarid/subhumid Sahel zones. Based on back-trajectory analyses, high mica/kaolinite values are associated with Sahara sources and lower mica/kaolinite values are associated with Sahel sources. Calculation of these values in the clay fractions of Canary Islands paleosols shows that some paleosols are derived dominantly from Saharan sources, some from Sahel sources, and some from both sources. These observations, along with the geochemical data, indicate that both Saharan and Sahel sources of dust have been important in the genesis of these paleosols over much of the Quaternary. It follows from this that droughts of the Sahel, which bring about conditions favorable for dust generation at present, likely have been occurring over many hundreds of thousands of years.

Paleosols in aeolian sand sequences on the Canary Islands show a consistent pattern of gradual upward-increasing concentrations of elements (SiO_2, Al_2O_3, K_2O, Ba, Rb, Cs, and REE) that proxy for exotic minerals. This distinct form of depth function can be explained by increasing land-surface stability, vegetation cover, and dust accretion as pedogenesis proceeds. Thus, these paleosols are good examples of what has been called accretionary-inflationary profile (AIP) development, a contrast to the classical model of "topdown" soil development. As such, the paleosols of the Canary Islands add to the growing body of evidence that LRT dust accretion is an important factor in pedogenesis in many parts of the world.

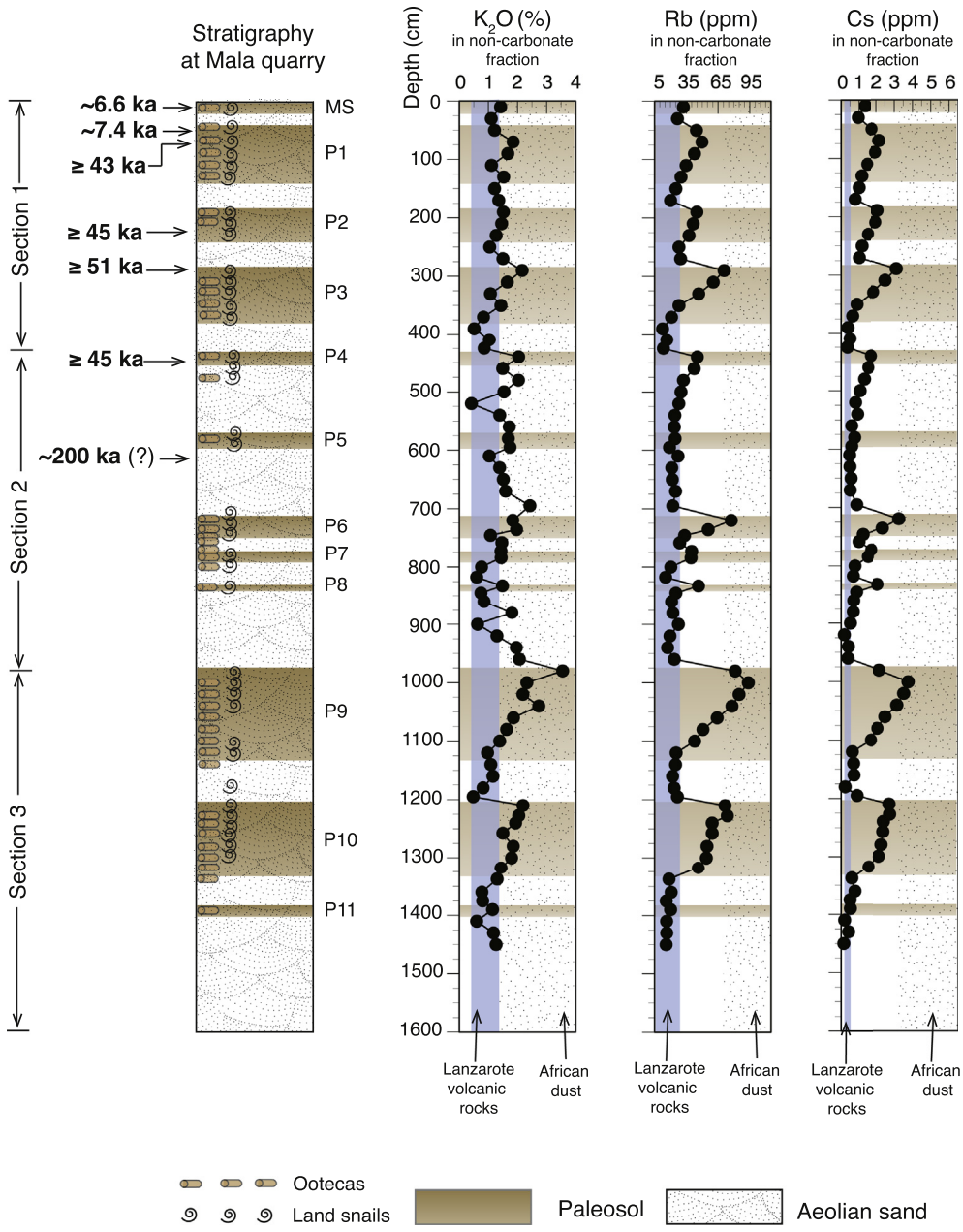

Fig. 28. Composite stratigraphy of aeolian sands (stipple pattern) and paleosols (brown shades) at Mala (see Figs. 7 and 8 for location of sections 1, 2, and 3), and concentrations of K_2O, Rb, and Cs as a function of depth, as in Fig. 15, but recalculated as abundances within the non-carbonate fraction only. Also shown are the ranges of these elements in Lanzarote volcanic rocks (from Fuster et al. (1968a), for K_2O and from Quaternary and Miocene volcanic rocks (SP-300, SP-310, SP-477; see Fig. 5 for localities, for Rb and Cs). (For interpretation of the references to color in this figure legend, the reader is referred to the Web version of this article.)

Author statement of contributions

DRM: Concept, field work, interpretations, writing. JM: Concept, field work, interpretations. JRR: All geochemistry. GLS: All mineralogy. KRS: All Sr isotope work. MCB: All back trajectory analyses. JFB: Field work. AL: Field work.

Declaration of competing interest

The authors declare that they have no known competing financial interests or personal relationships that could have appeared to influence the work reported in this paper.

Acknowledgements

The work by U.S. Geological Survey (USGS) authors is supported by the Climate Research and Development Program of the USGS. Field work in this study for Muhs was supported in part by the Farouk El-Baz Award of the Geological Society of America, and we thank Dr. El-Baz for his support and encouragement of this project. A sampling permit for field work on the Canary Islands was provided by Dr. Maria Aranzazu Gutiérrez Ávila, Directora General de Cooperación y Patrimonio Cultural, Gobierno de Canarias. Señor Isidro Morales Rodriguez kindly gave us permission to sample the La Rosa Negra quarry on Fuerteventura. Merci beaucoup to our French colleagues Dr. Isabelle Chiapello (LOA, CNRS/Université

Lille), Dr. Gilles Bergametti (Laboratoire Interuniversitaire des Systèmes Atmosphériques), and Dr. P. Formenti (Université Paris Est Créteil et Université Paris Diderot), who kindly gave us their data on Si, Al, and K concentrations from samples of various dust source areas in Africa. We appreciate the efforts of Zachary Muhs Rowland and Helen Roberts, who ably assisted with field work on Lanzarote and Fuerteventura, respectively. We thank Lisa Peters (New Mexico Institute of Mining and Technology) who provided the $^{40}Ar/^{39}Ar$ age, and DeAnna Laurel, who assisted with laboratory work. Our good friend and colleague Jack McGeehin (USGS, retired) generated all the radiocarbon ages from the section at Mala, which we greatly appreciate. Finally, our thanks go to QSR editor Giovanni Zanchetta, two anonymous reviewers, and Jeff Pigati and Janet Slate (both USGS) for helpful comments on an earlier version of this paper. Any use of trade, firm, or product names is for descriptive purposes only and does not imply endorsement by the U.S. Government.

Appendix A. Supplementary data

Supplementary data to this article can be found online at https://doi.org/10.1016/j.quascirev.2021.107024.

References

Abouchami, W., Näthe, K., Kumar, A., Galer, S.J.G., Jochum, K.P., Williams, E., Horbe, A.M.C., Rosa, J.W.C., Balsam, W., Adams, D., Mezger, K., Andreae, M.O., 2013. Geochemical and isotopic characterization of the Bodélé Depression dust source and implications for transatlantic dust transport to the Amazon Basin. Earth Planet Sci. Lett. 380, 112–123.

Ahijado, A., Casillas, R., Hernández-Pacheco, A., 2001. The dyke swarms of the Amanay massif, Fuerteventura, Canary Islands (Spain). J. Asian Earth Sci. 19, 333–345.

Alastuey, A., Querol, X., Castillo, S., Escudero, M., Avila, A., Cuevas, E., Torres, C., Romero, P.-M., Exposito, F., García, O., Diaz, J.P., Van Dingenen, R., Putaud, J.P., 2005. Characterisation of TSP and PM2.5 at Izaña and Sta. Cruz de Tenerife (Canary Islands, Spain) during a Saharan dust episode (July 2002). Atmos. Environ. 39, 4715–4728.

Allibon, J., Bussy, F., Lewin, É., Darbellay, B., 2011. The tectonically controlled emplacement of a vertically sheeted gabbro-pyroxenite intrusion: feeder-zone of an ocean-island volcano (Fuerteventura, Canary Islands). Tectonophysics 500, 78–97.

Almond, P.C., Tonkin, P.J., 1999. Pedogenesis by upbuilding in an extreme leaching and weathering environment, and slow loess accretion, south Westland, New Zealand. Geoderma 92, 1–36.

Ambrost, J.P., Nahon, D., Herbillon, A.J., 1986. The epigenetic replacement of kaolinite by hematite in laterite; petrographic evidence and the mechanisms involved. Geoderma 37, 283–294.

Baddock, M.C., Mockford, T., Bullard, J.E., Thorsteinsson, T., 2017. Pathways of high-latitude dust in the north Atlantic. Earth Planet Sci. Lett. 459, 170–182.

Balcells, R., Barrera, J.L., Gómez, J.A., 1991. Geological Map, Isla de Fuerteventura. Instituto Geológico y Minero de España scale, 1:100,000.

Balcells, R., Barrera, J.L., Gómez, J.A., 1994. Geological Map, Isla de Lanzarote, 24-17/18, 24-18/19. Instituto Geológico y Minero de España, scale, 1:100,000.

Bergametti, G., Gomes, L., Coudé-Gaussen, C., Rognon, P., Le Coutumer, M.-N., 1989. African dust observed over Canary Islands: source-regions identification and transport pattern for some summer situations. J. Geophys. Res. 94, 14855–14864.

Birkeland, P.W., 1999. Soils and Geomorphology. Oxford University Press, New York, p. 430.

Bouab, N., Lamothe, M., 1997. Geochronological framework for the Quaternary paleoclimatic record of the Rosa Negra section (Fuerteventura-Canary Islands, Spain. In: Meco, J., Petit-Maire, N. (Eds.), Climates of the Past. International Union of Geological Sciences, UNESCO, Universidad de Las Palmas de Gran Canaria, pp. 37–42.

Bozlaker, A., Prospero, J.M., Price, J., Chellam, S., 2018. Linking Barbados mineral dust aerosols to North African sources using elemental composition and radiogenic Sr, Nd, and Pb isotope signatures. J. Geophys. Res. 123, 1384–1400.

Brady, N.C., Weil, R.R., 2002. The Nature and Properties of Soils, Thirteenth ed. Prentice Hall, Upper Saddle River, NJ, p. 960.

Bristow, C.S., Moller, T.H., 2018. Testing the auto-abrasion hypothesis for dust production using diatomite dune sediments from the Bodélé Depression in Chad. Sedimentology 65, 1322–1330.

Bristow, C.S., Drake, N., Armitage, S., 2009. Deflation in the dustiest place on Earth: the Bodélé depression, Chad. Geomorphology 105, 50–58.

Bristow, C.S., Hudson-Edwards, K.A., Chappell, A., 2010. Fertilizing the Amazon and equatorial Atlantic with west African dust. Geophys. Res. Lett. 37, L14807. https://doi.org/10.1029/2010GL043486.

Budahn, J.R., Wandless, G.A., 2002. Instrumental neutron activation by long count. U.S. Geological Survey Open-File. Report OF-02-0223, Y1-Y9.

Caquineau, S., Gaudichet, A., Gomes, L., Magonthier, M.-C., Chatenet, B., 1998. Saharan dust: clay ratio as a relevant tracer to assess the origin of soil-derived aerosols. Geophys. Res. Lett. 25, 983–986.

Carlson, T.N., Prospero, J.M., 1972. The large-scale movement of Saharan air outbreaks over the Northern Equatorial Atlantic. J. Appl. Meteorol. 11, 283–297.

Carmona, J., Romero, C., Dóniz, J., García, A., 2009. Las alteraciones silíceas de las lavas de Montaña Señalo, erupción de Timanfaya (1730-1736) (Lanzarote, Islas Canarias). Estud. Geol. 65, 79–89.

Carracedo, J.C., Troll, V.R., 2016. The Geology of the Canary Islands. Elsevier, Amsterdam, p. 621.

Carracedo, J.C., Torrado, F.J.P., Meco, J., 2005. La gea: análisis de una isla en estado post-erosivo de desarrollo. In: Delgado, O.R. (Ed.), Patrimonio Natural de la Isla de Fuerteventura. Gran Canaria: Centro de la Cultura Popular Canaria, pp. 27–44.

Chester, R., Elderfield, H., Griffin, J.J., Johnson, L.R., Padgham, R.C., 1972. Eolian dust along the eastern margins of the Atlantic Ocean. Mar. Geol. 13, 91–105.

Chiapello, I., Bergametti, G., Chatenet, B., Bousquet, P., Dulac, F., Santos Soares, E.S., 1997. Origins of African dust transported over the northeastern tropical Atlantic. J. Geophys. Res. 102, 13701–13709.

Coudé-Gaussen, G., Rognon, P., Bergametti, G., Gomes, L., Strauss, B., Gros, J.M., Le Coustumer, M.N., 1987. Saharan dust on Fuerteventura Island (Canaries): chemical and mineralogical characteristics, air mass trajectories, and probable sources. J. Geophys. Res. 92, 9753–9771.

Coudé-Gaussen, G., Rognon, P., 1993. Contrasting origin and character of Pleistocene and Holocene dust falls on the Canary Islands and southern Morocco: genetic and climatic significance, 72. Geological Society of London Special Publication, pp. 277–291.

Criado, C., Dorta, P., 2003. An unusual 'blood rain' over the Canary Islands (Spain). The storm of January 1999. J. Arid Environ. 55, 765–783.

Criado, C., Torres, J.M., Hansen, A., Lillo, P., Naranjo, A., 2012. Intercalaciones de polvo sahariano en paleodunas bioclásticas de Fuerteventura (Islas Canarias). Cuaternario Geomorfol. 26, 73–88.

Damnati, B., 1997. Mineralogical and sedimentological characterization of Quaternary eolian formations and paleosols in Fuerteventura and Lanzarote (Canary Islands, Spain). In: Meco, J., Petit-Maire, N. (Eds.), Climates of the Past. International Union of Geological Sciences, UNESCO, Universidad de Las Palmas de Gran Canaria, pp. 71–77.

Damnati, B., Petit-Maire, N., Fontugne, M., Meco, J., Williamson, D., 1996. Quaternary palaeoclimates in the eastern Canary Islands. Quat. Int. 31, 37–46.

Damnati, B., Maatouk, M., Meco, J., Petit-Maire, N., 2005. Sédimentologie et minéralogie de la séquence sédimentaire "Mala" située a Lanzarote (Iles Canaries, Espagne): les significations paléoclimatologies. Rev. Soc. Geol. Espana 18, 179–185.

Draxler, R.R., Hess, G.D., 1998. An overview of the HYSPLIT_4 modelling system for trajectories, dispersion and deposition. Aust. Meteorol. Mag. 47, 295–308.

Dubief, J., 1979. Review of the north African climate with particular emphasis on the production of eolian dust in the Sahel zone and in the Sahara. In: Morales, C. (Ed.), Saharan Dust: Mobilization, Transport, Deposition. John Wiley & Sons, Chichester, pp. 27–48.

Ducloux, J., Guero, Y., Sardini, P., Decarreau, A., 2002. Xerolysis: a hypothetical process of clay particles weathering under Sahelian climate. Geoderma 105, 93–110.

Engelstaedter, S., Washington, R., Mahowald, N., 2009. Impact of changes in atmospheric conditions in modulating summer dust concentration at Barbados: a back-trajectory analysis. J. Geophys. Res. 114, D17111. https://doi.org/10.1029/2008JD011180.

Engleman, E.E., Jackson, L.L., Norton, D.R., 1985. Determination of carbonate carbon in geological materials by coulometric titration. Chem. Geol. 53, 125–128.

Fanning, D.S., Keramidas, V.Z., 1977. Micas. In: Dixon, J.B., Weed, S.B. (Eds.), Minerals in Soil Environments. Soil Science Society of America, Madison, pp. 195–258.

Faure, P., Volkoff, B., 1998. Some factors affecting regional differentiation of the soils in the Republic of Benin (West Africa). Catena 32, 281–306.

Faust, D., Yanes, Y., Willkommen, T., Roettig, C., Richter, D., Richter, D., von Suchodoletz, H., Zöller, L., 2015. A contribution to the understanding of late Pleistocene dune sand-paleosol-sequences in Fuerteventura (Canary Islands). Geomorphology 246, 290–304.

Food and Agriculture Organization of the United States, Unesco, 1974. Soil Map of the World, 1:5,000,000, vol. 6. UNESCO, Paris, Africa.

Formenti, P., Rajot, J.L., Desboeufs, K., Caquineau, S., Chevaillier, S., Nava, S., Gaudichet, A., Journet, E., Triquet, S., Alfaro, S., Chiari, M., Haywood, J., Coe, H., Highwood, E., 2008. Regional variability of the composition of mineral dust from western Africa: results from the AMMA SOP0/DABEX and DODO field campaigns. J. Res. 113, D00C13. https://doi.org/10.1029/2008jd009903.

Formenti, P., Schuetz, L., Balkanski, Y., Desboeufs, K., Ebert, M., Kandler, K., Petzold, A., Scheuvens, D., Weinbruch, S., Zhang, D., 2010. Recent progress in understanding physical and chemical properties of mineral dust. Atmos. Chem. Phys. Discuss. 10, 31187–31251.

Formenti, P., Rajot, J.L., Desboeufs, K., Saïd, F., Grand, N., Chevaillier, S., Schmechtig, C., 2011. Airborne observations of mineral dust over western Africa in the summer Monsoon season: spatial and vertical variability of physico-chemical and optical properties. Atmos. Chem. Phys. 11, 6387–6410.

Formenti, P., Caquineau, S., Desboeufs, K., Klaver, A., Chevaillier, S., Journet, E.,

Rajot, J.L., 2014. Mapping the physico-chemical properties of mineral dust in western Africa: mineralogical composition. Atmos. Chem. Phys. 14, 10663–10686.
Fuster, J.M., Fernandez Santin, S., Sagredo, J., 1968a. Geology and Volcanology of the Canary Islands: Lanzarote. Instituto Lucas Mallada, Consejo Superior de Investigaciones Cientificas, Madrid, p. 177.
Fuster, J.M., Cendrero, A., Gastesi, P., Ibarrola, E., Lopez Ruiz, J., 1968b. Geology and Volcanology of the Canary Islands: Fuerteventura. Instituto Lucas Mallada, Consejo Superior de Investigaciones Cientificas, Madrid, p. 239.
García Herrera, R., Gallego Puyol, D., Hernández Martín, E., Gimeno Presa, L., Ribera Rodríguez, P., 2001. Influence of the north Atlantic oscillation on the Canary Islands precipitation. J. Clim. 14, 3889–3903.
Genise, J.F., Alonso-Zarza, A.M., Verde, M., Meléndez, A., 2013. Insect trace fossils in aeolian deposits and calcretes from the Canary Islands: their ichnotaxonomy, producers, and palaeoenvironmental significance. Palaeogeogr. Palaeoclimatol. Palaeoecol. 377, 110–124.
Gile, L.H., Hawley, J.W., Grossman, R.B., 1981. Soils and Geomorphology in the Basin and Range Area of Southern New Mexico–Guidebook to the Desert Project, vol. 39. New Mexico Bureau of Mines & Mineral Resources Memoir, pp. 1–222.
Giles, J., 2005. The dustiest place on Earth. Nature 434, 816–819.
Glaccum, R.A., Prospero, J.M., 1980. Saharan aerosols over the tropical north Atlantic – mineralogy. Mar. Geol. 37, 295–321.
Goodfriend, G.A., Hood, D.G., 1983. Carbon isotope analysis of land snail shells: implications for carbon sources and radiocarbon dating. Radiocarbon 25, 810–830.
Goudie, A.S., Middleton, N.J., 2001. Saharan dust storms: nature and consequences. Earth Sci. Rev. 56, 179–204.
Goudie, A.S., Middleton, N.J., 2006. Desert Dust in the Global System. Springer, Heidelberg.
Grousset, F.E., Rognon, P., Coudé-Gaussen, G., Pédemay, P., 1992. Origins of peri-Saharan dust deposits traced by their Nd and Sr isotopic composition. Palaeogeogr. Palaeoclimatol. Palaeoecol. 93, 203–212.
Grousset, F.E., Parra, M., Bory, A., Martinez, P., Bertrand, P., Shimmield, G., Ellam, R.M., 1998. Saharan wind regimes traced by the Sr-Nd isotopic composition of subtropical Atlantic sediments: last glacial maximum vs today. Quat. Sci. Rev. 17, 395–409.
Guillou, H., Carracedo, J.C., Paris, R., Torrado, F.J.P., 2004a. Implications for the early shield-stage evolution of Tenerife from K/Ar ages and magnetic stratigraphy. Earth Planet Sci. Lett. 222, 599–614.
Guillou, H., Torrado, F.J.P., Machin, A.R.H., Carracedo, J.C., Gimeno, D., 2004b. The Plio-Quaternary volcanic evolution of Gran Canaria based on new K-Ar ages and magnetostratigraphy. J. Volcanol. Geoth. Res. 135, 221–246.
Gutiérrez-Elorza, M., Lucha, P., Gracia, F.-J., Desir, G., Marín, C., Petit-Maire, N., 2013. Palaeoclimatic considerations of talus flatirons and aeolian deposits in Northern Fuerteventura volcanic island (Canary Islands, Spain). Geomorphology 197, 1–9.
Heinrich, H., Schmidt, C., Zieman, F., Mikolajewicz, U., Roettig, C.-B., 2021. Massive deposition of Sahelian dust on the Canary Island Lanzarote during North Atlantic Heinrich events. Quat. Res. 101, 51–66.
Holloway, M.I., Bussy, F., 2008. Trace element distribution among rock-forming minerals from metamorphosed to partially molten basic igneous rocks in a contact aureole (Fuerteventura, Canaries). Lithos 102, 616–639.
Hooghiemstra, H., Lézine, A.-M., Leroy, S.A.G., Dupont, L., Marret, F., 2006. Late Quaternary palynology in marine sediments: a synthesis of the understanding of pollen distribution patterns in the NW African setting. Quat. Int. 148, 29–44.
Howarth, R.J., McArthur, J.M., 1997. Statistics for strontium isotope stratigraphy: a robust LOWESS fit to the marine Sr-isotope curve for 0 to 206 Ma, with look-up table for derivation of numeric age. J. Geol. 105, 441–456.
Hudson-Edwards, K.A., Bristow, C.S., Cibin, G., Mason, G., Peacock, C.L., 2014. Solid-phase phosphorus speciation in Saharan Bodélé Depression dusts and source sediments. Chem. Geol. 384, 16–26.
Huerta, P., Rodríguez-Berriguete, Á., Martín-García, R., Martín-Pérez, A., Fernández, Á.L.I., Alonso-Zarza, A.M., 2015. The role of climate and aeolian dust input in calcrete formation in volcanic islands (Lanzarote and Fuerteventura, Spain). Palaeogeogr. Palaeoclimatol. Palaeoecol. 417, 66–79.
Johnson, D.L., 1985. Soil thickness processes. Catena Suppl. 6, 29–40.
Kalu, A.E., 1979. The African dust plume: its characteristics and propagation across west Africa in winter. In: Morales, C. (Ed.), Saharan Dust: Mobilization, Transport, Deposition. John Wiley & Sons, Chichester, pp. 95–118.
Klaver, A., Formenti, P., Caquineau, S., Chevaillier, S., Ausset, P., Calzolai, G., Osborne, S., Johnson, B., Harrison, M., Dubovik, O., 2011. Physico-chemical and optical properties of Sahelian and Saharan mineral dust: in situ measurements during the GERBILS campaign. Q. J. R. Meteorol. Soc. 137, 1193–1210.
Kohfeld, K.E., Tegen, I., 2007. Record of mineral aerosols and their role in the Earth system. In: Holland, H.D., Turekian, K.K. (Eds.), Treatise on Geochemistry. Elsevier, p. 26. http://www.sciencedirect.com/science/referenceworks/9780080437514.
Kuiper, K.F., Deino, A., Hilgen, F.J., Krijgsman, W., Renne, P.R., Wijbrans, J.R., 2008. Synchronizing rock clocks of earth history. Science 320, 500–504.
Kumar, A., Abouchami, W., Galer, S.J.G., Singh, S.P., Fomba, K.W., Prospero, J.M., Andreae, M.O., 2018. Seasonal radiogenic isotopic variability of the African dust outflow to the tropical Atlantic Ocean and across to the Caribbean. Earth Planet Sci. Lett. 487, 94–105.
Lomoschitz, A., Marco, A.S., Huertas, M.J., Betancort, J.F., Isern, A., Sanz, E., Meco, J., 2016. A reappraisal of the stratigraphy and chronology of Early Pliocene palaeontological sites from Lanzarote Island containing fossil terrestrial animals. J. Afr. Earth Sci. 123, 338–349.
Mahowald, N.M., Baker, A.R., Bergametti, G., Brooks, N., Duce, R.A., Jickells, T.D., Kubilay, N., Prospero, J.M., Tegen, I., 2005. Atmospheric global dust cycle and iron inputs to the ocean. Global Biogeochem. Cycles 19. https://doi.org/10.1029/2004GB002402(GB4025).
Mahowald, N.M., Muhs, D.R., Levis, S., Rasch, P.J., Yoshioka, M., Zender, C.S., Luo, C., 2006. Change in atmospheric mineral aerosols in response to climate: last glacial period, preindustrial, modern, and doubled carbon dioxide climates. J. Geophys. Res. 111 https://doi.org/10.1029/2005JD006653.
McArthur, J.M., Howarth, R.J., Bailey, T.R., 2001. Strontium isotope stratigraphy: LOWESS Version 3: best fit to the marine Sr-isotope curve for 0-509 Ma and accompanying look-up table for deriving numerical age. J. Geol. 109, 155–170.
McArthur, J.M., Howarth, R.J., Shields, G.A., Zhou, Y., 2020. Strontium isotope stratigraphy. In: Gradstein, F., Ogg, J., Schmitz, M., Ogg, G. (Eds.), Geologic Time Scale 2020, vol. 1. Elsevier, Amsterdam, pp. 211–238. https://doi.org/10.1016/B978-0-12-824360-2.00007-3.
McConnell, C.L., Highwood, E.J., Coe, H., Formenti, P., Anderson, B., Osborne, S., Nava, S., Desboeufs, K., Chen, G., Harrison, M.A.J., 2008. Seasonal variations of the physical and optical characteristics of Saharan dust: results from the dust outflow and deposition to the ocean (DODO) experiment. J. Geophys. Res. 113, D14S05. https://doi.org/10.1029/2007jd009606.
McFadden, L.D., 2013. Strongly dust-influenced soils and what they tell us about landscape dynamics in vegetated aridlands of the southwestern United States. Geological Society of America Special Paper 500, pp. 501–532.
McGee, D., deMenocal, P.B., Winckler, G., Stuut, J.B.W., Bradtmiller, L.I., 2013. The magnitude, timing and abruptness in North African dust deposition over the last 20,000 yr. Earth Planet Sci. Lett. 371–372, 163–176.
McLennan, S.M., 1989. Rare earth elements in sedimentary rocks: influence of provenance and sedimentary processes. Rev. Mineral. 21, 169–200.
McTainsh, G.H., Walker, P.H., 1982. Nature and distribution of Harmattan dust. Z. Geomorphol. 26, 417–435.
Meco, J., Petit-Maire, N., Fontugne, M., Shimmield, G., Ramos, A.J., 1997. The Quaternary deposits in Lanzarote and Fuerteventura (eastern Canary Islands, Spain): an overview. In: Meco, J., Petit-Maire, N. (Eds.), Climates of the Past. International Union of Geological Sciences, UNESCO, Universidad de Las Palmas de Gran Canaria, pp. 123–136.
Meco, J., Ballester, J., Betancort, J.F., Cilleros, A., Scaillet, S., Guillou, H., Carracedo, J.C., Lomoschitz, A., Petit-Maire, N., Ramos, A.J.G., Perera, N., Meco, J.M., 2006. Paleoclimatología del Neógeno en las Islas Canarias: Geliense, Pleistoceno y Holoceno. Ministerio de Medio Ambiente, Universidad de Las Palmas de Gran Canaria, Las Palmas, p. 203.
Meco, J., Ballester, J., Betancort, J.F., Cilleros, A., Scaillet, S., Guillou, H., Carracedo, J.C., Lomoschitz, A., Petit-Maire, N., Ramos, A.J.G., Perera, N., Meco, J.M., 2008. Historia Geológica del Clima en Canarias. Las Palmas de Gran Canaria, p. 296.
Meco, J., Muhs, D.R., Fontugne, M., Ramos, A.J.G., Lomoschitz, A., Patterson, D., 2011. Late Pliocene and Quaternary Eurasian locust infestations in the Canary Archipelago. Lethaia 44, 440–454.
Meco, J., Koppers, A.A.P., Miggins, D.P., Lomoschitz, A., Betancort, J.-F., 2015. The Canary record of the evolution of the North Atlantic Pliocene: new $^{40}Ar/^{39}Ar$ ages and some notable palaeontological evidence. Palaeogeogr. Palaeoclimatol. Palaeoecol. 435, 53–69.
Menéndez, I., Díaz-Hernández, J.L., Mangas, J., Alonso, I., Sánchez-Soto, P.J., 2007. Airborne dust accumulation and soil development in the north-East sector of Gran Canaria (Canary Islands, Spain). J. Arid Environ. 71, 57–81.
Menéndez, I., Cabrera, L., Sánchez-Pérez, I., Mangas, J., Alonso, I., 2009. Characterisation of two fluvio-lacustrine loessoid deposits on the island of Gran Canaria, Canary Islands. Quat. Int. 196, 36–43.
Menéndez, I., Pérez-Chacón, E., Mangas, J., Tauler, E., Engelbrecht, J.P., Derbyshire, E., Cana, L., Alonso, I., 2014. Dust deposits on La Graciosa Island (Canary Islands, Spain): texture, mineralogy and a case study of recent dust plume transport. Catena 117, 133–144.
Menéndez, I., Mangas, J., Tauler, E., Barrón, V., Torrent, J., Betancort, J.F., Santana, Á., Recio, J.M., Quevedo-González, L.A., Alonso, I., Méndez-Ramos, J., 2019. Aeolian influx and related environmental conditions on Gran Canaria during the early Pleistocene. Quat. Res. 91, 35–50.
Milliman, J.D., 1974. Marine Carbonates, Part 1. Springer-Verlag, New York, NY, p. 375.
Min, K., Mundil, R., Renne, P.L., Ludwig, K.R., 2000. A test for systematic errors in $^{40}Ar/^{39}Ar$ geochronology through comparison with U/Pb analysis of a 1.1-Ga rhyolite. Geochem. Cosmochim. Acta 64, 73–98.
Moore, D.M., Reynolds Jr., R.C., 1997. X-ray Diffraction and the Identification and Analysis of Clay Minerals. Oxford University Press, Oxford, p. 378.
Moskowitz, B.M., Reynolds, R.L., Goldstein, H.L., Berquó, T.S., Kokaly, R.F., Bristow, C.S., 2016. Iron oxide minerals in dust-source sediments from the Bodélé Depression, Chad: implications for radiative properties and Fe bioavailability of dust plumes from the Sahara. Aeolian Res. 22, 93–106.
Muhs, D.R., 2013. The geologic records of dust in the Quaternary. Aeolian Res. 9, 3–48.
Muhs, D.R., Budahn, J.R., Prospero, J.M., Carey, S.N., 2007. Geochemical evidence for African dust inputs to soils of western Atlantic islands: Barbados, the Bahamas, and Florida. J. Geophys. Res. 112, F02009. https://doi.org/10.1029/2005JF000445.
Muhs, D.R., Budahn, J., Skipp, G., Prospero, J.M., Patterson, D., Bettis III, E.A., 2010. Mineralogical and geochemical evidence for Sahara and Sahel dust additions to Quaternary soils on Lanzarote, eastern Canary Islands, Spain. Terra. Nova 22,

399–410.
Muhs, D.R., Budahn, J.R., Prospero, J.M., Skipp, G., Herwitz, S.R., 2012. Soil genesis on the island of Bermuda in the Quaternary: the importance of African dust transport and deposition. J. Geophys. Res. 117, F03025. https://doi.org/10.1029/2012JF002366.
Muhs, D.R., Pigati, J.S., Schumann, R.R., Skipp, G.L., Porat, N., DeVogel, S.B., 2018. Quaternary sea-level history and the origin of the northernmost coastal aeolianites in the Americas: Channel Islands National Park, California, USA. Palaeogeogr. Palaeoclimatol. Palaeoecol. 491, 38–76.
Muhs, D.R., Meco, J., Budahn, J.R., Skipp, G.L., Betancort, J.F., Lomoschitz, A., 2019. The antiquity of the Sahara Desert: new evidence from the mineralogy and geochemistry of Pliocene paleosols on the Canary Islands, Spain. Palaeogeogr. Palaeoclimatol. Palaeoecol. 533, 109245. https://doi.org/10.1016/j.palaeo.2019.109245.
Ortiz, J.E., Torres, T., Yanes, Y., Castillo, C., de la Nuez, J., Ibáñez, M., Alonso, M.R., 2006. Climatic cycles inferred from the aminostratigraphy and aminochronology of Quaternary dunes and palaeosols from the eastern islands of the Canary Archipelago. J. Quat. Sci. 21, 287–306.
Paquet, H., Coudé-Gaussen, G., Rognon, P., 1984. Etude minéralogique de poussières sahariennes le long d'un itinéraire entre 19° et 35° de latitude nord. Rev. Geol. Dyn. Geogr. Phys. 25, 257–265.
Patey, M.D., Achterberg, E.P., Rijkenberg, M.J., Pearce, R., 2015. Aerosol time-series measurements over the tropical Northeast Atlantic Ocean: dust sources, elemental composition and mineralogy. Mar. Chem. 174, 103–119.
Pigati, J.S., Quade, J., Wilson, J., Jull, A.J.T., Lifton, N.A., 2007. Development of low-background vacuum extraction and graphitization systems for ^{14}C dating of old (40-60 ka) samples. Quat. Int. 166, 4–14.
Pigati, J.S., Rech, J.A., Nekola, J.C., 2010. Radiocarbon dating of small terrestrial gastropods in North America. Quat. Geochronol. 5, 519–532.
Pigati, J.S., McGeehin, J.P., Muhs, D.R., Bettis III, E.A., 2013. Radiocarbon dating late Quaternary loess deposits using small terrestrial gastropods. Quat. Sci. Rev. 76, 114–128.
Pourmand, A., Prospero, J.M., Sharifi, A., 2014. Geochemical fingerprinting of trans-Atlantic African dust based on radiogenic Sr-Nd-Hf isotopes and rare earth element anomalies. Geology 42, 675–678.
Prospero, J.M., Carlson, T.N., 1972. Vertical and areal distribution of Saharan dust over the western equatorial North Atlantic Ocean. J. Geophys. Res. 77, 5255–5265.
Prospero, J.M., Nees, R.T., 1977. Dust concentration in the atmosphere of the equatorial North Atlantic: possible relationship to the Sahelian drought. Science 196, 1196–1198.
Prospero, J.M., Lamb, P.J., 2003. African droughts and dust transport to the Caribbean: climate change implications. Science 302, 1024–1027.
Prospero, J.M., Bonatti, E., Schubert, C., Carlson, T.N., 1970. Dust in the Caribbean atmosphere traced to an African dust storm. Earth Planet Sci. Lett. 9, 287–293.
Prospero, J.M., Ginoux, P., Torres, O., Nicholson, S.E., Gill, T.E., 2002. Environmental characterization of global sources of atmospheric soil dust identified with the Nimbus 7 Total Ozone Mapping Spectrometer (TOMS) absorbing aerosol product. Rev. Geophys. 40 (1), 1002. https://doi.org/10.1029/2000RG000095.
Prospero, J.M., Barkley, A.E., Gaston, C.J., Gatineau, A., Campos y Sanso, A., Panechou, K., 2020. Characterizing and quantifying African dust transport and deposition to South America: implications for the phosphorus budget in the Amazon Basin. Global Biogeochem. Cycles. https://doi.org/10.1029/2020GB006536.
Pye, K., 1987. Aeolian Dust and Dust Deposits. Academic Press, London.
Reimer, P.J., Bard, E., Bayliss, A., Beck, J.W., Blackwell, P.G., Bronk Ramsey, C., Grootes, P.M., Guilderson, T.P., Haflidason, H., Hajdas, I., Hatte, C., Heaton, T.J., Hoffmann, D.L., Hogg, A.G., Hughen, K.A., Kaiser, K.F., Kromer, B., Manning, S.W., Niu, M., Reimer, R.W., Richards, D.A., Scott, E.M., Southon, J.R., Staff, R.A., Turney, C.S.M., van der Plicht, J., 2013. IntCal13 and Marine 13 radiocarbon age calibration curves 0-50,000 Years cal BP. Radiocarbon 55, 1869–1887.
Roettig, C.-B., Kolb, T., Wolf, D., Baumgart, P., Richter, C., Schleicher, A., Zöller, L., Faust, D., 2017. Complexity of Quaternary aeolian dynamics (Canary Islands). Palaeogeogr. Palaeoclimatol. Palaeoecol. 472, 146–162.
Roettig, C.-B., Varga, G., Sauer, D., Kolb, T., Wolf, D., Makowski, V., Espejo, J.M.R., Zöller, L., Faust, D., 2019. Characteristics, nature, and formation of palaeosurfaces within dunes on Fuerteventura. Quat. Res. 91, 4–23.
Roettig, C.-B., Kolb, T., Zöller, L., Zech, M., Faust, D., 2020. A detailed chronostratigraphical record of Canarian dune archives - interplay of sand supply and volcanism. J. Arid Environ. 183, 104240. https://doi.org/10.1016/j.jaridenv.2020.104240.
Rognon, P., Coudé-Gaussen, G., 1987. Reconstitution paléoclimatique à partir des sédiments du Pleistocène supérior et de l'Holocène du nord de Fuerteventura (Canaries). Z. Geomorphol. 31, 1–19.
Rognon, P., Coudé-Gaussen, G., 1996a. Paleoclimates off northwest Africa (28°-35°) about 18,000 yr B.P. based on continental eolian deposits. Quat. Res. 46, 118–126.
Rognon, P., Coudé-Gaussen, G., 1996b. Changements dans les circulations atmosphérique et océanique à la latitude des Canaries et du Maroc entre les stades isotopiques 2 et 1. Quaternaire 7, 197–206.
Rognon, P., Coudé-Gaussen, G., Le Coustumer, M.-N., Balouet, J.C., Occhietti, S., 1989. Le massif dunaire de Janida (Fuerteventura, Canaries): évolution des paléoenvironnments de 20 000 BP à l'actuel. Bull. Assoc. Fr. Étude Quat. 26, 31–37.
Rognon, P., Coudé-Gaussen, G., Revel, M., Grousset, F.E., Pedemay, P., 1996. Holocene Saharan dust deposition on the Cape Verde Islands: sedimentological and Nd-Sr isotopic evidence. Sedimentology 43, 359–366.
Rowe, M.P., Bristow, C.S., 2015a. Landward-advancing Quaternary eolianites of Bermuda. Aeolian Res. 19, 235–249.
Rowe, M.P., Bristow, C.S., 2015b. Sea-level controls on carbonate beaches and coastal dunes (eolianite): lessons from Pleistocene Bermuda. Geol. Soc. Am. Bull. 127, 1645–1665.
Sarnthein, M., Tetzlaff, G., Koopmann, B., Wolter, K., Pflaumann, U., 1981. Glacial and interglacial wind regimes over the eastern subtropical Atlantic and north-west Africa. Nature 293, 193–196.
Schaetzl, R.J., Thompson, M.L., 2015. Soils: Genesis and Geomorphology, second ed. Cambridge University Press, New York, p. 778.
Scheuvens, D., Schütz, L., Kandler, K., Ebert, M., Weinbruch, S., 2013. Bulk composition of northern African dust and its source sediments – a compilation. Earth Sci. Rev. 116, 170–194.
Schneider, B., Kuiper, K.F., Mai, K., Foeken, J.P.T., Stuart, F.M., Wijbrans, J.R., 2014. Fuerteventura – assessment of a calibration site for cosmogenic ^{3}He exposure dating with the $^{40}Ar/^{39}Ar$ incremental heating method. Quat. Geochronol. 21, 58–69.
Schwanghart, W., Schütt, B., 2008. Meteorological causes of harmattan dust in west Africa. Geomorphology 95, 412–428.
Skonieczny, C., Bory, A., Bout-Roumazeilles, V., Abouchami, W., Galer, S.J.G., Crosta, X., Diallo, A., Ndiaye, T., 2013. A three-year times series of mineral dust deposits on the West African margin: sedimentological and geochemical signatures and implications for interpretation of marine paleo-dust records. Earth Planet Sci. Lett. 364, 145–156.
Stein, R., Sarnthein, M., 1984. Late Neogene events of atmospheric and oceanic circulation offshore northwest Africa: high-resolution record from deep-sea sediments. Palaeoecol. Afr. Surround. Isl. 16, 9–36.
Stuiver, M., Reimer, P.J., 1993. Extended ^{14}C database and revised CALIB radiocarbon calibration program. Radiocarbon 35, 215–230.
Stuut, J.-B., Zabel, M., Raymeyer, V., Helmke, P., Schefuß, E., Lavik, G., Schneider, R., 2005. Provenance of present-day eolian dust collected off NW Africa. J. Geophys. Res. 110, D04202. https://doi.org/10.1029/2004JD005161.
Stuut, J.-B., Smalley, I., O'Hara-Dhand, K., 2009. Aeolian dust in Europe: African sources and European deposits. Quat. Int. 198, 234–245.
Taylor, S.R., McLennan, S.M., 1985. The Continental Crust: its Composition and Evolution. Blackwell Scientific Publications, Oxford, p. 312.
Tetzlaff, G., Peters, M., 1986. Deep-sea sediments in the eastern equatorial Atlantic off the African coast and meteorological flow patterns over the Sahel. Geol. Rundsch. 75, 71–79.
Todd, M.C., Washington, R., Martins, J.V., Dubovik, O., Lizcano, G., M'Bainayel, S., Engelstaedter, S., 2007. Mineral dust emission from the Bodélé depression, northern Chad, during BoDEx 2005. J. Geophys. Res. 112, D06207. https://doi.org/10.1029/2006JD007170.
Tornare, E., Pilet, S., Bussy, F., 2016. Magma differentiation in vertical conduits revealed by the complementary study of plutonic and volcanic rocks from Fuerteventura (Canary Islands). J. Petrol. 57, 2221–2250.
Torres-Padrón, M.E., Gelado-Caballero, M.D., Collado-Sánchez, C., Siruela-Matos, V.F., Cardona-Castellano, P.J., Hernández-Brito, J.J., 2002. Variability of dust inputs to the CANIGO zone. Deep-Sea Res. II 49, 3455–3464.
Van der Does, M., Pourmand, A., Sharifi, A., Stuut, J.-B.W., 2018. North African mineral dust across the tropical Atlantic Ocean: insights from dust particle size, radiogenic Sr-Nd-Hf isotopes and rare earth elements (REE). Aeolian Res. 33, 106–116.
Varga, G., Roettig, C.-B., 2018. Identification of Saharan dust particles in Pleistocene dune sand-paleosol sequences of Fuerteventura (Canary Islands). Hungaria. Geogr. Bullet. 67, 121–141.
Von Suchodoletz, H., Fuchs, M., Zöller, L., 2008. Dating Saharan dust deposits on Lanzarote (Canary Islands) by luminescence dating techniques and their implication for paleoclimate construction of NW Africa. Geochem. Geophys. Geosyst. 9, Q02Q07. https://doi.org/10.1029/2007GC001658.
Von Suchodoletz, H., Faust, D., Zöller, L., 2009a. Geomorphological investigations of sediment traps on Lanzarote (Canary Islands) as a key for the interpretation of a paleoclimate off NW Africa. Quat. Int. 196, 44–56.
Von Suchodoletz, H., Kühn, P., Hambach, U., Dietz, M., Zöller, L., Faust, D., 2009b. Loess-like and palaeosol sediments from Lanzarote (Canary Islands/Spain)–Indicators of palaeoenvironmental change during the late Quaternary. Palaeogeogr. Palaeoclimatol. Palaeoecol. 278, 71–87.
Von Suchodoletz, H., Blanchard, H., Hilgers, A., Radtke, U., Fuchs, M., Dietze, M., Zöller, L., 2012. TL and ESR dating of middle Pleistocene lava flows on Lanzarote island, Canary Islands (Spain). Quat. Geochronol. 9, 54–64.
Von Suchodoletz, H., Glaser, B., Thrippleton, T., Broder, T., Zang, U., Eigenmann, R., Kopp, B., Reichert, M., Zöller, L., 2013. The influence of Saharan dust deposits on La Palma soil properties (Canary Islands, Spain). Catena 103, 44–52.
Walker, T.R., 1979. Red Color in Dune Sand. U.S. Geological Survey Professional Paper 1052, pp. 61–81. Chapter D.
Warren, A., Chappell, A., Todd, M.C., Bristow, C., Drake, N., Engelstaedter, S., Martins, V., M'bainayel, S., Washington, R., 2007. Dust-raising in the dustiest place on Earth. Geomorphology 92, 25–37.
Washington, R., Todd, R., Middleton, N.J., Goudie, A.S., 2003. Dust-storm source areas determined by the Total Ozone Monitoring Spectrometer and surface observations. Ann. Assoc. Am. Geogr. 93, 297–313.
Washington, R., Todd, M.C., Lizcano, G., Tegen, I., Flamant, C., Koren, I., Ginoux, P., Engelstaedter, S., Bristow, C.S., Zender, C.S., Goudie, A.S., Warren, A.,

Prospero, J.M., 2006. Links between topography, wind, deflation, lakes and dust: the case of the Bodélé Depression, Chad. Geophys. Res. Lett. 33, L09401. https://doi.org/10.1029/2006GL025827.

Weaver, C.E., Pollard, L.D., 1973. The Chemistry of Clay Minerals. Elsevier, New York, p. 213.

Williams, R.H., McGee, D., Kinsley, C.W., Ridley, D.A., Hu, S., Fedorov, A., Tal, I., Murray, R.W., deMenocal, P.B., 2016. Glacial to Holocene changes in trans-Atlantic Saharan dust transport and dust-climate feedbacks. Sci. Adv. 2 (11), e1600445 https://doi.org/10.1126/sciadv.1600445.

Williamson, D., Jackson, M., Banerjee, S.K., Petit-Maire, N., 2004. The magnetism of a glacial aeolianite sequence from Lanzarote (Canary Islands): coupling between luvic calcisol formation and Saharan dust trapping processes during wet deposition events off northwestern Sahara. Geophys. J. Int. 157, 1090–1104.

Yanes, Y., Kowalewski, M., Ortiz, J.E., Castillo, C., Torres, T., Nuez, J., 2007. Scale and structure of time-averaging (age mixing) in terrestrial gastropod assemblages from Quaternary eolian deposits of the eastern Canary Islands. Palaeogeogr. Palaeoclimatol. Palaeoecol. 251, 283–299.

Yanes, Y., Tomasovych, A., Kowalewski, M., Castillo, C., Aguirre, J., Alonso, M.R., Ibáñez, M., 2008. Taphonomy and compositional fidelity of Quaternary fossil assemblages of terrestrial gastropods from carbonate-rich environments of the Canary Islands. Lethaia 41, 235–256.

Yanes, Y., Aguirre, J., Alonso, M.R., Ibáñez, M., Delgado, A., 2011. Ecological fidelity of Pleistocene-Holocene land snail shell assemblages preserved in carbonate-rich paleosols. Palaios 26, 406–419.

Yu, Y., Kalashnikova, O.V., Garay, J.J., Lee, H., Notaro, M., Campbell, J.R., Marquis, J., Ginoux, P., Okin, G.S., 2020. Disproving the Bodélé depression as the primary source of dust fertilizing the Amazon rainforest. Geophys. Res. Lett. 47, e2020GL088020 https://doi.org/10.1029/2020GL088020.